Departament d'Enginyeria Mecànica

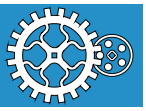

UNIVERSITAT POLITÈCNICA DE CATALUNYA

Approach to acoustic mapping through continuous mobile monitoring

by

Guillermo Quintero Perez

Supervisors:

Jordi Romeu Garbí

Andreu Balastegui Manso

A thesis submitted in partial fulfillment for the degree of Doctor of Philosophy of Environmental Engineering

in the

Escola Tècnica Superior d'Enginyeries Industrial, Aeroespacial i Audiovisual de Terrassa

Department of Mechanical Engineering

May 21, 2019

Abstract

Escola Tècnica Superior d'Enginyeries Industrial, Aeroespacial i Audiovisual de Terrassa
Department of Mechanical Engineering

Doctor of Philosophy in Environmental Engineering

by Guillermo Quintero Perez

For the production of representative noise maps, a large amount of information is necessary, which includes, among others, on-site measurements of environmental noise. Thus, for noise maps based on measurements, mobile sampling emerges as a possible solution for the enhancement of data acquisition.

The present research proposes a complete framework to perform mobile sampling. Since the normative requires long-term values to be presented in a noise map, a sampling strategy based on temporal stratification, which reduces the required sampled days to estimate the annual equivalent noise level, is presented. Furthermore, to compute long-term values for the night period, since they are usually affected by noise sources different to traffic, specifically leisure noise, a complementary temporal and spatial stratification is also presented.

Then, the statistical requirements to perform mobile noise measurements using bicycles is evaluated. The vehicles and bicycles journeys are reproduced based on micro-traffic simulation and then coupled with an acoustic modeling. The estimation error of L_{Aeq} for the mobile sampling is compared to reference static samples, in terms of the Root Mean Square Error (RMSE), and is computed for different aggregation radius of mobile receivers, and as a function of the number of passes-by and to the distance to its nearest cross street.

To perform the mobile sampling on a real scenario, a low-cost noise monitoring device with the aim of performing georeferenced noise sampling, is developed. The accuracy tests suggest that it is able to acquire noise levels with an equivalent accuracy as a Class 2 sound level meter.

Finally, to validate the results obtained through the modeling framework, a noise monitoring device is mounted on a bicycle and on-site mobile measurements are

performed simultaneously to reference static ones. The same scenario is again recreated based on micro-simulation of traffic complemented with acoustic modeling. Then, for the simulated framework and the on-site measurements, the RMSE of the estimation of L_{Aeq} for different aggregation radius of mobile samples is compared to the reference static ones. It is confirmed that mobile sampling is a solution to improve noise data acquisition, which reduces the resources required to produce a noise map without sacrificing the accuracy and representativeness.

Acknowledgements

First of all, I would like to thank to my thesis supervisors, Jordi Romeu and Andreu Balastegui, for guiding me through this tortuous but satisfying process of becoming a doctor, it has been a pleasure to work with both of you. Thank you for the time you spent with me!

Also, one can not achieve succesfully any goal if the working environment is not adequate. Hopefully, at the LEAM this requirement is perfectly fulfilled. I would like to thank all the members for your support and friendship.

Almost that important are my friends who accompanied me in the late-night working sessions, mainly intended to reduce the stress of a PhD student. Thank you all for going along with me in this 3 years of hard work, taking care and worrying even a little bit.

Finally, I want to thank to my family, there are no words to express how grateful I feel for all your support. The goals achieved so far are because you always believed in me and motivated me to move forward. Also, because in your own way, made me note when was I moving away a little bit from the road.

Thank you all!

Contents

List of Figures

List of Tables

To my family and friends

Chapter 1

Introduction

1.1 Background of the research

Health problems related to environmental noise exposure such as the elevation of the auditory threshold, total hearing loss or problems in communication have been widely studied[5]. But the harmful effects of exposure to noise pollution are not only limited to hearing problems, it could bring other non-auditory affections such as sleep disturbance, lead to cardiovascular diseases, cause cognitive problems and more [6, 7].

Noise, among other environmental pollutants in urban areas, are mainly caused by the vehicular transit. In order to evaluate the exposure of population to traffic noise pollution, noise maps have become the main tool since they allow the characterization of the acoustic pollution and noise exposure in a specific area [8] under different temporal, environmental and activity conditions. The use that is given to noise maps is wide, starting from just informing the community of the acoustic situation of their place of residence, to making decisions to establish maximum levels of noise or city planning [9, 10].

The Environmental Noise Directive 2002/49/EC [11] has emerged as a framework for the Member States to evaluate and manage the environmental noise. Through the use of strategic noise mapping to estimate the population exposure, action plans should be generated to reduce noise pollution in cities, whose results are requested to be updated and published every five years. According to the Noise Directive, as a minimum, the indicators that should be shown in a noise map are: the night-time equivalent noise level L_{night}, for the evaluation of sleep disturbance, and the day-evening-night equivalent level, L_{DEN}, for the evaluation of overall annoyance, which should be presented for the equivalent time of one year.

For the estimation of the noise levels to be presented in the noise maps, mainly 3 methods are used [12, 13]:

- On-site measurements.
- Computational methods.
- Computational methods, validating results through on-site measurements.

The computational methods present as main inconvenience that the amount of information required is very large and is not always available, since several parameters such as the variety of noise sources, traffic properties and composition, road characteristics, climatological variables or building configurations, should be considered for the calculations [14, 15]. Furthermore, to compute the perceived noise level at a receiver (façade), noise propagation models should be used which usually requires high computational power to provide accurate results [16].

The on-site measurement method is based on the direct measurement of environmental noise using sound level meters. The main drawback of this strategy is that it consumes more resources than the computational methods for large areas under assessment [17], since apart from recording noise levels at several sampling points for long periods, a high intensity of further noise data processing of the measurements is required. Furthermore, the noise measurement representativeness is dependent on many factors such as environmental conditions, distance from the noise sources, reflections or absorptions of near obstacles or the qualification of the measuring personnel [18, 19].

In both cases, either for direct noise levels sampling or detailed traffic flow measurements, proper sampling planning, and the error that inherently causes in the estimation of the sound levels, are key points to obtain representative values that describe, with an adequate precision, the impact of urban noise in the population. So, when it comes about performing noise assessment of a place, the number of sampling points, their location and the measurement time is directly related to the accuracy that is desired and to the resources to be invested.

1.1.1 Noise mapping using on-site measurements

Although the preferred tool to produce a noise map has been the computational methods [20, 21], noise measurements are required to calibrate the noise modeling tools [22, 23], in complex environments where the traffic is not the main noise source [24] or when more accurate results are required [25].

Since the use of on-site noise measurements is a task that demands many resources, temporal and spatial sampling techniques are used to reduce the required measurement time and amount of sampling points when the noise source is traffic.

However, those sampling strategies could lead to significant differences between the estimated and the actual values [26, 27].

1.1.1.1 Spatial optimizations

The traditional method used to select the location where the noise measurements should be performed was through the use of a sampling grid [28, 29], which places measurement points at equal distances, randomly or according to a specific characteristic.

In order to increase the spatial resolution of samples, the distance between receivers shall be reduced [13]. In the practice, when assessing city-wide zones, shortening the distance between receivers becomes unfeasible after some point. Thus, interpolation methods are used to compute noise level across the whole spatial extent of the study zone [30]. This process brings an associated uncertainty that affects the accuracy of the obtained results [14, 31, 32].

Spatial sampling strategies have been developed so that smaller number of measurement points are required. There are some authors who propose a classification of pathways, that would reduce the number of sampling points as well as it opens the possibility of noise levels extrapolation to non-measured points. This classification is based primarily on the concept of classifying streets according to the type or use of the road [17, 33, 34] which would also reduce the variability within each category [35–40]. Anyway, special care should be taken for the night period since land use can affect urban noise levels [10, 41–44], specially in case of leisure activities [24, 38, 45–48].

1.1.1.2 Temporal optimizations

As stated in Section 1.1, annual equivalent levels should be presented in a noise map in separated time periods such as L_{day}, $L_{evening}$, L_{night} or L_{den} [11]. Analogous to the spatial optimizations, a temporal sampling method is required in order to estimate long-term noise levels with an adequate level of precision and representativeness. Long-term equivalent levels could be approximated by the use of sampling techniques that imply sampling times whose length is far smaller than

the total period to estimate [49], and whose characteristics in terms of measurement duration and placement of the receiver must generate a representative value of the study area.

To estimate the L_{den} value, one or a small number of short time measurements of length much lower than the 24 hours period can be used, usually between minutes to a few hours [17, 50, 51]. In this way, the year equivalent value can be estimated with certain precision using noise levels from a number of days much lower than the whole year [52].

For the calculation of L_{day}, authors reduce the estimation error by limiting sampling to some specific characteristic. As an example [17], shows that it is possible to estimate day time noise level by taking short time measurements which, depending on the category, could be improved by limiting the measurements to certain periods of the day. Regarding the minimum time needed for a sample to be representative of a specific place, it is found that measurements between 10-20 minutes are enough to stand for the day value [17, 53]. Also, it has been proposed using as a stop parameter the time taken for the sound pressure to stabilize, e.g., that its fluctuation range be within certain error interval, which is called stabilization time [54].

For annual noise levels estimation, it has been shown that sampling random days during the year, gives better precision and representativeness than other techniques such as sampling consecutive days, only working-days, only weekends or random full weeks [27, 52]. Moreover, several authors use random sampling as a base for comparison of optimizations in sampling techniques for long term values estimation [8, 26, 34, 55].

1.1.1.3 On-site noise data acquisition approaches

For noise maps produced through on-site measurements, the tasks that were traditionally executed by experts using expensive certified equipment [56], are being replaced by other data acquisition approaches. One of them are the sensor networks, which are comprised by a set of spatially distributed sensor nodes that work collaboratively to perform a global task and communicate the gathered data through wireless links [57–60]. However, the measurement points are representative of a very specific environment, basically the section of street on which the

nodes are located, unlike other environmental agents that have a more homogeneous distribution.

Thus, to improve the temporal and spatial coverage of samples, participatory sensing has recently emerged as another option to perform noise mapping. Its main characteristic is that it lets to the citizens the sampling process [61], which is performed mainly through their mobile phones. It has been shown that, when measurements are performed following specific requirements such as calibrated handsets, spatio-temporal density, proper measurement protocols and trained citizens, participatory sensing could be another approach to address the Noise Directive guidelines, since the noise maps can be produced with similar accuracy to the standard ones [61–63]. Nevertheless, participatory sensing has many drawbacks that are already under study. One of them is the data trustworthiness, that, as the sampling is left entirely in the hands of the citizen, the data integrity and representativeness is not fully assured [64].

Mobile sampling is another approach that has not been widely studied, which would increase the temporal and spatial resolution as well, but in a more controlled environment compared to participatory sensing, thus, the data trustworthiness would be improved. The term mobile refers to the way that the measurement is taken, i.e., the noise sensor is mounted on a vehicle and it is able to change its position while acquiring noise information. Nevertheless some drawbacks should be addressed for the case of mounting the measuring device on any vehicle such as the noise contribution of the vehicle itself, the air flow or the position of the microphone [60, 65, 66]. Furthermore, to deal with the temporal and spatial sparseness of the collected measurements, task related to the mobile noise data processing should be accounted to ensure the representativeness of the computed noise levels [30, 66].

1.2 Justification

Due to the need to generate policies aimed to prevent and control problems related to noise emissions, it is necessary to have tools and instruments that allow the generation of criteria to support the decision-making of action plans to control noise emissions. Nevertheless, nowadays acoustic mapping techniques demand a

large amount of resources and do not have a known degree of precision, which makes them difficult to expand.

It is clear that traditional methods of noise monitoring, such as an expert moving from place to place performing static measurements using a small number of expensive sound level meters, are not adequate to quantify the problem of noise pollution, which is ubiquitous and variable in time by nature. A high number of new strategies for the production of noise maps are emerging, such as the use of mobile devices (smartphones) to obtain georeferenced noise data, which brings many benefits such as cost, citizen participation and constant updating of data. However there are still some problems to address such as the representativeness of samples or the data processing to create a noise map.

Since the on-site measurements are required for noise mapping [22–25], a sampling strategy that allows to reduce the measurement time required to estimate long-time periods, which also allows to know the estimation error, and that increases the spatial resolution without having a negative impact on the required resources, should be developed.

One possibility of reducing costs while increasing the amount of information obtained is through the use of a low-cost mobile monitoring system, which would capture both, the noise levels and the position of the vehicle, as it moves through predefined routes across the city with enough precision to be representative of the place under assessment.

Mobile monitoring is a technique that could bring a high reduction of costs and resources, since an acoustic map could be created from the circulation of a group of vehicles equipped with noise measurement devices, but not necessarily dedicated ones, as well as a reduction in the uncertainty of the results since a greater amount of information would be available in both spatial and temporal aspects.

1.3 Objective

This research aims to settle the basis for a methodology to perform the acquisition and processing of noise data measured in a moving vehicle, required for the realization of acoustic maps for traffic noise in a more efficient and accurate way compared to traditional sampling methods.

1.4 Outline of the thesis

The content of the present thesis is divided in seven chapters. Except Chapters 1 and 7, Introduction and Conclusions and further work, respectively, each chapter has its own state of the art within the introduction. The content of each chapter is as follows:

Chapter 1 presents a general introduction of the research, the justification, objective and outline of the thesis.

Chapter 2 proposes a sampling strategy that, based on a weekdays stratification which separates working-days and weekends, shows that performing measurements of L_{Aeq} on working days and estimating the noise levels of weekends, increases the accuracy of long-term noise level estimation, which led to a reduction in the number of required sampled days compared to taking samples randomly, and allows to establish the estimation error according to the number of sampled days.

Chapter 3 complements the proposed sampling technique in previous chapter to enhance the results for the night period. The analysis aims to find the influence of the land use in the weekdays stratification to improve the accuracy of the long-term noise level estimation. Depending on the land use of the place under assessment, the weekdays temporal and spatial stratification are affected by the intensity of the surrounding leisure activities. It is proposed to adapt the spatio-temporal sampling technique to the new stratification to reduce the required sampling days compared to random sampling.

Chapter 4 introduces mobile sampling through a modeling framework that allows checking the statistical requirements for building noise maps based on mobile measurements. A reference noise map is created based on a micro-simulation traffic modeling coupled with acoustic modeling. Then, mobile targets performing measurements evolve within the simulation, aiming to estimate the reference noise map indicators. The difference between the reference noise map and the one generated by the moving receivers, characterized by the Root Mean Square Error (RMSE), is computed for different aggregation radius of mobile receivers, and as a function of the number of passes-by and to the distance to its nearest cross street.

Chapter 5 shows the development of a low-cost noise monitoring device. It is intended to take georeferenced mobile measurements at each 1/3 octave band

(63 Hz - 10 kHz) with an equivalent accuracy as a Class 2 sound level meter. The design, implementation, calibration and accuracy tests of the equipment are presented. Laboratory and field tests are performed together with a Class 1 sound level meter to test the accuracy of the device. Additionally, a set of preliminary mobile measurements are performed with the noise sensor mounted on a bicycle.

Chapter 6 validates noise mapping based on mobile measurements by means of a comparison between the noise levels acquired on-site with mobile and static receivers, where the noise levels at the static receivers are also calculated through dynamic noise modeling. To perform the mobile noise measurements, the noise sensor is again mounted on a bicyle and one hour of measurements with the mobile receiver simultaneously to 6 static measurement points were taken around a main avenue. The same scenario was recreated based on micro-simulation of traffic complemented with acoustic modeling. For the mobile receiver, L_{Aeq} was computed aggregating samples within a radius from 1 m to 100 m around the measurement points. Then, the Root Mean Square Error (RMSE) between the aggregated L_{Aeq} of the mobile receivers and the one hour L_{Aeq} of the static receivers was computed.

Finally, Chapter 7 presents the general conclusions of the study as well as the possible research lines that could be followed in the future.

Chapter 2

Annual traffic noise levels estimation based on temporal stratification

2.1 Introduction

Noise pollution is one of the main environmental issues in cities as it leads to health problems for inhabitants. The exposure to high noise levels can affect sleep, lead to cardiovascular diseases, cause cognitive problems and even cause property prices to fall [5–7, 67, 68]. It is therefore essential to accurately assess the noise levels to which the population is exposed in order to draw up and evaluate the effect of environmental noise management strategies [69]. The main basic tool for this purpose are noise maps. According to European Directive 2002/49/EC [11], for strategic noise mapping, the minimum time recommended for noise assessment is one year and should be done (at least) for the indicators L_{DEN} and L_{night}. Such maps are available for many agglomerations in Europe but in most cases the information is incomplete due to the lack of data [70]. Models and standards are also applied inconsistently [71] and the accuracy of the given results is unknown.

Although numerical noise models are the preferred tool for noise mapping, [20, 21], undertaking noise measurements is an essential task for: calibrating noise map modelling tools [22, 23], evaluating the effect of local noise reduction strategies such as green zones [72–74], obtaining results in complex environments where the traffic is not the main noise source [24] or traffic data is not available [23], and obtaining more accurate results [25]. The use of experimental noise measurements is a highly demanding task that is usually simplified using sampling strategies that, as a drawback, could lead to significant differences between the estimated and the actual annual values.

A good approach to reduce variability is to take into account the spatial and temporal correlation [33, 75]. In terms of the temporal aspect of noise assessment, many studies have been carried out to estimate the day equivalent value, for which the actual noise level is approximated by one or a few short time measurements, for a duration that is much shorter than the full-day period, usually between minutes to a few hours [17, 49–51]. An example of street categorization method shows that it is possible to estimate the day-time noise level by taking short time measurements which, depending on the category, could be improved by restricting the measurements to certain periods of the day [17]. Regarding the minimum time needed for a sample to be representative of a specific place, it has been found that measurements between 10 and 20 minutes are enough to represent the day value [17, 53]. Generally speaking, the criteria used to define the quality of the results is

the time taken for the sound pressure to stabilize, e.g., that its fluctuation range be within a certain error interval, which is known as stabilization time [54].

In this way, the year equivalent value can be estimated with a certain level of precision using noise levels from a number of days corresponding to a time period much shorter than a whole year. For annual L_{DEN} estimation, researchers have shown that sampling random days during the year gives better precision and representativeness of year equivalent levels than other techniques such as sampling consecutive days, only workdays or only weekends, or random full weeks [52]. Moreover, several authors use random sampling as a basis for comparison of optimizations or improvements proposed in sampling techniques for long-term level estimation [8, 26, 34, 55].

The main objective of this study is to determine a sampling strategy which minimizes the estimation error and, consequently, allows for the estimation of the annual value with a reduced temporal sampling. A procedure involving temporal stratification could be used to reduce variability. It is possible to identify days within a week with lower variability that can be used to estimate unsampled days and lead to a better annual estimation. This study computes the average difference between weekend and workday equivalent noise levels, $L^{Wd} - L^{We}$, and uses it to estimate the weekend levels from the measurement of randomly selected workdays.

2.2 Data

Barcelona is the capital of Catalonia, which is one of the 17 autonomous communities of Spain. It is an important hub for services and tourism, with a land area of around 102.2 km^2 and a population of about 1.6 million people according to the municipal register of inhabitants. It is the centre of a conurbation of about 3 million inhabitants. In summer, the climate is humid and hot, with temperature ranging between 23 and 30, while in winter it ranges between 9 and 12. Average annual rainfall is approximately 600 mm, with autumn being the most rainy season of the year.

A total of 14 Type 1 CESVA and 01dB sound level meters, equipped with an outdoor protection kit, were placed in 14 different streets in the city of Barcelona, at an equivalent height of around one storey (approximately 4m above the ground

according to the European Noise Directive). Measurements of L_{Aeq} were continuously taken between 2010 and 2015. The measurement equipment was calibrated every year to ensure proper operation and accurate measurements according to regulations. Time integration for the noise level was originally set at between 1 second and 10 minutes for different sound meters. In the end, this study only used the data of one full year for each street. The chosen year for each street was the one with the fewest missing measurements.

Streets were categorized according to three different categories in which urban traffic is considered to be the main source of noise [38, 76]:

- Category 1: Urban ring roads or access roads. Roads that surround the city or that allow access to the city.
- Category 2: Main streets. Roads within the city which mainly distribute traffic throughout the urban area.
- Category 3: Ordinary streets. Mainly destination streets which are commonly used for residential, commercial or leisure purposes.

The locations of the measurements points are shown in Figure 6.1. According to previous experience [17, 36, 76], higher traffic flow means more stable values and the categorization is established according to traffic flow order. The number of streets was also selected according to this previous knowledge in order to get representative results. For category 1, less points were selected and measurement points were located in places where it is known to exist constant traffic flow. For category 2 and 3, the number of points was increased and they were located in streets with different traffic conditions and different use of the territory in order to verify that the proposed strategy was applicable in a more general way, i.e. not to be limited to certain types of streets or cities. Categories and supplementary information about each measurement point can be found in Table 2.1.

2.3 Methodology

The values in dBA of L_{DEN} and L_{day} (from 7 a.m. to 7 p.m.), $L_{evening}$ (from 7 p.m. to 11 p.m.) and L_{night} (from 11 p.m. to 7 a.m.) for every single day and

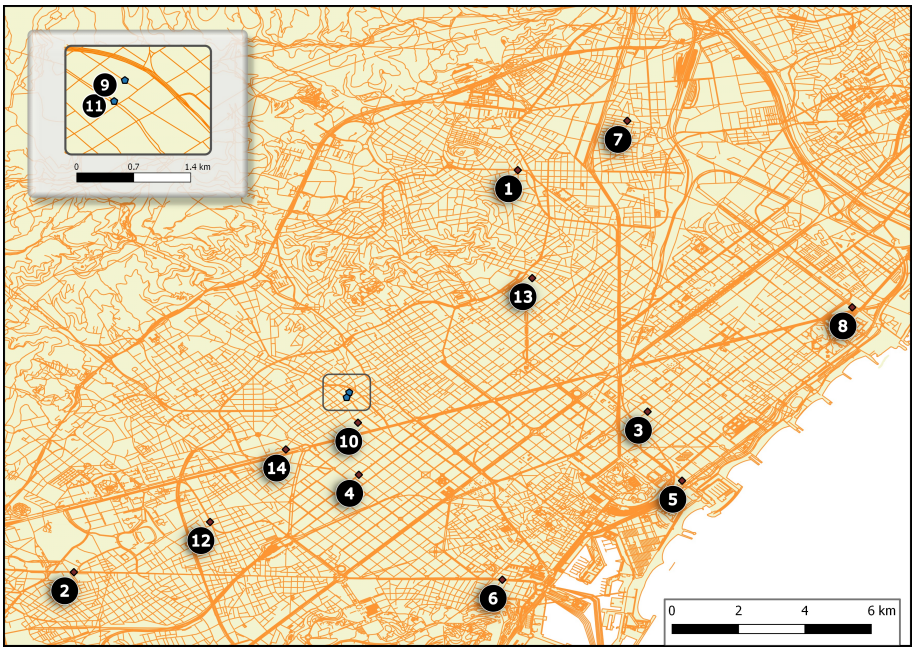

FIG. 2.1: Location of the 14 measurement points.

Point No.	Category	Street	Lanes	Parking	Year
1	2	Passeig de Fabra i Puig	3	1	2012
2	1	Carretera de Collblanc	4	-	2014
3	3	Carrer dels Almogàvers	4	1	2014
4	3	Carrer de Villarroel	4	2	2011
5	2	Carrer de la Marina	6	-	2011
6	2	Av. del Paral·lel	9	2	2012
7	3	Carrer de Servet	2	-	2011
8	2	Rambla de Prim	8	4	2013
9	3	Carrer de Lincoln	2	1	2014
10	3	Carrer de Tuset	3	2	2014
11	2	Carrer de Balmes	4	-	2010
12	3	Carrer de Joan Güell	3	1	2010
13	3	Carrer de Sant Quintí	4	2	2011
14	1	Carrer de Beethoven (Side of Diagonal)	3	1	2013

TABLE 2.1: Supplementary information regarding the measurement points. Data regarding the total number of lanes and how many of them are specifically designated for parking is shown. It also shows the measurement year chosen from the total sampled years (2010-2015).

the actual annual level in each measurement point were calculated and stored in a local database. As described in [11], L_{DEN} is calculated using the following equation:

$$L_{DEN} = 10log\left\{\frac{1}{24} \times (12 \times 10^{\frac{L_{day}}{10}} + 4 \times 10^{\frac{L_{evening}+5}{10}} + 8 \times 10^{\frac{L_{night}+10}{10}})\right\} \quad (2.1)$$

For each street, noise levels were analysed in order to find any anomaly that could

alter the actual year value [77]. For all the data presented in this paper, a total of 14 days had L_{DEN} values larger than $< L_{DEN} > + 4\sigma$. These 14 values were considered abnormal and eliminated. Furthermore, 70% of these eliminated days had values of L_{DEN} larger than $< L_{DEN} > + 6\sigma$. 9 of the eliminated days were especially noisy local celebrations (Sant Joan, la Mercè and a Champions League celebration). The reason for the high levels of the other 5 days eliminated could not be found.

2.3.1 Statistical data calculation

This paper presents a methodology for long term L_{DEN} estimation based on temporal stratification. The methodology proposed is compared to the random days sampling strategy [27, 52].

Then, for each measurement point i, 1,000 samples of N measurement days are taken according to each sampling strategy. The difference in dBA between the equivalent level of each sample and the actual value is computed as:

$$\Delta L_j^{i,N} = L_p^{i,N}(j) - < L_p^i > \tag{2.2}$$

where $< L_p^i >$ is the actual annual value computed using all the days of the year for measurement point i and period p. Where p is *day*, *evening*, *night* or DEN. $L_p^{i,N}(j)$ is the level for period p and measurement point i computed from the sample of N days. j is the current sample and runs from 1 to 1,000. The number of sampling days N runs from 1 to 28.

The parameter used to perform the comparison between the proposed strategy and the random sampling strategy is the number of days that have to be measured in order to have 90% of the 1,000 samples inside the interval $< L_p^i > \pm 1dB$. In specific cases where 28 days is not enough to reach the desired percentage, N was increased until an appropriate number of days was reached.

Therefore, to compute the percentage of samples for N days, the first step is to obtain the noise data which is stored in a local database. This connection provides a whole year of data for point i and for the required period p. $< L_p^i >$ is then computed to be used in Equation 2.2. After this, $L_p^{i,N}(j)$ is computed according to each sampling strategy and $\Delta L_j^{i,N}$ is calculated for $1 \leq j \leq 1,000$ and stored

in the array

$$\overrightarrow{L_p^{i,N}} = \left\{ \Delta L_1^{i,N}, \Delta L_2^{i,N}, ..., \Delta L_{1000}^{i,N} \right\} \tag{2.3}$$

Then, within the array, the percentage of samples inside $< L_p^i > \pm 1dB$ is obtained. Afterwards, the next measurement point data is selected from the data base and the whole process is repeated until all measurement points (i=14) and p periods are evaluated.

2.3.2 Temporal stratification

Apart from the physical characteristics of the street, noise depends on the types of noise sources, which could be due to traffic or other activities [36]. As this paper is focused only on traffic noise, the temporal noise evolution in each street depends mainly on the type and number of vehicles circulating through them, since physical street characteristics such as type of paving, obstacles and geometry usually never change within a street. For the purpose of this study, a temporal categorization is proposed, differentiating working days from weekends. The temporal sampling for annual value estimation is limited to only workdays and the weekend level is calculated based on the workday/weekend difference. The following equation is proposed to estimate the weekend equivalent level in dBA as:

$$L_p^{We} = L_p^{Wd} + < L_p^{We-d} > \tag{2.4}$$

where $< L_p^{We-d} >$ should be an approximation of the difference between workday and weekend noise levels of the place under study for period p and L_p^{Wd} is the workdays equivalent value for the same period computed according to:

$$L_p^{Wd} = 10log \left\{ \frac{1}{N} \sum_{k=1}^{N} 10^{\frac{L_p(k)}{10}} \right\} \tag{2.5}$$

where N is the total number of sampled days and $L_p(k)$ is the day level for period p in dBA.

Within a year [5/7] of the days are weekdays, L^{Wd}, and [2/7] are weekends, L^{We}. Based on Equation 2.1 and changing parameters to adapt it to the aforementioned two temporal strata, the following equation is proposed to estimate the annual level

in dBA for period p based on N working days chosen at random:

$$L_p^{i,N}(j) = 10log\left\{\frac{1}{7}(5 \times 10^{\frac{L_p^{Wd}}{10}} + 2 \times 10^{\frac{L_p^{We}}{10}})\right\} \tag{2.6}$$

Then, estimating L_p^{We} from measurements taken during weekdays with Equation 2.4, the proposed temporal stratification strategy computes $L_p^{i,N}(j)$ as:

$$L_p^{i,N}(j) = 10log\left\{\frac{1}{7}(5 \times 10^{\frac{L_p^{Wd}}{10}} + 2 \times 10^{\frac{L_p^{Wd}+<L_p^{We-d}>}{10}})\right\} \tag{2.7}$$

For the case of the random sampling strategy, the following formulation is applied to calculate $L_p^{i,N}(j)$:

$$L_p^{i,N}(j) = 10log\left\{\frac{1}{N}\sum_{j=1}^{N} 10^{\frac{L_p(j)}{10}}\right\} \tag{2.8}$$

2.4 Results

As stated in [55, 78, 79], differences between workdays and weekends can be found when studying the variability of days of the week. In the city under study, the working days are from Monday to Friday and the weekend days correspond to Saturday and Sunday.

Figure 2.2 shows the differences between the equivalent level computed only for workdays L_p^{Wd} and only for weekends L_p^{We}, with the actual level $< L_p^i >$ as well as the levels L_p^{Wd} with L_p^{We} for all periods p. As one can see, $L_p^{Wd} > L_p^{We}$ except for some specific cases in the night period (Figure 2.2c). It can also be seen that workday levels are higher than the annual value $< L_p^i >$ with the day period being the one with the highest workday/weekend differences $< L_p^{We-d} >$. This seems to indicate stratification within the week that would allow $< L_p^{We-d} >$ to be calculated for the estimation of weekend levels.

Figure 2.3 shows L_p^{Wd} and L_p^{We} levels for all periods and their 68% confidence interval for each of the measurement points with the aim of observing the overlapping of the confidence intervals. Workdays always show less variation than weekend days. Furthermore, for the day period, it is seen that the overlapping between workday and weekend confidence intervals is close or equal to zero in most cases.

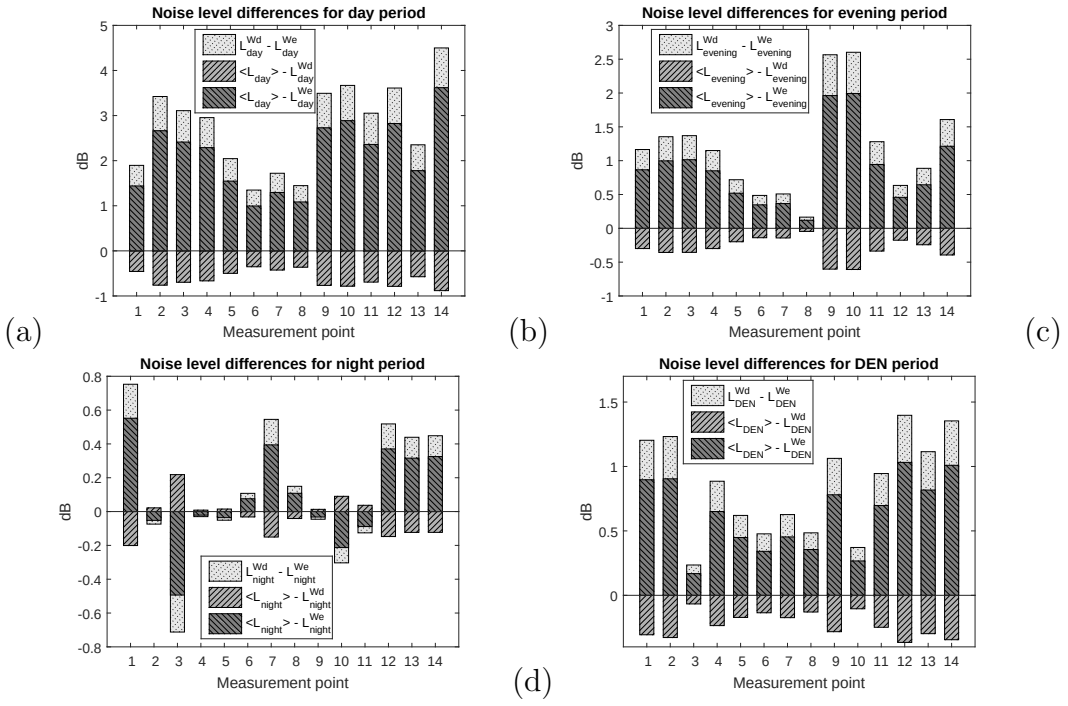

FIG. 2.2: Difference between $< L_p >$, L_p^{Wd} and L_p^{We} for all the periods and measurement points.

However, this trend is not clearly seen for the other periods. In order to estimate L_p^{We} from L_p^{Wd}, both quantities must come from populations with different means. Since according to a Chi-square goodness-of-fit test not all the distributions can be considered as normal, a non-parametric test should be used. The Wilcoxon rank-sum test was applied to both L_p^{Wd} and L_p^{We} to test the null hypothesis that both of them come from distributions with equal means. The result of this test is shown in Table 2.2. It can be seen that for L_{day}, workdays and weekends belong to different distributions; for $L_{evening}$ and L_{DEN}, mean independence is not achieved in only one of the measurement points; and for L_{night}, only four of the measurement points present distributions mean independence.

Thus, given the independence between L_p^{Wd} and L_p^{We} and the smaller variability of L_p^{Wd}, it is possible to establish a temporal stratification that separates workdays and weekends. However, this would not reduce the size of the sample unless the weekend values are estimated from workday levels [36]. Estimating the weekend level by setting $< L_p^{We-d} >$ as close as possible to the actual difference for each point would bring a very accurate approximation of the actual weekend level; this should be better in cases where $< L_p^{We-d} >$ is higher, since L_p^{We} estimation takes greater importance when its value is much smaller than L_p^{Wd} as it is related to

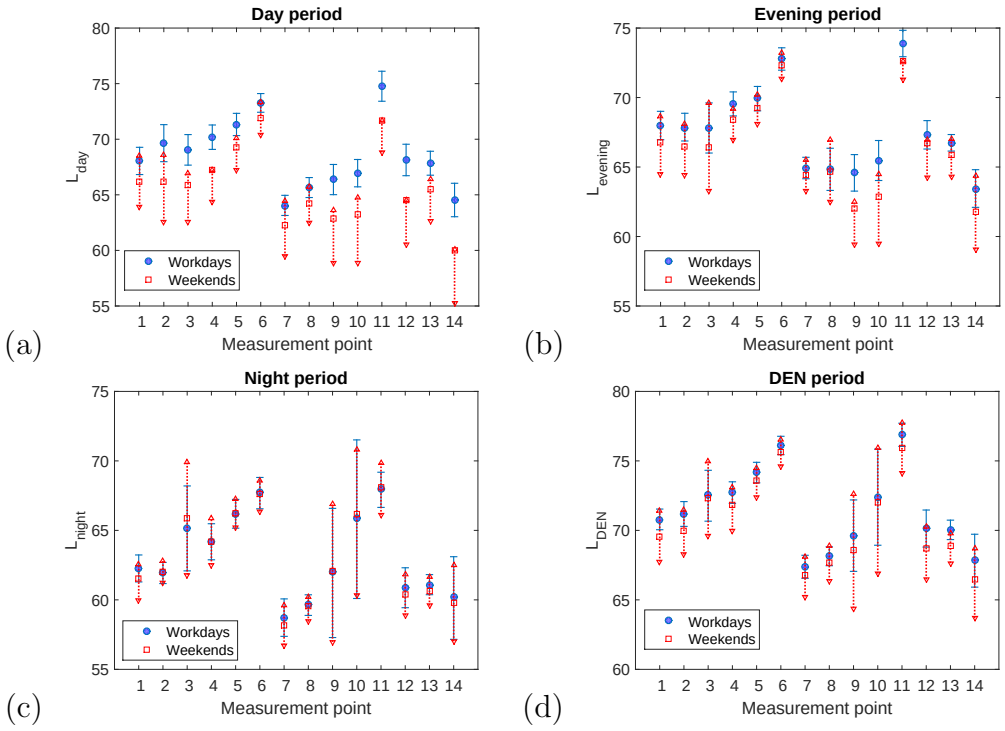

FIG. 2.3: L_p^{Wd} and L_p^{We} mean and 68% confidence interval.

Point	L_{day}	L_{eve}	L_{night}	L_{den}
1	$9E^{-18}$	$3E^{-13}$	$4E^{-11}$	$2E^{-17}$
2	$8E^{-35}$	$1E^{-17}$	0.745	$2E^{-21}$
3	$7E^{-41}$	$8E^{-13}$	0.075	0.132
4	$4E^{-39}$	$2E^{-21}$	0.141	$2E^{-10}$
5	$3E^{-35}$	$1E^{-10}$	0.864	$2E^{-10}$
6	$1E^{-10}$	$8E^{-04}$	0.977	$3E^{-03}$
7	$4E^{-25}$	$8E^{-07}$	$7E^{-03}$	$9E^{-09}$
8	$4E^{-21}$	0.079	$1E^{-03}$	$5E^{-10}$
9	$3E^{-37}$	$3E^{-31}$	0.965	$2E^{-05}$
10	$2E^{-35}$	$8E^{-25}$	0.562	$4E^{-02}$
11	$1E^{-11}$	$2E^{-06}$	0.982	$2E^{-04}$
12	$1E^{-17}$	$1E^{-07}$	0.076	$4E^{-08}$
13	$6E^{-25}$	$6E^{-16}$	$5E^{-06}$	$1E^{-20}$
14	$5E^{-20}$	$6E^{-09}$	0.559	$2E^{-04}$

TABLE 2.2: Test for distribution mean independence. Grey box indicates rejection that the data sets come from the same distribution (p=5%). The p value is shown inside each cell.

a higher distribution mean separation. Nevertheless, the noise level difference between workdays and weekends $< L_p^{We-d} >$ should be known for each of the sampling points, which is not always possible. The calculation of $< L_p^{We-d} >$ requires the accurate measurement of L_p^{We} and L_p^{Wd} from a large sample of days. Therefore, if one had the actual values of L_p^{We} and L_p^{Wd} it would not be necessary to estimate $< L_p^{We-d} >$.

2.4.1 Annual L_p estimation by using $< L_p^{We-d} >$ as computed average

Since previous noise data for each sampling point is not always available for noise assessment of a city, the overall average for all measurement points and the average by category is used as the $< L_p^{We-d} >$ parameter.

Then, $< L_p^{We-d} >$ was first calculated for each measurement point using the following formula obtained from Equation 2.4:

$$< L_p^{We-d} >= L_p^{We} - L_p^{Wd} \tag{2.9}$$

Table 2.3 shows the values of $< L_p^{We-d} >$ for each p period computed individually for street categories and for all the streets.

The required number of days to have 90% of $\Delta L_p^{i,N}$ within ±1dB are shown in Table 2.4 for both strategies and for all periods.

2.5 Discussion

Even though there is a reduction in the required number of days in most of the cases presented in Table 2.4, there are some specific measurement points where the random sampling strategy is not improved or equalled.

For L_{day}, it is observed that, in almost all of the measurement points there is a reduction in the required number of days using Equation 2.7 compared to using the random sampling strategy. The total reduction in days sampled by applying the temporal stratification strategy compared to random sampling strategy is more

		$< L_{day}^{We-d} >$		$< L_{evening}^{We-d} >$		$< L_{night}^{We-d} >$		$< L_{DEN}^{We-d} >$	
Cat	*Point*	*C*	*G*	*C*	*G*	*C*	*G*	*C*	*G*
1	**2**	-4.0		-1.5		-0.3		-1.3	
	14								
2	**1**	-2.0		-0.8		-0.2		-0.7	
	5								
	6								
	8								
	11		-2.8		-1.2		-0.3		-0.9
3	**3**	-3.0		-1.4		-0.4		-0.8	
	4								
	7								
	9								
	10								
	12								
	13								

TABLE 2.3: $< L_p^{We-d} >$ computed for each category (C) and overall for all the streets (G) for all periods.

		L_{day}			$L_{evening}$			L_{night}			L_{DEN}		
Point	**Cat**	D_R	D_G	D_C	D_R	D_G	D_C	D_R	D_G	D_C	D_R	D_G	D_C
1	**2**	7	6	5	7	6	6	10	8	9	4	3	3
2	**1**	10	5	5	5	4	4	2	2	2	4	3	3
3	**3**	9	6	6	19	16	15	23	***30***	***30***	12	12	11
4	**3**	6	3	3	4	3	3	6	5	5	4	3	3
5	**2**	4	3	3	3	3	3	4	4	4	3	3	2
6	**2**	3	3	2	2	***3***	2	5	4	4	3	2	2
7	**3**	8	5	5	4	4	4	7	7	***8***	5	4	4
8	**2**	6	5	4	13	***18***	***14***	5	4	4	4	3	3
9	**3**	12	7	7	9	6	7	48	***51***	48	25	21	23
10	**3**	16	10	11	11	9	10	39	***42***	***44***	27	***28***	24
11	**2**	7	3	4	4	3	3	7	6	5	4	3	2
12	**3**	11	6	6	17	10	10	10	9	8	8	6	7
13	**3**	7	4	5	4	3	3	3	2	2	3	2	2
14	**1**	13	7	6	10	6	6	23	***24***	22	13	11	12
Total		**119**	**73**	**72**	**112**	**94**	**90**	**192**	**198**	**195**	**119**	**104**	**101**

TABLE 2.4: Number of days required to make the 90% confidence interval of $< L_p^i > \pm 1dB$ for the random sampling strategy (D_R) and temporal stratification strategy, computing $< L_p^{We-d} >$ as the measurement point average (D_G) and category average (D_C) for all periods. Measurement points are shown in bold italics where there is an increase in the required number of days with respect to the random sampling strategy.

than 38% using $< L_{day}^{We-d} >$ from the overall average and more than 39% using $< L_{day}^{We-d} >$ from the category average. For measurement point 6, as shown in Figures 2.2 and 2.3, the combination of the low variability, which requires fewer days to reach the desired confidence interval, and the fact that $< L_{day}^{We-d} >$ by category is closer to the actual value, leads to a reduction in the required days when using the value per category and not with the overall average.

For $L_{evening}$, in all but two streets, the random sampling estimation is equalled or improved with an average reduction in the required days by more than 16% and 19% by computing $< L_{evening}^{We-d} >$ as the overall or category average, respectively. The low variability of measurement point 6 is reflected in the low number of required measured days. Furthermore, the fact that $< L_{evening}^{We-d} >$ as the overall average is more than double the value compared to the individual one, makes the overall average less suitable for this measurement point than the category one. For measurement point 8, there are several reasons that could lead to the increase in the number of required days. As seen in Table 2.2, this measurement point is the only one for this period that does not meet the distribution mean independence which, combined with its high variability, causes the estimation of L_p^{We} using the temporal stratification strategy to be inaccurate.

For the *night* period, in all but four measurement points, the random sampling estimation is equalled or improved. As seen in the total number of days for this period, there is no overall reduction; however, if we look at the measurement points individually, the increase in the number of days is concentrated in only four of the whole set of measurement points: 3, 9, 10 and 14. For the particular case of measurement point 3, 28 days are not enough using both, overall or category average as $< L_{night}^{We-d} >$. This lack of improvement may be associated with the combination of high variability, the fact that L_{night}^{Wd} and L_{night}^{We} come from the same distribution and that the condition $L_{night}^{Wd} > L_{night}^{We}$ is not fulfilled. This is also observed in points 9, 10 and 14. It can be seen that, for the *night* period, some specific measurement points do not give as good results as for other periods. In order to establish the reason for this, a revision of the surrounding area was performed.

For measurement point 14, which is one of the main ring roads of Barcelona and also a commercial hub of the city, it was found that the possible reason for L_{night} to be higher at weekends could be due to its extensive link with commercial areas,

as the road is full of large shopping centres, high-fashion clothing and jewellery stores, and some night clubs which could increase traffic flow on non-working days.

For measurement points 3 and 9, it was observed that their location is in the same street as well-known nightclubs. This means that their proximity to the clubs could increase the traffic flow during early and late *night* periods, as well as noise due to human interactions.

Measurement point 7 is located in front of a park on a narrow street with vehicle circulation mainly from the people living in the neighbourhood. Something to emphasize for this point is that, even though the test for distribution mean independence indicated means separation and that it meets the condition $L_{night}^{Wd} > L_{night}^{We}$, a reduction in the number of required days was not achieved. The possible reason for obtaining this result could be that $< L_{night}^{We-d} > \approx 0.6\ dB$, which for the overall and category average is even lower ($< 0.5\ dB$). This small value is a negligible difference and makes the temporal stratification strategy unsuitable for this point.

Measurement point 10 is located in a narrow street in which there is a high concentration of commercial areas and restaurants. At approximately 150 meters from the measurement point there are two small-sized night clubs which could greatly affect the traffic flow, as there is only one lane for circulation.

It is observed that almost all of the aforementioned measurement points are affected by leisure activity. This activity implies that the variability of the L_p^{We} levels is very high (as seen in Figure 2.3) which, combined with the fact that L_p^{We} and L_p^{Wd} come from the same distributions, means that the estimation based on L^{Wd} is not a suitable strategy for these measurement points.

Finally, for L_{DEN}, a similar result as the *day* period is obtained. It is seen that, by using $< L_{DEN}^{We-d} >$ as the category average, the required number of days is reduced for every measurement point. When using the overall average there is a reduction in the required days in all but one measurement point.

If the proposed strategy were to be used in different cities, the parameters to be adapted to each place under assessment are $< L_p^{We-d} >$ and the number of working days and weekend days, which for Barcelona are 5 (from Monday to Friday) and 2 (Saturday and Sunday), respectively. The selection of an accurate $< L_p^{We-d} >$ value is essential to obtain significant improvements. In terms of noise data, if there is enough previous information available, $< L_p^{We-d} >$ could be computed as

the category average and, in cases where there is little information available, an overall average could be used. As shown in Table 2.4, for the temporal stratification strategy, results are better when using $< L_p^{We-d} >$ for each street category, as the required number of days is reduced even further compared to $< L_p^{We-d} >$ obtained as an overall average for all streets. As shown in this research, a combination of the proposed methodology together with the street categorization method is a very good option; this would help to save resources and increase the estimation accuracy as it would only require as many $< L_p^{We-d} >$ values as street categories under study. As noise pollution is becoming a priority issue in cities, the number of fixed networks is growing [80–85]. This means that the $< L_p^{We-d} >$ could easily be obtained for a larger number of measurement points, which would increase the accuracy of the temporal stratification strategy.

2.6 Conclusions

It has been shown that, in the city of Barcelona, there is a temporal stratification for days of the week as their values follow different distributions, with the workday noise level being higher and the variability being lower than for weekends. Based on this temporal stratification, a new sampling strategy was introduced. It was shown that measuring only on workdays and estimating weekend noise level from the $< L_p^{We-d} >$ value, brings a significant improvement in accuracy compared to the random sampling strategy for the estimation of the annual $< L_p^i >$. For the case of the annual $< L_{DEN}^i >$ estimation, using $< L_{DEN}^{We-d} >$ by category led to an improvement for each of the sampling points studied, for which the average reduction is 1.29 days per measurement point compared to the random sampling strategy.

The temporal stratification strategy works well for streets with normal traffic, but in those with significant leisure activity, a high variability is detected for night period values, which leads to poorer results than the random sampling strategy, for the aforementioned reasons. The proposed method assumes that $< L_p^{Wd} > \neq < L_p^{We} >$; if this is not true, as it is in most of the cases for the night period, the temporal stratification strategy does not bring a significant improvement as $< L_p^{We-d} > \approx 0$. This means that, at this time, it is advisable to apply the temporal stratification strategy to streets where traffic is due to regular people

displacement, and for the streets with a strong presence of leisure activities, further research is required as the performance is not so good because of the local effect of these activities on the surrounding traffic. All this suggests that it is necessary to carry out double categorization: one by type of street and the other by use of the area.

For the entity in charge of the noise assessment of a city, using the categorization method together with the proposed strategy, makes the sampling process less demanding as the measurements only have to be done on working days and in a reduced number of sampling points. Furthermore, the improvements in accuracy lead to a reduction in the number of sampling days required to equal or improve the population coverage with respect to using the random sampling strategy. The proposed methodology, allows the authorities in charge of environmental management to get traffic noise data faster and saving resources without compromising the precision and representativeness of the noise levels.

Chapter 3

Temporal and spatial stratification for the estimation of nocturnal long-term noise levels

3.1 Introduction

Exposure to noise pollution can generate both auditory and non-auditory negative health effects as it is related to annoyance, stress and cognitive problems [86]. Some recent researches state that, according to epidemiological studies, noise could also bring different cardiovascular diseases as well as psychological problems [5, 6, 68, 87]. Specifically, night noise exposure propitiates a reduction in the quality of sleep [88, 89] and hypertension [90]. However, in order to properly carry on epidemiological studies of noise exposure for long periods, long-term noise information is required which is not usually available [69, 70, 90].

Several studies have been conducted in order to improve the estimation of annual values by using temporal sampling strategies which tend to reduce the required measurement time when the noise source is traffic. Random sampling is taken in most cases as a benchmark strategy [8, 26, 27, 34, 52, 55]. Some procedures related to extrapolate short time measurements to long-term values are shown in [17, 49–53] and some works suggest that a spatial stratification based on street traffic [34, 91] or the role of the streets within the city regarding traffic distrubution [17, 36, 38] led to a reduction of sampling points.

There are many other studies also indicating that land use can affect urban noise level, such as [10, 41, 43, 44], specially in case of leisure activities for the night period [24, 38, 45–48]. Concretely, a spatial stratification of streets based on traffic characteristics fails to improve the estimation of night levels [91] as it does for day and evening periods, probably due to the presence of leisure activities nearby the streets.

The research proposed in this chapter aims to find the influence of land use, and in particular leisure activity, for the nocturnal noise assessment in order to improve the long-term noise level estimation. The objective is to optimize the estimation of the annual value of L_{night} [11], through a temporal and spatial stratification that does not come from the street classification based only on traffic, but done by clustering procedures to determine the influence of leisure noise in the categorization.

3.2 Material and methods

3.2.1 Material under study

The present research was carried out in the city of Barcelona which is located in the north-east of Spain. Barcelona has 1.6 million of inhabitants within a land area of about 102.2 km^2. It is the administrative center of a region of more than 7 millions of inhabitants, a commercial center of about 3 million customers and an important tourism destination with more than 4 million people received during 2016 according to official information of the city hall [92].

Continuous noise measurements were performed between 2010 and 2015 in 19 sampling points, close to different recreational and leisure activities in the city of Barcelona, using Type 1 sound level meters (CESVA and 01dB brands). Their placement can be observed in Figure 3.1. The sound meters were calibrated every year to ensure their proper operation according to regulations. They were also equipped with outdoor protection kit and placed according to the European Noise Directive, approximately at 4 m above the ground, mostly on light poles. These points belong to places affected by some leisure or recreational activities in order to study the differences between the real land uses. The noise source of leisure is not the recreational activity itself but the concentration of traffic caused by these activities which may alter the temporal traffic pattern distribution. The measurement point is placed to be representative of the street segment between intersections, to guarantee that the whole nocturnal sound environment was assessed and all noise sources are considered (differences above 10 dB between sources would result in source omission). Table 3.1 extends the information about the sampling points.

All the considered streets have a mix of different activities and residential buildings, as a result, most of them are considered "residential" by the land use classification of the city (Figure 3.1). Moreover, the definition of leisure activity is rather complex as many activities can be tagged as leisure. The hypothesis is that leisure activities influence the night noise patterns, which could depend on the type of leisure activity. For this study, a classification of leisure activities is defined as:

- Commercial (Com): Mostly focused in shopping centers. Mainly daytime activities.

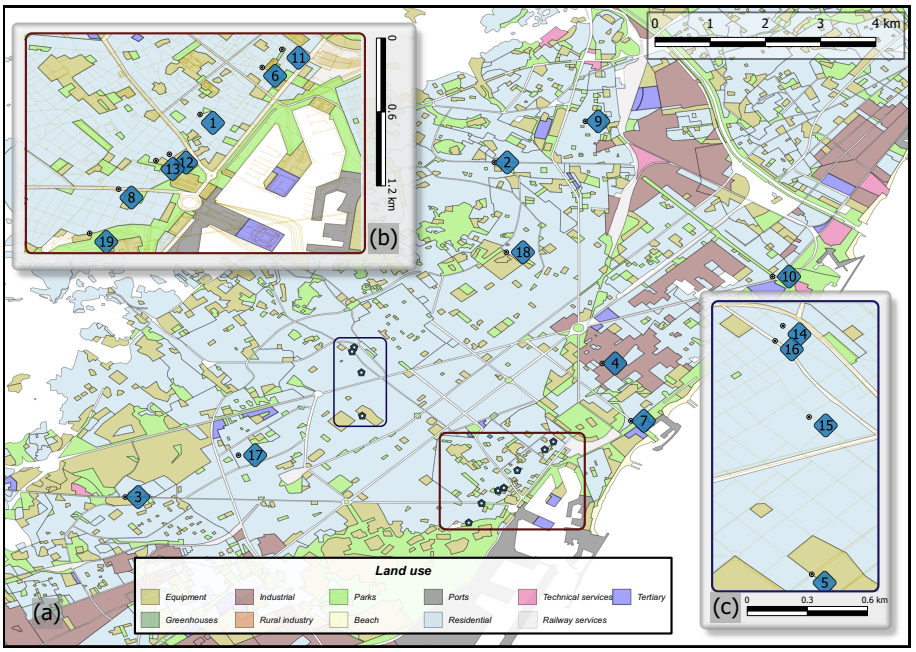

FIG. 3.1: Location of the 19 sound meters in the city of Barcelona and its corresponding land use [1]. Figure 3.1(b), corresponds to the downtown, which has high tourism and shopping/restoration activity. Figure 3.1(c), has mostly local recreational activity. Figure 3.1(a) has points distributed all over the city of Barcelona, also in zones with nighttime noise problems.

Point No.	**T.C.**	**Nearby act.**	**Address**	**T. lanes**	**P. lanes**	**Year**	**Land use**
1	4	Tou	Carrer dels Escudellers, 53	-	-	2012	Residential
2	2	Com	Passeig de Fabra i Puig, 274	3	1	2012	Residential
3	1		Carretera de Collblanc , 126	4	-	2014	Equipment
4	2		Carrer dels Almogàvers, 120	4	1	2014	Industrial
5	2	Fs	Carrer de Villarroel, 170	4	2	2011	Equipment
6	4	Tou, Com	Carrer de l'Argenteria, 69	-	-	2013	Residential
7	2	Tou	Carrer de la Marina, 33	6	-	2011	Residential
8	2		Av. del Paral·lel, 55	9	2	2012	Residential
9	3		Servet, 37	2	-	2011	Residential
10	2	Com, Fs	Rambla de Prim, 19	4	-	2013	Residential
11	4	Fs, Lei, Tou	Passeig del Born, 19	4	2	2014	Residential
12	4	Tou	Carrer de Montserrat, 4	-	-	2014	Residential
13	4	Tou	Carrer de l'Arc del Teatre, 5	1	-	2014	Residential
14	3	Lei, Com	Carrer de Lincoln, 8	2	1	2014	Residential
15	3	Fs, Lei	Carrer de Tuset, 17	3	2	2014	Residential
16	2	Com	Carrer de Balmes, 246	4	-	2010	Residential
17	3	Fs, Lei	Carrer de Joan Güell, 153	3	1	2010	Residential
18	3	Fs	Carrer de Sant Quintí, 112	4	2	2011	Equipment
19	3	Lei	Carrer de Beethoven, 2	3	1	2013	Residential

TABLE 3.1: Supplementary information of the measurement points. The address, traffic categorization (T.C.), nearby activities, total number and parking exclusive lanes are shown. The column year shows the selected measurement year from the whole set of measurement (2010-2015). The land use is also shown as obtained from [1].

- Food and services (Fs): Restaurants, pubs, with some retail shops nearby. Mainly day or early night activities.
- Leisure (Lei): Streets with taverns, discotheques, mostly focused in night-time leisure. Mainly night activities.
- Tourism (Tou): Tourism spots or places with high tourism activity. Mainly day and night activities.

The mentioned zone characteristics were selected based on the nearby activities that the place under assessment has (maximum around 3 blocks of radius).

The traffic categorization of streets (T.C.) is the same as used in previous studies, but adding pedestrian streets [36, 38, 76, 91]:

- Category 1 : Urban ring roads or access roads. Roads that surround the city or that allow access to the city.
- Category 2 : Main streets. Roads within the city which mainly distribute traffic throughout the urban area.
- Category 3 : Ordinary streets. Mainly destination streets.
- Category 4 : Pedestrian streets. Streets whose traffic is very limited or they are only pedestrian.

According to [11], the night period corresponds to the time between 23:00 hours of the current day until 7:00 hours of the next day. Then, from the original data, the daily equivalent L_{night} was computed [93] together with its corresponding measurement date/time and was stored in a local database for all the sampling points. Only one year of data from the total measurement period (2010-2015) of each sampling point was used for this research, the year with more measured days excluding the days removed after an analysis of days with abnormal noise levels that affected the annual average [91].

3.2.2 Procedure

In order to increase the long-term estimation accuracy of L_{night} and to shorten the temporal sampling, an estimation based on the temporal and spatial stratification

methodology proposed in [91] are followed. To face the uncertainties to establish the categories due to the different leisure activities included in this work, the categorization is performed through a statistical analysis of clusters according to following procedure:

1) A **temporal stratification** is performed to find how the weekdays are grouped within the week.

2) A **spatial classification** to group streets with similar weekly noise patterns is done.

3) A **long-term estimation** is performed by employing the found time-space stratas. Results are compared to random sampling.

3.2.2.1 Temporal stratification

The steps to follow are:

(a) Determine the optimal number of clusters for each of the sampling points, obtained through the *silhouette* method [94]. The input data is the L_{night} of all the sampled days within each street.

(b) A cluster analysis for an automatic classification of weekdays in each measurement points is performed. The selected clustering algorithm is *k-means* [95] and the input data is the same as for *silhouette* method (L_{night}).

(c) To proof that the found stratas are actually independent subsets, the Wilcoxon rank-sum test is used to reject the null hypothesis that the found stratas come from continuous distributions with equal means. This non-parametric test was selected because not all the data is normally distributed and due to the small number of samples. A statistical analysis is then performed to find the stratas with less variability, which would be the selected to perform the measurements.

3.2.2.2 Spatial classification

The procedure is:

(a) Similar to what was found in [40], a cluster analysis to group sampling points by the weekly noise pattern is performed using again the $k-means$ clustering algorithm. The input data, in order to classify streets by the variations of the noise levels during the week, is the night equivalent noise level for each day of the week (DOW), $< L_{i,DOW} >$. It is centered to the long-term equivalent level ($< L^i_{night} >$) to perform the classification by the noise pattern of the week, rather than the actual noise levels, and it is computed according to:

$$< L_{i,DOW} >= 10log \left\{ \frac{1}{M} \sum_{j=1}^{M} 10^{\frac{L^i_{night}(j)}{10}} \right\} - < L^i_{night} > \tag{3.1}$$

where i represents the sampling point and j runs from 1 to the M total days of each DOW within each sampled set. The cluster analysis is performed using the data of the whole set of streets.

(b) A Principal Component Analysis (PCA) is done to extend the information about how the noise level of each DOW influences the spatial classification. A PCA gives information about how each variable affects the clustering process and allows to observe the composition of each cluster itself. It also helps to reduce the input variables (usually correlated) into uncorrelated variables called principal components retaining most of the information. The input parameter is the same used for the cluster analysis (Equation 3.1).

3.2.2.3 Long-term estimation

For the long-term L_{night} estimation and the accuracy comparison to random sampling, the procedure is as follows:

(a) L_{night} estimation. To estimate the long-term reference period with fewer samples, it is proposed to take samples during the days of the strata with less variability (S_L), and estimate the noise level of the strata with the highest variability, based on an approximation of the noise level difference

between their equivalent noise levels [26]. Then, for the annual estimation of L_{night}, for k clusters of D_j weekdays, the following equation is proposed:

$$< L_{night} >= 10log \left\{ \frac{1}{7} \times \left[\sum_{j=1}^{k} \left(D_j \times 10^{\frac{L_j}{10}} \right) \right] \right\} \tag{3.2}$$

where D_j is the number of days of each strata and $D_1 + D_{(...)} + D_K$ must be equal to 7 and L_j is the night equivalent noise level of each strata computed by:

$$L_j = 10log \left\{ \frac{1}{N_j} \sum_{m=1}^{N_j} 10^{\frac{L_j}{10}} \right\} \tag{3.3}$$

where N_j is the number of sampled days, used only fot the stratas with lesser variability. For the strata with highest variability, L_j is estimated by:

$$L_j = L_{j,min} - < L_{j,min-j} > \tag{3.4}$$

where $L_{j,min}$ is the noise level of the strata with the lowest variability, and $< L_{j-j,min} >$ is the difference between the noise level of the strata with low and the one with highest variability.

(b) Statistical data computation. The data used to compare the accuracy of the long-term estimation is the N sampling days required to have 90% of the estimated values inside the interval $< L^i_{night} > \pm 1$ dB, where $< L^i_{night} >$ is the year average [93] for each i street. Then, for computing the percentage of samples inside $< L^i_{night} > \pm 1$ dB, 1000 samples are taken from the data stored in the database for each i and for $1 \leq N \leq 50$ sampling days. The long-term estimation is then computed using Equation 3.2 and its difference to the actual long-term level $< L^i_{night} >$ is calculated as [91]:

$$\overline{\Delta L^{i,N}_j} =< L^{i,N}_{night} > - < L^i_{night} > \tag{3.5}$$

where $< L^{i,N}_{night} >$ is the $1 \leq j \leq 1000$ equivalent night level for the N sampled days in measurement point i, computed according to Equation 3.2 for the proposed stratas and according to:

$$< L_{night}^{i,N} >= 10log \left\{ \frac{1}{N} \sum_{j=1}^{N} 10^{\frac{L_{night}^{i}(j)}{10}} \right\} \tag{3.6}$$

for the random sampling strategy. Finally, from the vector of data $\overline{\Delta L_j^{i,N}}$, the N number of days required to have 90% of the 1000 estimation values inside ±1 dB is obtained.

3.3 Results

3.3.1 Cluster analysis for temporal stratification

The optimal number of cluster is 2 in all but 3 streets (Table 3.2). For the objective of the present research, the value is fixed at $k = 2$ since computing the silhouette value with $k = 2$ for those points, the difference to the optimal is very low (0.01, 0.01 and 0.03 for points 4, 8 and 18 respectively).

Point	**Silhouette**	**Optimal K**	***p*-value**
1	0.75	2	4.04E-24
2	0.91	2	4.47E-07
3	0.73	2	3.16E-10
4	0.74	**3**	3.49E-27
5	0.76	2	3.77E-31
6	0.76	2	2.45E-34
7	0.75	2	2.83E-22
8	0.76	**6**	5.98E-13
9	0.75	2	***0.51***
10	0.89	2	3.21E-02
11	0.80	2	5.07E-42
12	0.84	2	4.32E-25
13	0.75	2	1.08E-22
14	0.81	2	1.38E-39
15	0.85	2	1.84E-34
16	0.77	2	7.49E-11
17	0.74	2	7.43E-10
18	0.72	**7**	7.79E-06
19	0.75	2	1.38E-12

TABLE 3.2: Silhouette average, optimal number of clusters and p-value of the test for distribution mean independence for each measurement point. Values of optimal $k > 2$ are in bold italics. Values of $p > 0.05$ are also in bold italics and mean that the hypothesis that the datasets belongs to distributions with the same mean could not be rejected (p=5%).

Figure 3.2 shows the DOW density of all streets within each cluster. As it can be seen, the highest concentration of days is Friday/Saturday in one of the clusters and the remaining days in the other cluster, which could be interpreted as a stratification. The *Wilcoxon rank-sum* test showed that the weekends and working-days subsets in all but one point (Table 3.2), come from different distributions

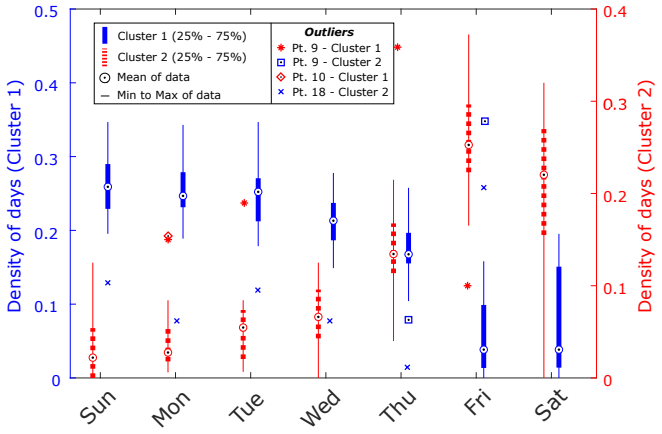

FIG. 3.2: Box-plot of each day of the week density for all of the measurement point within each of the two clusters.

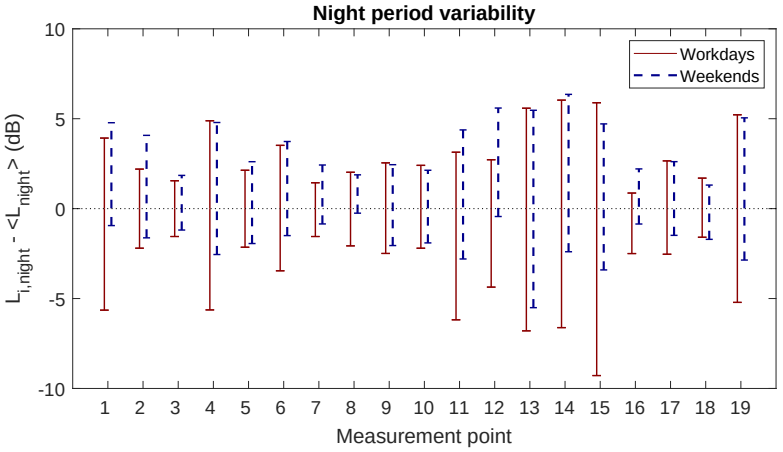

FIG. 3.3: Variability of the night period. L^{Wd}_{night} and L^{We}_{night} centered to the $< L_{night} >$ and its 95% confidence interval in dB.

($p = 0.05$). The only exception is the sampling point 9 which, as seen in Figure 3.2, is a clear outlier for several days in both clusters.

The variability analysis is then performed. The working-days equivalent level L^{Wd}_{night}, the weekends equivalent level L^{We}_{night} and the corresponding 95% confidence interval of the new stratas were computed. The results are presented in Figure 3.3. As it can be observed, in most of the streets, the 95% confidence interval of the new weekend strata is lower than the working-days interval, thus, L^{We}_{night} would correspond to the strata with low variability. Then, it is proposed to take samples during weekends and estimate the working-days equivalent level for the night period.

3.3.2 Street categorization by land use

Table 3.3 shows the corresponding cluster category of each sampling point as well as the $< L_{j,min-j} >$ parameter, computed for each point and for the cluster average. As it can be seen, $< L_{j,min-j} >$ increases as the cluster does (Cluster A with the lowest value to Cluster D with the highest).

	Categories		$< L_{j,min-j} >$		N Days		Estimations		
Point	**T.C.**	**Cl.**	**Ind.**	**Cl.**	**Ran**	L_{night}	$< L_{night} >$	$< L^N_{night} >$	**Nearby Act.**
2	2	A	1.02	0.69	10	***11***	62.0	63.6	Com
3	1		0.58		2	2	61.9	61.1	
7	2		1.13		4	4	66.2	66.4	Tou
8	2		1.50		5	5	67.6	68.2	
9	3		0.07		7	***12***	58.5	58.1	
10	2		0.07		5	***19***	59.7	59.7	Com, Fs
18	3		0.45		3	3	60.9	60.1	Fs
4	2	B	2.95	2.39	23	14	65.3	64.8	Lei
5	2		1.86		6	5	64.1	63.9	Fs
6	4		2.75		11	5	59.4	59.0	Tou, Com
16	2		2.07		7	3	67.9	66.5	Com
17	3		1.69		10	***12***	60.7	61.2	Fs, Lei
19	3		3.02		23	13	60.1	60.9	Lei
1	4	C	3.20	4.52	30	7	64.4	64.6	Tou
11	4		4.57		42	6	64.4	63.6	Fs, Lei, Tou
12	4		5.10		31	9	61.5	62.0	Tou
13	4		3.46		24	20	70.3	70.1	Tou
14	3	D	6.15	5.60	48	15	62.0	61.5	Lei, Com
15	3		5.04		39	9	65.9	65.2	Fs, Lei
Total					**330**	**174**			

TABLE 3.3: Traffic categories (T.C.), cluster categorization of sampling points (Cl.) and $< L_{j,min-j} >$ computed individually for each sampling point and as the cluster category average is shown. The required number of days to have 90% of samples within $< L_{night} > \pm 1$ dB for random sampling strategy (Ran) and for the proposed stratas, setting the $< L_{j,min-j} >$ as the cluster category (Cl.) average for night period, is also shown. N is bold italic when the required days is higher for cluster category than for random sampling. Finally, the actual annual level $< L_{night} >$ and estimated noise level using N sampled days $< L^N_{night} >$ for each sampling point is presented as well.

To observe the week noise level dynamics for each cluster, the streets were grouped by the obtained classification and the mean $< L_{i,DOW} >$ and the standard deviation for all streets within each cluster was computed. The results are shown in Figure 3.4. It can be appreciated that each cluster has different $< L_{i,DOW} >$ patterns during the week. It is seen that the classification of streets is related to the noise level difference between working-days and weekends, $< L_{j,min-j} >$.

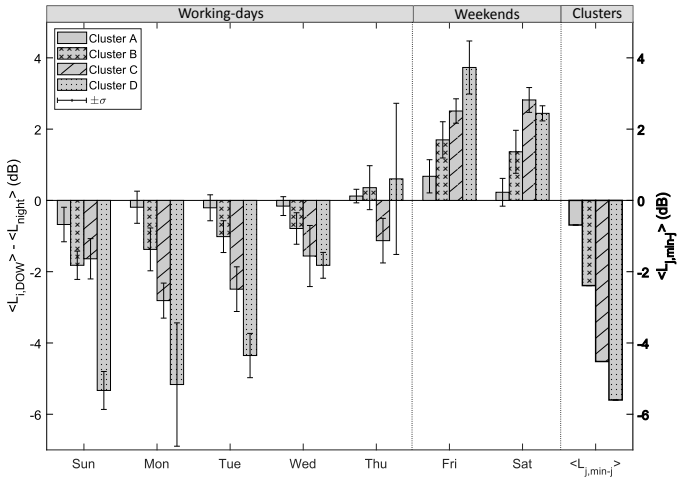

FIG. 3.4: Mean value for each day of the week (Equation 3.1) of the streets within each cluster category and its corresponding standard deviation. The noise level difference ($< L_{j,min-j} >$) is also shown.

To get more information of the spatial classification of streets, a PCA analysis was performed. More than 90% of the variability is explained by the first 2 principal components. Figure 3.5 shows the scatter plot of each sampling point by using the new coordinates defined by the principal components. The influence that Friday and Saturday have in the streets defines half of the clusters, with a negative influence in Clusters C and D, which means that the noisy days are weekends. The rest of the working-days (except Thursday) have a direct influence in Cluster A and B since the streets of these clusters are in the positive side of Component 1, which means that the important days for this type of clusters are working-days. Component 2 has direct influence in the Cluster C, since it is totally on its negative side. The streets that belong to this cluster are the pedestrian ones. As seen in Figure 3.4, for the pedestrian streets all the working-days have similar $< L_{i,DOW} >$, including Thursday, but, for the rest of the clusters, Thursday is observed to have a $< L_{i,DOW} >$ level between working-days and weekends. The absence of traffic in pedestrian streets, could increase the stratification for the night period (with constant values for working-days and for weekends, but with a marked difference between them) as the noise would be mostly due to leisure and human interactions, which tends to be higher during weekends.

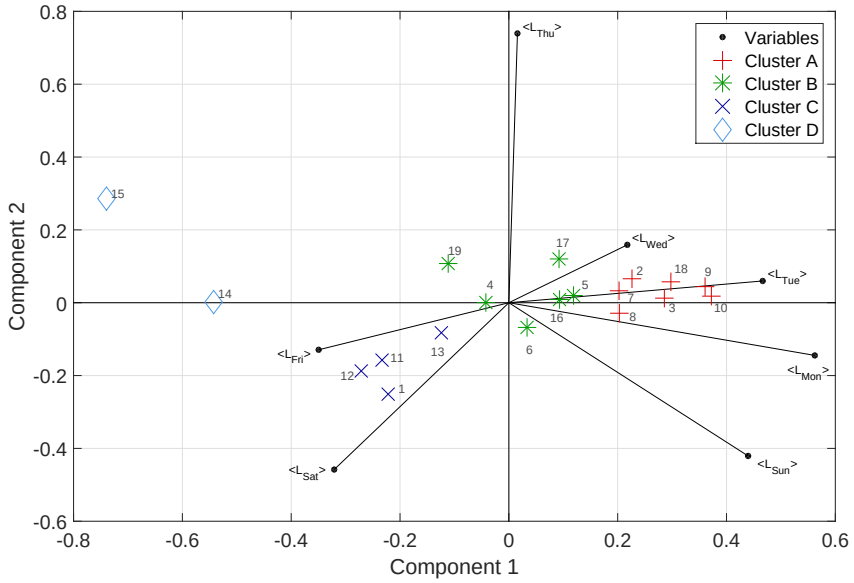

FIG. 3.5: Scatter plot of P.C. 1 vs P.C. 2 for each street. Every point in the scatter plot shows the street number and a symbol corresponding to its cluster. Black dots represent the coefficients of P.C. 1 and P.C. 2 for each DOW and the length and direction of each vector of the input variables, represent the contribution of each of the variables into the first two principal components.

3.3.3 Long-term estimation

In order to set the $< L_{j,min-j} >$ for the estimation of $< L^{Wd}_{night} >$, since previous noise data will not always be available for all the places under assessment, the average value of all the streets within each one of the proposed cluster categories is used for the long-term estimation.

The N required number of days to have 90% of samples within the interval $< L_{night} > \pm 1$ dB was computed for each street (Table 3.3). It is also computed for the random sampling strategy to be used as a reference [27, 52, 96]. The results are shown in Table 3.3. The global reduction using spatiotemporal stratification compared to random sampling is about 47%.

3.4 Discussion

Four different street categories are found according to the night noise levels behaviour for the whole week. Relating these categories to the nearby activities of each street (Table 3.3), some trends can be found depending, basically, of the

activity period (day/night). Moreover, as traffic noise is also considered, there is some influence of the traffic category (T.C.) of each street (also in Table 3.3). Considering these variables, the land use categories found can be generally described from the cluster letter as:

- Category A: Streets with daytime activities, with almost no night life, and supporting considerable traffic (T.C. 1 and 2), so that there is little influence of land use on the categorization. The influence is observed since two T.C. are put together in a same category. These streets could be targeted as Commercial Streets.
- Category B: This category is rather similar to category A, but these streets have a greater density of commercial and food related services, basically daytime activities but with some presence of leisure activities. Mainly composed by T.C. 2 and 3, so the weight of ordinary traffic in the weekly acoustic pattern is not so high as in the category A. These streets could be targeted as a High Density Commercial Streets.
- Category C: Clearly composed by pedestrian streets with great influence of tourism activity. Noise is caused basically by street crowds. These streets could be targeted as Pedestrian Recreational Streets.
- Category D: Streets mainly intended for nighttime leisure activities, with many bars and nightclubs in the surroundings, but with streets opened to traffic. In this case, noise comes from street crowds and traffic as well, but probably the weekly acoustic pattern of traffic is influenced by the traffic flow attending to those activities. These streets could be targeted as Recreational Streets.

This is clearly a tentative classification as, for example, there are only two streets in Category D, so further research is required in order to give a quantitative value to the nearby activities that would make the classification more objective.

There are some measurement points that seem not to fit within the new categorizations due to their lack of improvement, but most of them are in Cluster A, which is the one with less influence of leisure noise during nighttime. Within this category, measurement point 9 is a special case, as it fails the independence test

and it is considered an outlier as seen in Figure 3.2. It is a street with very few activity (some small businesses) and very few traffic as well. However, its $< L_{night} >$ is above 57 dB. This value is caused by the traffic noise of the Meridiana Avenue, a main access to Barcelona with a traffic flow over 100,000 vehicles per day, which is only 2 blocks away and point 9 is directly connected to it. Points 2 and 10 from the same category, a reduction in the required days is also not achieved. Both streets have high traffic flow as they are main avenues, although both have influence of commerce activity, probably it is not enough to have an effect into the land use, which is also reflected in a low $< L_{j,min-j} >$ and should be classified according to T.C.

For sampling point 17, from Cluster B, also no improvements are obtained. Computing $< L_{DOW} >$, it was observed that $< L_{Thu} >$ is as high as the weekend (Friday and Saturday) which brings an estimation error, then, Thursday should be separated from working-days for this particular point. The temporal cluster of Street 17 should include Thursday in the weekend cluster which perhaps could define one more category, although it has not been considered in this work as only this case has been found.

As seen in Table 3.3, for the estimation of long-term values, the cluster categorization brings good improvements as it reduces the global required days in about 47%. It is also observed that the obtained reduction is higher when the $< L_{j,min-j} >$ is high.

Based on a scheme of spatial categorization by temporal evolution, similar as presented in [97], the classification proposed in Section 3.3.2, extends the temporal evolution to be a whole week pattern in order to take into account the noise level variations due to the nearby activities, which was first observed in [91] to be reflected during the nighttime in the weekly noise evolution. The present research also complements the traffic categorization, whose methodology was proved to be applicable at nighttime [98] based only on traffic noise [38], since now the influence of leisure noise is taken into account as well.

The actual and estimated long-term night noise levels, as shown in Table 3.3, are consistent with previous studies carried out in other cities around the world [99–103], but all in all, they are above the WHO recommended limits [104],

The proposed methodology is a tool that, by addressing the spatiotemporal influence of recreational noise, would help authorities to perform the noise assessment for these types of noise scenarios in a more efficient manner and draw action plans accordingly. The parameter $< L_{j,min-j} >$, for the case of practical application of the methodology, should be computed based on previous noise levels (where available) or extrapolated from other urban zones with similar characteristics.

3.5 Conclusion

The effect of the land use in the street categorization for the night period is found. Based on a cluster analysis, 4 street categories are proposed: Category A (Commercial Streets), comprises streets almost without night life activities and high traffic flow; Category B (High Density Commercial Streets) is formed by streets that include a wide range of businesses such as schools, health care, financial institutions, which are mostly open only during commercial hours; Category C (Pedestrian Recreational Streets), is mainly formed by pedestrian streets that could have recreational places focused on people passing by or tourism activity; finally, Category D (Recreational Streets), comprises streets whose main land use is for leisure, they could have many nightclubs and pubs nearby. For sampling points affected by leisure activities at night, the weekends are found to be Friday and Saturday, and not Saturday and Sunday as for the day period. Also contrary to what happens during the day period, the variability for the night period is lower during the weekends.

The long-term estimation was performed using the spatiotemporal categorization procedure and $< L_{j,min-j} >$ as the category average. For the annual L_{night} estimation, the reduction in the required number of days to have 90% of the samples inside $< L_{night} > \pm 1$ dB was higher than 47%. As observed in Figure 3.4, the clusters are separated by the difference of noise level between working-days and weekends, being Category A the one with the lowest difference, which means that its land use is more residential with a few or without leisure places, and is suggested to be used the categorization based on traffic, and Category D the one with the highest difference which means it is the one with more influence of leisure noise.

Chapter 4

Statistical requirements for noise mapping based on mobile measurements using bikes

4.1 Introduction

To evaluate the noise exposure of the population, the European Noise Directive [11] requires that the Member States develop noise maps and actions plans for noise reduction every 5 years, for agglomerations higher than 100,000 inhabitants. The parameters suggested to be plot in the noise maps are, at least, L_{night} and L_{den} for the equivalent time of 1 year.

For the production of a noise map, the noise levels are mainly based on on-site measurements or calculated based on computational models. Both approaches share the need of huge amount of input data, whether they are large sampling campaigns for noise maps based on measurements or detailed traffic information for noise maps based on simulations.

For noise maps based on simulations, there is a wide variety of traffic noise models [105], which are meant to predict the sound pressure level of a single vehicle in the road. Anyway, since they are usually developed at a local scale, mainly for action plans on noise reduction, they do not allow a direct comparison of the presented data between different models [31, 106], even with commercial software [69]. For instance, as indicated in [11], the CNOSSOS framework emerges as a solution to standardize noise modeling, which would allow results from different countries to be compared [23, 107].

A common way to represent the vehicles as the noise source in the computational models, which also reduces the required computations, is using long-term average values such as speed or traffic flow rates. Since it disregards the vehicle dynamics along the roads, a correction factor for each segment of the road can be used [108]. Furthermore, the dynamic traffic representation is shown to improve the noise level estimations [109, 110]. As the different situations that can be observed on real scenarios such as traffic jams, free flow, accelerations, decelerations, roundabouts, among others, are considered (usually 1 s), it would bring noise estimations closer to reality, but with an increase in the computational complexity since the amount of input data would considerably increase. Moreover, different paradigms have been investigated to represent the noise from multiple sources [30, 111] to emulate on-site sampling, where sources that exists in urban environments are measured [112].

For the case of noise maps based on measurements, it is necessary to perform

spatio-temporal sampling. Thus, to improve the temporal sampling process, several techniques have been proposed to estimate long-term noise levels from short-term measurements [17, 34, 49–53, 91]. For the spatial sampling, many ways reduce the amount of sampling points through street classifications have also been proposed [36, 38, 76, 97, 113].

In addition, the tasks that were traditionally executed by experts using certified equipment [56] are being replaced by other sampling approaches such as sensor networks, that are usually developed with low-cost hardware to cover large areas [57–60, 114, 115]. Another sampling scheme that has gained interest recently is the participatory sensing, which enables any person to take measurements either with a specific measurement equipment or through their mobile phones with enough accuracy as the standard noise maps [61–63]. A comparison between traditional mapping methods and participatory noise mapping is presented in [61]. The study states that, when measurements are performed following specific requirements such as calibrated handsets, spatio-temporal density, proper measurement protocols and trained citizens, participatory sensing could be another approach to address the Noise Directive guidelines. Some past and current projects regarding participatory sensing are shown in [116–120].

A common practice, which mixes both noise mapping schemes, is to take on-site measurements to calibrate the noise map based on computational models or to use them to dynamically update noise maps based on interpolation methods [14, 69, 121].

Finally, an approach that has not been widely studied, is the mobile sampling. One of the advantages of mobile sampling is that it would increase the temporal and spatial resolution, even with short length samples [122], in a more controlled environment than participatory sensing, since the measurement is carried out by professionals or trained people. Furthermore, combining the mobile sampling with the static one could enhance the advantages of making noise maps based on measurements [66]. Nevertheless many drawbacks should be addressed for the case of mounting the measuring device on any vehicle such as the noise contribution of the vehicle itself, the air flow and the position of the microphone among others [60, 65, 66]. Beyond these metrological issues, the temporal variations of noise due to the traffic dynamics (vehicle passes-by, vehicle platoons due to traffic lights,

heterogeneity between vehicle noise emissions, etc.) define the feasibility and statistical requirements for noise mapping based on mobile measurements.

Therefore, through a controlled simulated framework that reproduces the actual spatial and temporal noise variations, which is based on road traffic dynamic modeling, the present paper evaluates the statistical requirements for making a noise map based on mobile measurements, where the noise meter is simulated as mounted on a moving vehicle, ideally a bicycle to diminish the mentioned drawbacks. The aim of this chapter is to obtain the number of bikes passes-by required for different traffic flow rates and different distances to intersections. Furthermore, in order to reduce the estimation error, a spatial aggregation of mobile samples is also evaluated.

4.2 Methodology

4.2.1 Study area

The place under study is an area of almost 4.5 km^2 located at the northeast of the city of Lyon, France (Figure 4.1). The total length of the traffic network, which also includes Tram and Bus trajectories, is about 51.4 km. The micro-simulation software SYMUVIA [123] was used to provide the traffic input data for the dynamically modeled noise maps and also to simulate the mobile receivers (bikes). SYMUVIA is a software able to reproduce all the dynamics that would occur in the studied area, such as bus stops, traffic lights, lane changing and queues, giving as output the position $x_i(t)$, speed $v_i(t)$ and acceleration/deceleration $a_i(t)$ of each i vehicle within the studied road network for each time-step ($\Delta t = 1$ s).

Two independent traffic simulations, but performed for the same time period, were executed. The first one for the vehicles, that would be the input for the noise emission (sources), and the second one, that corresponds to the mobile receivers (bikes). This means that interactions between bicycles and vehicles are neglected when considering the position of bicycles on the network. However, their difference in kinematics is taken into account as detailed later in the investigation.

The vehicles demand, for the case of the sources simulation, was set to match the actual behavior of the traffic in the zone during 1 hour, from 8:00 to 9:00 hrs.

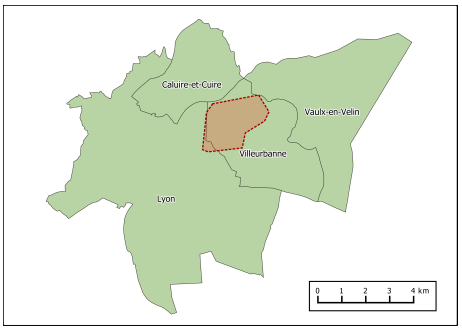

FIG. 4.1: Area under study located in the northeast of Lyon, France.

Furthermore, the traffic lights, Bus and Tram stops, trajectories and speed limits are also set to match the real scenario.

For the case of the mobile receivers, the bikes were simulated as a regular car but their speed was limited to a maximum of 5 m/s. Additionally, to have a constant demand and a similar distribution of bikes through most of the studied streets, some input parameters related to the route calculation algorithm were also adjusted. A video of the whole simulation of the mobile noise sampling can be found in *.

4.2.2 Dynamic noise modeling

The dynamic simulation methodology is based on [30, 109, 110], where the vehicles are mapped into fixed grids and some steps are suggested for the dynamic modeling. The main difference of the present research is that the microscopic traffic simulations are not only used for the sources (noise emission), but also for the mobiles receivers. Then, the modeling steps are as follow:

(a) Traffic model: Simulation of individual vehicle trajectories at each t. Matched to a fixed grid of sources.

(b) Noise emission: Calculation of the noise power of each individual vehicle at each t.

(c) Mobile receivers: Simulation of individual bikes trajectories at each t. Matched to a fixed grid of receivers.

*https://vimeo.com/315221179

(d) Sound propagation: Attenuation between fixed sources and receivers grids to compute noise level at each receiver, whether they are static or mobile.

(e) Indicators calculation: Sound level indicators to compare static and mobile sampling.

The geographical information system OrbisGIS together with the NoiseModeling plug-in (v 2.2.0) [124, 125] are used for the noise emission and propagation computations. This version of the plug-in is based on the CNOSSOS [107] standard for road noise emission, and the NMPB [126] method for sound propagation. The validity of a similar modeling chain to reproduce the spatio-temporal noise variations in urban areas has been demonstrated in [110, 127].

4.2.2.1 Fixed grids for sources and receivers

Since the output of the simulations for traffic and mobile receivers could bring infinite different positions for sources and receivers, which could have a huge negative impact on the calculation time, the sources and receivers are matched into fixed grids close enough not to alter the expected noise level.

Therefore, to place the fixed sources points, each road/street is taken as a single lane and divided into equal segments of $D = 3$ m. A fixed point is placed on one side of each segment and every vehicle is then attached to its nearest fixed point (modeling chain step (a)). The grid of sources is finally created selecting only the fixed source points, P_s, that have a vehicle attached. Almost the same procedure is followed for the grid of receivers (modeling chain step (c)), but the positions of the fixed receiver points, P_r, are displaced 1 m perpendicular to the trace of the road to avoid an overlapping with the cars (Figure 4.2).

4.2.2.2 Vehicle noise emission

The input parameters for the CNOSSOS standard are obtained from the each second outputs from the SYMUVIA software, and from the actual characteristics of the zone under study. According to [107], five classes of vehicles are considered for the noise emission computation. For the present research, since the aim is to compare the differences between mobile and static sampling for traffic noise,

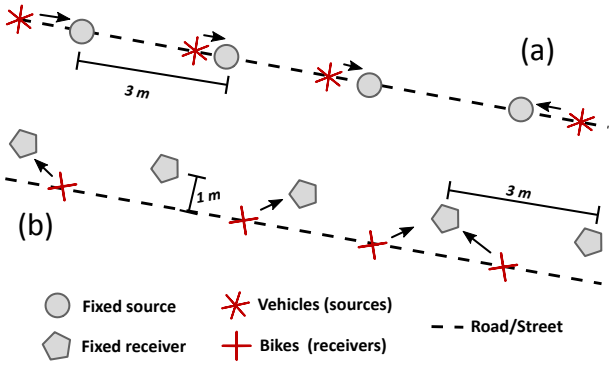

FIG. 4.2: (a) Vehicles and (b) bikes mapped into a fixed grid. The fixed grid of the bikes is displaced 1 meter perpendicular to the road.

three vehicle classes are considered: light vehicles (Cars), medium heavy vehicles (Buses) and heavy vehicles (Tram).

Since on a real scenario not all the vehicles emit the same noise level, an uncertainty with a standard deviation of 2 dB was added to the noise power calculated for each vehicle (constant during its whole life). Thus, the spectrum power for every time-step and each vehicle $Lw_b(i,t)$ (dB) is computed for the b octave bands with a central frequency in the range 63 Hz - 8 kHz (modeling chain step (b)).

4.2.2.3 Attenuation matrix

To compute the attenuation between sources and receivers, the input parameters were configured to have an appropriate calculation time without affecting the accuracy. Thus, the calculation takes into account only the sources that are within a maximum radius of 250 m from a receiver (maximum propagation distance), and reflections and diffractions are computed only for walls within 50 m from the sources-receivers propagation line. The road surface is specified as dense asphalt concrete [107] and the temperature is set to 20 °C. Other configured parameters for the computation of the attenuation of each octave band are:

- Reflection order: 2
- Diffraction order: 1
- Wall absorption: 0.2

Based on the condition that the acoustic propagation for the studied period does not change [30], and using as input the buildings information and the fixed grids of

sources and receivers, the attenuation $Att_b(x, y)$ is computed for each combination of $x \in Pr$ and $y \in P_s$ (modeling chain step (d)) with the spatial conditions previously mentioned.

4.2.3 Noise maps and indicators calculation

Using the power spectrum of each vehicle and the attenuation matrix for each b octave band, Subsections 4.2.2.2 and 4.2.2.3 respectively, the noise level at each x for any t can be computed as (modeling chain step (e)):

$$L_b(x,t) = 10log\left(\sum_{i\in I} 10^{[Lw_b(i,t)-Att_b(P_s(i),P_r(x))]} + 10^{\frac{L_{BK}}{10}}\right) \tag{4.1}$$

where $I = \{x \diagdown\!\!\diagdown^{250} P_s\}$* and L_{BK} is the background noise set at 40 dB, which is relevant for the cases where there are not cars nearby a fixed or mobile receiver.

The L_b is representative of the interval of one second, with the error that this entails, since a fixed position is assumed for the whole second, when both emitter and receiver are actually moving during this period. Once the L_b is computed for all the octave bands, the A-weighted equivalent level of each time-step is obtained [128].

4.2.3.1 Reference and mobile noise maps

Two different types of noise maps are created: the reference noise map, which is based on fixed measurements and computed for the whole set of fixed receivers, and the mobile noise maps based on mobile measurements, which are the ones to be evaluated.

Thus, to obtain the final noise maps, a temporal aggregation for the whole simulation time T is performed for each receiver. Furthermore, to homogenize the results of the reference noise map, and to find the optimal aggregation radius for the mobile noise maps, a spatial aggregation of the surrounding receivers is also performed.

*$\{x \diagdown\!\!\diagdown^{y} Z\}$ is a subset of the elements in Z that are within a radius of y meters from x.

Therefore, for the total simulation time T and for each $x \in P_r$, each time-step samples $L_{Aeq}(x,t)$ are joint into a subset of P_r as:

$$L = \bigcup_{x \in X} \left\{ \bigcup_{t=1}^{T} L_{Aeq}(x,t) \right\} \tag{4.2}$$

where T is the total simulation time and $X = \{x \diamond^{15} P_r\}$ for the reference noise map or $X = \left\{x \diamond^{[1,100]} P_r\right\}$ for the mobile noise maps.

Then, the aggregated A-weighted equivalent level is computed as:

$$\overline{L_{Aeq}}(x) = 10log\left(\frac{1}{N}\sum_{l \in L} 10^{\frac{l}{10}}\right) \tag{4.3}$$

where N is the number of elements in L (Equation 4.2).

For the case of the reference noise map, all $x \in Pr$ are used for the spatial and temporal aggregations. For the case of the mobile noise maps, only the fixed points that are active at t are taken into account for aggregations.

4.2.3.2 Complementary indicators

For the whole simulation period, the number of bikes passes-by (B_{pb}) and the traffic flow (T_f) for each static receiver is computed. Moreover, since the type of road junctions, whether they are traffic lights, roundabouts, cross streets, etc. are shown to bring noise level variations [109, 129], the distance to the nearest cross street (streets intersections D_{in}) is also computed. Then, the Root Mean Square Error (RMSE) between the reference and mobile noise maps is obtained as:

$$RMSE = \sqrt{\left(\frac{1}{N}\sum_{x \in P_r} (\overline{L^{ref}_{Aeq}(x)} - \overline{L^{mob}_{Aeq}(x)})^2\right)} \tag{4.4}$$

where L^{ref}_{Aeq} and L^{mob}_{Aeq} are the A-weighted noise levels from the reference and mobile receivers respectively and N is the number of receivers.

Thus, three types of noise maps are computed according to the following conditions:

(C_1) **Optimal aggregation radius:** Using all the receivers, the mobile noise maps are computed using Equation 4.2 for a spatial aggregation distance from 1 m to 100 m. The RMSE is computed for each aggregated noise map.

(C_2) **Minimum passes-by:** The RMSE is computed for subsets of P_r. First, the receivers are separated according to 4 traffic flow rates $Q = \{i, ii, iii, iv\}$ where ***i)*** 0 - 100 veh/hr, ***ii)*** 102 - 245 veh/hr, ***iii)*** 246 - 561 veh/hr and ***iv)*** 562 - 2185 veh/hr. Then, for each traffic flow, the receivers are grouped according to their number of bikes passes-by, $B_{pb} = \{1, ..., 100\}$. Thus, RMSE is computed for each combination of Q and B_{pb}, i.e. $\text{RMSE}_{Q,B_{pb}}$.

(C_3) **Distance to intersection error estimation:** The RMSE is computed for subsets of P_r grouped according their distance to the nearest intersection, $D_{in} = \{1, ..., 100\}$ meters, i.e. $\text{RMSE}_{D_{in}}$.

Before the RMSE calculations in (C_2) and (C_3), the maps are aggregated by the optimal radius as obtained in (C_1). The receivers were separated into traffic flows to enhance the rest of the parameters [130]. Then, the ranges of traffic flow in (C_2) were chosen so that each category has the same amount of receivers and the comparison be as homogeneous as possible.

4.3 Results

4.3.1 RMSE vs Aggregation radius

As stated in [108, 122], the spatial aggregation of short-term samples is necessary to deal with their high spatial variations. Furthermore, in [131] for the aggregation of L_{Aeq} samples, a radius of 50 m is suggested to ensure that a minimum of 10 samples are aggregated in each point, since the typical speed of a bicycle is 5 m/s. Thus, for the present research, the noise maps were computed for aggregation radius from 1 m to 100 m according to Equation 6.1 and to condition C_1. Then, the RMSE for each map was computed with Equation 6.3. Figure 4.3 shows the RMSE as a function of the aggregation radius. It is seen that the radius that minimizes the estimation error is 34 m. The lower radius obtained for L_{Aeq} compared to the one suggested in [131], is obtained since the simulation limits the maximum speed to 5 m/s which, would only be obtained in cases of free flow. The

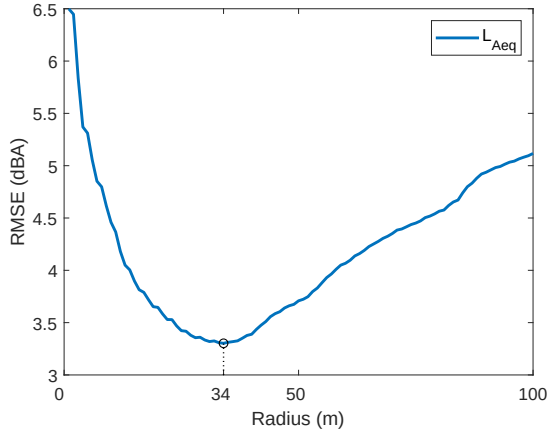

FIG. 4.3: RMSE for mobile measurements aggregation from 1 m to 100 m. The minimum error is pointed with a circle.

actual speed average of bikes is 3.5 m/s, that for a radius of 34 m, gives around 19 samples for each spatial aggregation.

4.3.2 RMSE vs Pass-by

The SYMUVIA output file gives to each vehicle a unique ID, then, in order to calculate the number of passes-by or the traffic flow, the different IDs attached to each receiver are accounted. For cases where an ID appears more than 1 time at the receiver, which means that it stayed more than 1 s near to it, a time aggregation was performed and it is counted as 1 pass-by.

Figure 4.4 shows the RMSE according to different traffic flows from 1 to 50 passes-by. It can be observed that, before a certain number of passes-by, the RMSE decreases as the passes-by increase. Except for traffic category i), after 20 passes-by the decrease in the RMSE is lower, which suggests a stabilization. Furthermore, about 42 passes-by brings almost the same error for the other 3 categories (approximately 0.5 dBA difference).

4.3.3 RMSE vs Distance to intersection

The distance to the nearest street intersection was computed for each of the fixed receivers. The RMSE for L_{Aeq} was then computed for 25 passes-by and for the 4 traffic categories. Figure 4.5 shows the mean error according to the distance to the

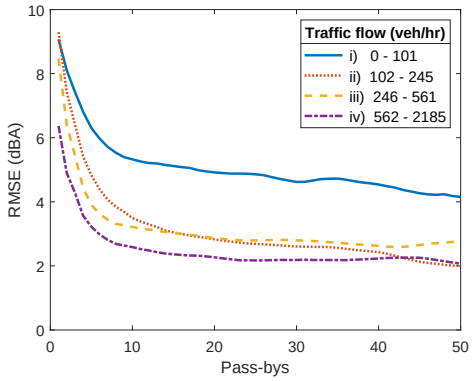

FIG. 4.4: RMSE for mobile measurements as a function of the number of passes-by for different traffic flows.

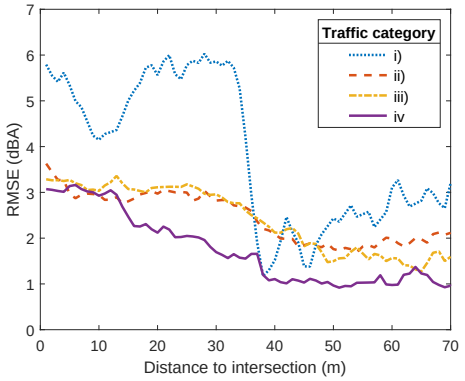

FIG. 4.5: RMSE for mobile measurements for 4 traffic categories as a function of the distance to the nearest intersection (1 m to 70 m).

nearest street intersection. It is observed that, except for category 1, the farther from the intersection, the lower the calculated RMSE.

Figure 4.6 shows a 3D bar plot of the RMSE as a function of the number of passes-by and the distance to the nearest intersection for traffic category 4. The plot was smoothed to better observe the possible patterns. It is seen that after a distance of 20 m from intersection, the number of passes-by gains more importance since the decrease in the RMSE is higher for each increment in the passes-by.

4.3.4 Noise maps

A map to represent the traffic count for the mentioned categories, as well as the number of passes-by (bikes) at each receiver point is shown in Figure 4.7. Furthermore, noise maps were computed for the whole simulation time for the

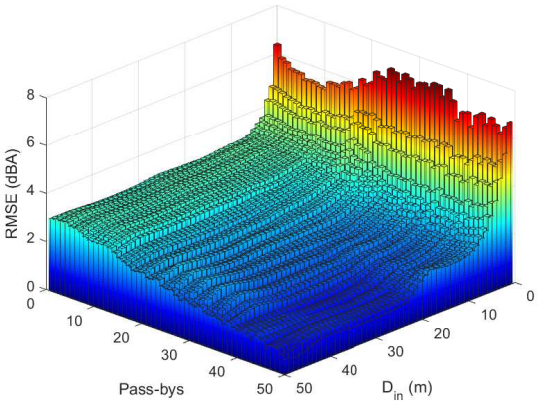

FIG. 4.6: RMSE for 1-50 passes-by and 1-50 m from intersection for L_{Aeq} estimation.

reference receivers, the mobile receivers (aggregated by its optimal radius) and their noise level difference computed by subtracting the reference noise level minus the mobile noise level as follows:

$$L_{reff-mobile}(x) = L_{Aeq}^{reff}(x) - L_{Aeq}^{mob}(x),\ \forall x \in P_r \tag{4.5}$$

where L_{Aeq}^{reff} and L_{Aeq}^{mob} stands for the L_{Aeq} of the reference noise map and the mobile noise map respectively. The resulting noise maps are shown in Figure 4.8. Although the reference and mobile noise maps seem to be similar at first sight, the map of the noise level differences (Figure 4.8d) highlights the discrepancies between them. If one compares Figure 4.8d to Figure 4.7, it can be appreciated that the highest estimation errors are mostly observed for streets with low traffic flow and low number of passes-by. The histogram of the estimation error for the mobile sampling (Figure 4.8d) according to the number of receivers is shown in Figure 4.9. The mean value and the standard deviation is also shown. It is observed that 95% of the samples fall in the range [-5.4, 5] dBA for L_{Aeq} estimation.

Finally, based on the three input parameters: B_{pb}, T_f and D_{in}, a linear regression analysis was performed to approximate the absolute error of the L_{Aeq} estimation. The independent variables were transformed into a logarithm function (log_{10}) to match their non linear relation. Table 4.1 shows the results of the analysis. It is observed that there is a positive correlation ($p<0.05$) with an explained variance about 15%. It is important to point out that, although the explained variance is

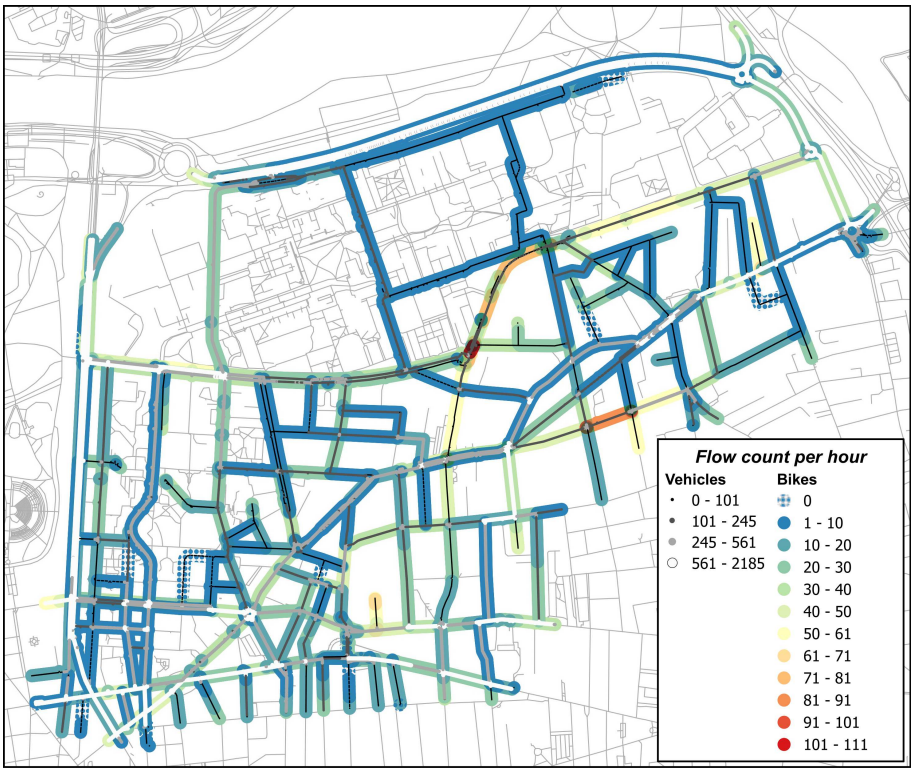

FIG. 4.7: Bikes passes-by and traffic counts for each receiver.

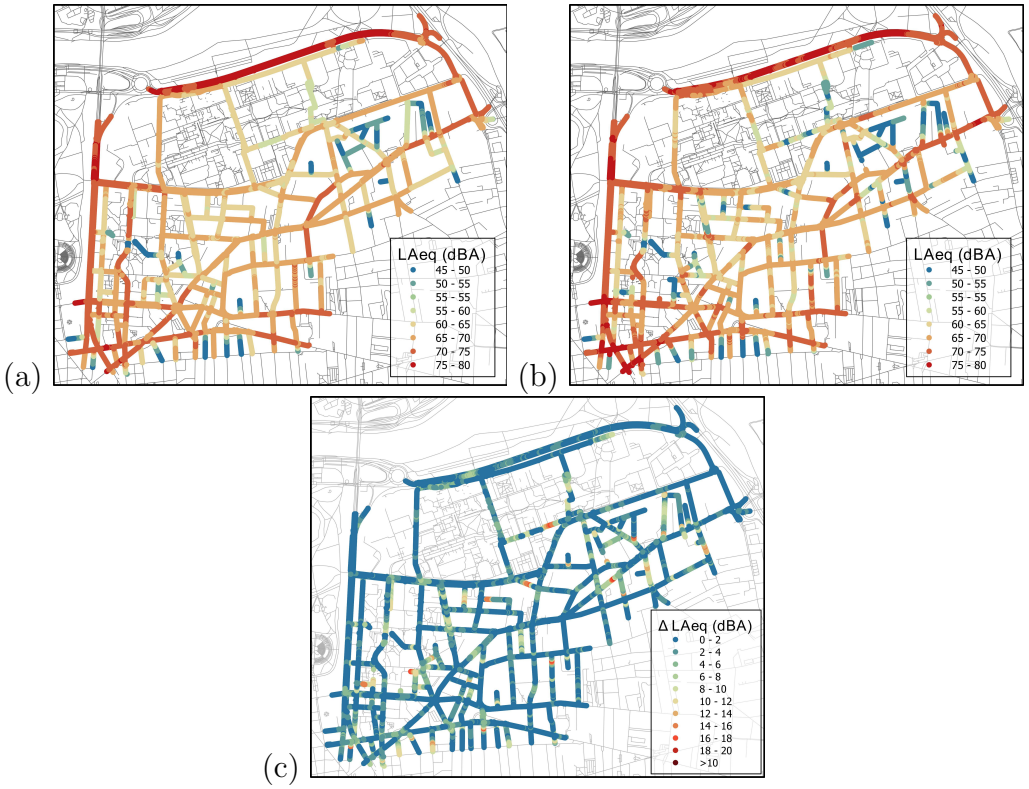

FIG. 4.8: Reference noise map (a), mobile noise map (b) and difference between reference and mobile noise maps (c).

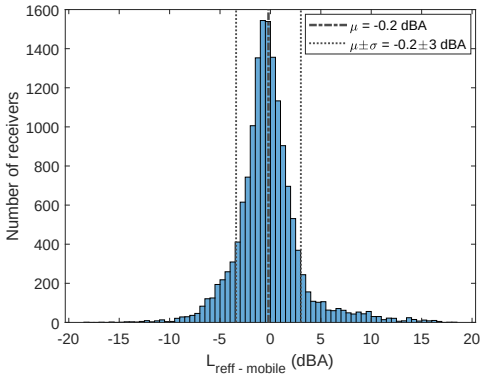

FIG. 4.9: Histogram of the noise level difference for each receiver of the reference noise map minus the mobile noise map (L_{Aeq}).

	Coeff.	**Std. err.**	**t-values.**
(Constant)	7.33	$16.29E^{-03}$	450.2
$\mathbf{B_{pb}}$	-1.75	$7.33E^{-03}$	-239.1
$\mathbf{T_f}$	-0.60	$3.96E^{-03}$	-151.8
$\mathbf{D_{in}}$	-0.82	$6.70E^{-03}$	-122.7

TABLE 4.1: Multiple linear regression between absolute estimation error in the L_{Aeq} estimates, and the independent variables B_{pb}, T_f and D_{in}. All variables are significant with a $p-value < 0.05$. The multiple and adjusted R^2 are both equal to 0.1554 and the residual standard error is 2.446.

low, it is an expected value since the moment of the measurement is what explains the largest part of the variance.

4.4 Discussion

The present chapter shows the possibility to perform mobile sampling with a certain precision, although some considerations should be taken into account in order to improve the estimation accuracy, or if one wanted to put this sampling approach into practice.

To improve the estimation accuracy, Figure 4.3 shows that by aggregating the mobile samples, the RMSE can be reduced up to 3 dBA for the estimation of L_{Aeq}. In addition, Figure 4.4 shows that a minimum of passes-by could be set depending on the traffic flow. For the case of streets with low traffic flow, it is clear that the higher the number of passes-by the lower the estimation error. For the case of streets with higher traffic flow, a stabilization time related to the number of passes-by, similar to the one shown in [54], could be proposed as a stop parameter, since at a given number of passes-by, the estimation error seems to remain almost constant.

Furthermore, the present chapter showed that intersections introduce some uncertainty to the mobile measurement (higher than 2 dBA for distances around 20 m). It is observed that the closer the intersection is, the higher the error. This result is in concordance to what is presented in [108, 109, 129, 132], where the influence of the acceleration/deceleration, which is mostly observed at the intersections, is studied and some corrections are proposed for static noise mapping.

Although in Section 4.3.4 it is mentioned that 95% of the estimations falls into a wide error range, [-5.4, 5.0] dBA for L_{Aeq}, this range could be reduced by setting some minimum sampling parameters. For example, if a minimum of 30 passes-by and a distance to intersection higher than 30 m for the traffic categories iii) and iv) is considered, the 95% confidence interval is reduced down to [-3, 2.2] dBA.

The present chapter proposes techniques to deal with the high spatial and temporal resolution of the samples, that is, the spatial and temporal aggregation, which, complemented with some minimum requirements help to reduce the estimations errors. Anyway, the studied simulation would be an ideal scenario for mobile sampling. If one wanted to put the methodology into practice on a real scenario, several external issues that the simulation neglects and that would certainly affect the actual sampling, should be taken into account:

- Vehicle reflections: The simulations do not include the reflections that would occur between the sources themselves (cars). Furthermore, in [18], the screening effect of the parked cars is also shown as a source of uncertainty, which for the proposed sampling, could probably be reduced by increasing the microphone height.
- Vehicle self generated and impulsive noise: Although the vehicle proposed is a bike, which would have a low floor noise compared to a car [65], impulsive noise, probably due to potholes or poor condition of traffic lanes, should be identified and processed.
- External noise sources: In a real scenario, several natural noise sources, such as birds, wind, climatological variables, or human induced such as constructions, commercial zones, schools, would be captured by the sampling device, which are not considered in the simulation.

4.5 Conclusion

The present chapter tested the statistical requirements for noise mapping based on mobile measurements, under a simulation framework. It was shown that it is actually possible to perform noise mapping based on mobile measurements, however, some considerations should be set in order to reduce the uncertainties.

In order to minimize the estimation error, a minimum number of passes-by, which depends on the traffic flow, should be selected. Furthermore, an optimal radius of 34 m for mobile samples aggregation to minimize the L_{Aeq} estimation error is proposed. For the distance to intersection, some correction could be set to compensate the error that it introduces.

Finally, in case that the mobile sampling is put into practice, some extra considerations that should be addressed are also suggested, some of them related to the vehicle itself such as reflections, self-generated noise and impulsive noise, or to external noise sources such as those related to the nature or human interactions.

Chapter 5

Design and implementation of a low-cost spectrum analyzer for georeferenced mobile measurements

5.1 Introduction

To create a noise map based on measurements, the levels shown in the noise map must be representative, which requires having a large amount of data in both the duration of the measurements [17, 34, 91, 133] and in sampling sites [38, 113]. The measurement equipment should fulfill minimum requirements regarding its accuracy which makes more expensive the sampling process. As a consequence, the production of a noise map becomes a complex task that demands many resources.

Advances in technology have allowed the development of sensor nodes provided with communication modules at a reduced cost but that have enough processing power to perform different sensing and data transfer tasks [134]. In recent years, several studies regarding the design and implementation of environmental monitoring stations have been carried out [56, 135–137]. Their main objective is to propose measuring tools at lower costs but that also guarantee the precision of the acquired samples. Having several nodes interconnected and working collaboratively to perform a global task, makes possible the idea of a sensor network [58, 138], which could be applied over a wide range of tasks such as environmental monitoring, medical applications, traffic counting, security and more [139–141]. However, the measurement points when assessing street traffic noise are representative of a very specific environment, basically the section of street on which they are located, unlike other environmental agents with more homogeneous distribution.

Other sampling method that, in general, nowadays is being more common is the participatory sensing or citizen oriented model [62]. Participatory sensing encourages the use of mobile devices, specially smartphones, to collect, analyze and share the sampled data which would increase the granularity in both spatial and temporal aspects [61]. However, participatory sensing for the specific case of environmental noise assessment has many drawbacks that are already under study. One of them is the data trustworthiness, since the sampling is left entirely in the hands of the citizen, the data integrity and representativeness is not fully assured. In [61, 62], information related to challenges and requirements to correctly address noise mapping through participatory sensing is presented. Moreover, since different devices have different sensors, their individual calibration for the wide variety of apps would reduce the advantages of participatory sensing [63, 64].

Another approach to increase spatial and temporal resolution in a more controlled environment is mobile monitoring, which enables the noise sensor to change its position while acquiring noise information. To properly represent the noise levels for map creation, the sampled data should be synchronized with its positioning information [65, 142]. Then, as the data is acquired over a large range of points across a predefined route, the spatial resolution is increased considerably, and if the route is repeated several times, the temporal resolution will also be considerably increased [122]. Thus, an important task to perform the mobile sampling is selecting the proper vehicle to mount the noise sensor. It has been shown that measurements taken walking may be convenient [66]. For the case of samples taken by car or bicycle, it is suggested that more tests should be performed since other variables such as the microphone position, the GPS accuracy and the noise contribution of the vehicle itself should be taken into account [65]. Furthermore, mounting the measuring device in a bus for real-time noise mapping has been proposed and the requirements that should be addressed have been analyzed [60].

In order to perform mobile sampling, the first part of the present chapter proposes the design, implementation, calibration and accuracy tests of a low-cost Georeferenced Noise Sensor (GNS) designed to measure the noise spectrum at each 1/3 octave bands ($^1/_3$OB) in the frequency range from 63 Hz to 10 kHz. The aim is to take georeferenced mobile measurements with an equivalent accuracy of a Type 2 sound level meter. The device consists in a Microcontroller, a digital MEMS microphone, a Micro SD card and a GPS module. For the second part of the chapter, the monitoring device is mounted in a bicycle and several mobile measurements are taken simultaneously to static ones to validate the proper operation of the equipment, and to compare the mobile sampling versus the static one for three different conditions: center of the road, free field and façade.

5.2 Methodology

5.2.1 Georeferenced Noise Sensor (GNS)

5.2.1.1 Hardware considerations

Two goals should be addressed by the proposed mobile measurement device, one is the low price of the whole set of components, and the other one regarding the accuracy, that should be equivalent to a Type 2 sound level meter for L_{Aeq} [115].

Additionally, since the spectrum data could be very useful for the post-processing of measurements to perform more complex tasks such as vehicle classification [143], soundscapes differentiation [144] or differentiating traffic from leisure noise [47], the device is designed to obtain noise levels for each $^1/_3$OB in the mentioned frequency range. The core components of the prototype are as follows:

- **Processing unit:** The main processing unit should be able to perform digital signal processing tasks as well as communicating with the different modules to acquire and store the noise data and location information. Thus, the selected microcontroller is the STM32F411RE from STMicroelectronics. Its main characteristics are:
  - 100 Mhz clock speed
  - 512kB Flash
  - 128kB RAM
  - 13 communication interfaces
- **Digital MEMS microphone:** MEMS microphones have been replacing the condenser ones in most of the consumer electronics [145]. Furthermore, it has been shown that the MEMS technology is able to fulfill the requirements for noise measurements [115, 146]. Moreover, the digital versions of the MEMS microphones are replacing the analog ones, as they offer some advantages such as the reduction in possible noise sources, since most of the components are integrated in the same chip. Therefore, the digital MEMS microphone SPH0645LM4H-B from Knowles Corporation is proposed as the noise sensor. Its frequency response is shown in Figure 5.1 and its main characteristics are summarized as follows:

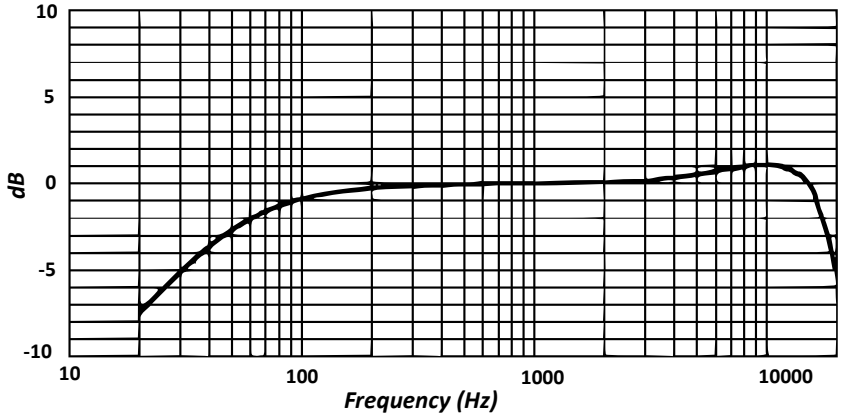

FIG. 5.1: Frequency response of the SPH0645LM4H-B MEMS microphone according to the specification sheet of the microphone [2].

- SNR of 65 dBA
- Typ. current 600 μA
- I2S Output
- Omnidirectional

- **GPS:** For the positioning information, the module RXM-GPS-RM-B from Linx Technologies was selected. Its main characteristics are: low current consumption, high precision, serial communication and low price. The module was complemented with an external passive antenna that matches the GPS frequency range (1.575 to 1.602 GHz) and the required impedance (50 Ohms).

- **Micro-SD:** Although the microcontroller is able to integrate wireless modules for data sharing, the GNS is designed to work off-line and to store the gathered data in a Micro-SD card attached to the processing unit.

- **Other components:** A 3V cell battery is connected to the processing unit to keep the Real Time Clock (RTC) synchronized. It is also used to power the Static Random Access Memory (SRAM) and RTC of the GPS module to have a faster Time To First Fix (TTFF). A 3.3V voltage regulator is connected at the input to regulate the voltage of the whole set of components. The GNS is designed to work with three AA batteries but also could be powered by an external source such as a mobile phone charger (up to 12v). Table 5.1 shows a list of the whole set of electronic components required for the measurement equipment and its price. The total cost of one unit is also shown.

Name	**Description**	**Price (€)**
STM32F411RE	Microcontroller with evaluation board	11.09
SPH0645LM4H-B	Digital MEMS microphone with evaluation board	5.70
RXM-GPS-RM-B	GPS Module (single chip)	16.44
Passive antenna	GPS antenna with micro coaxial connector	2.45
MIC5504-3.3YM5-TR	LDO voltage regulator	0.12
Micro SD	16GB Micro SD memory	11.91
Connectors and case	Coin cell, AA battery holder, plastic case, microphone connectors, Micro SD connector, leds, push button, cables, resistors and capacitors	17.68
	Total cost:	65.39

TABLE 5.1: List of materials and total price for a prototype unit.

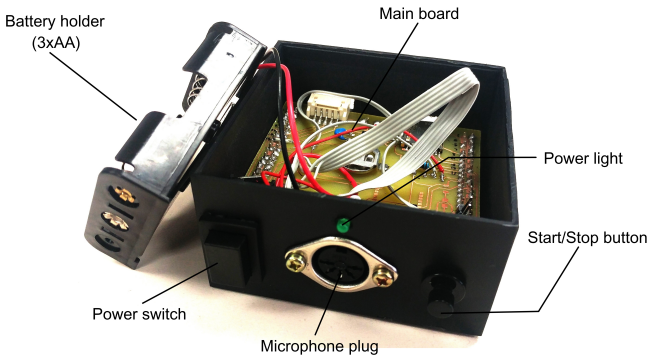

(a)

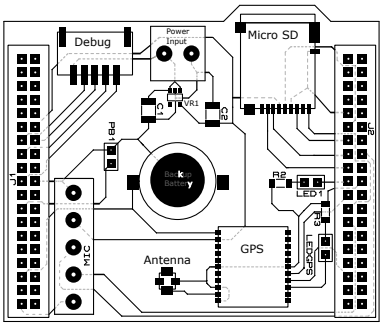

(b)

FIG. 5.2: Prototype of the georeferenced noise sensor (a) and PCB with components location to be mounted on the microcontroller evaluation board (b).

A printed circuit board (PCB), which includes all the components, was designed to be attached to the microcontroller evaluation board. Figure 5.2 shows the final design of the GNS and its PCB.

5.2.1.2 Software considerations

Since multiple task should be performed almost at the same time, the core of the software implementation is programmed based on the Real Time Operative System (RTOS) of the Mbed platform developed by ARM company and its partners [**?**]. The data must be sampled continuously to avoid losing information, and the signal processing, georeferencing and data storage tasks must not influence the sampling process. Then, proper timing and task synchronization should be carried on. The scheme presented in Figure 5.3, shows the 3 main tasks of the software implementation:

(a) **Data sampling:** This task performs the sound acquisition from the digital MEMS microphone. To ensure that no data is lost, since the samples must be taken continuously, it is configured with the highest priority. The sampled data is temporarily stored in an array of 4000 elements, according to capacity of RAM, which for a sampling frequency of $Fs = 32$ kHz, the vector is filled every 125 ms. Thus, once a full vector of data is obtained, it is copied to another 4000 vector array to process the data. Then, the signal processing task is triggered.

(b) **Signal processing:** Since the frequency response of the microphone is not totally flat for the whole range of frequencies, previous to all calculations, a filter designed to compensate the frequency response is applied to the sampled data. Then, the 125 ms A-weighted equivalent level ($SPL_{A,125ms}$) is computed. The following step is to compute the SPL for the 1/3OB ($SPL_{f_c,125ms}$). The 1/3OB filters are designed in accordance to [128, 147] for an equivalent Class 1. Moreover, in order to reduce the processing load and to improve the filter response, for frequency bands under 2.5 kHz, a decimation filter with a factor of 2 is applied (groups of 4 bands). Then, the signal is filtered for each 1/3OB (f_c = 63 Hz - 10 kHz) and the $SPL_{f_c,125ms}$ for each frequency is computed. The signal processing task is repeated 8 times to achieve a sampling time of 1 s. Then, the storage task is triggered.

(c) **Georeferencing and data storage:** Although it is possible to store the 125 ms data, since the GPS provides positioning information each 1 s, the each second equivalent level of the 1/3OB ($Leq_{f_c,1s}$) and the A-weighted one ($Leq_{A,1s}$) are computed based on the eight $SPL_{f_c,125ms}$ and $SPL_{A,125ms}$.

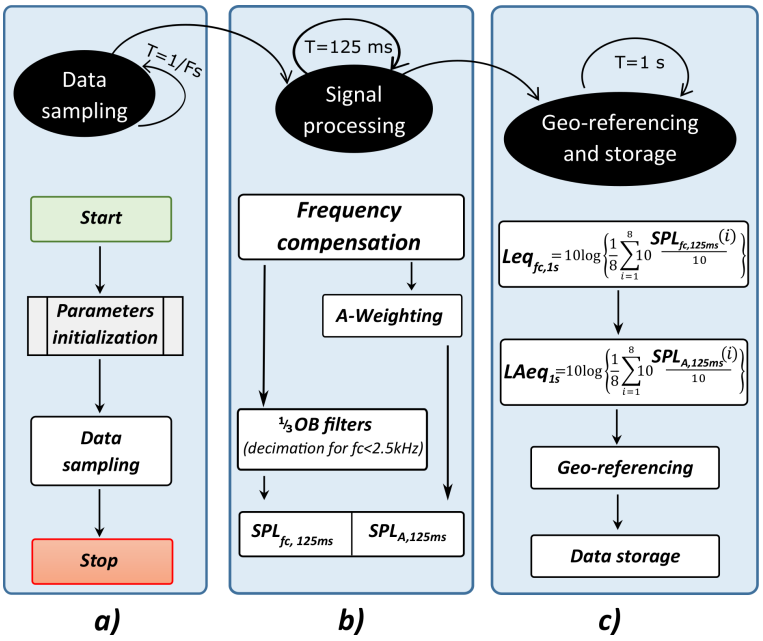

FIG. 5.3: Flow chart of the (a) data acquisition, (b) signal processing and (c) data storage tasks of the RTOS implementation.

Then, the data is appended with the time-stamp and the geographical information. Finally the data is stored in the Micro-SD card and the cycle is repeated until the measurement is stopped.

5.2.1.3 Laboratory tests

The laboratory tests were performed inside a semi-anechoic chamber using 5 GNSs and one Type 1 sound level meter (SC-310 CESVA) as a reference. A studio quality speaker with a frequency range from 50 Hz to 12 kHz was employed to produce the testing noise. The 5 MEMS microphones of the GNSs were put as close as possible surrounding the sound level meter microphone in a circular shape. The height of the microphones array was 1 m and its distance to the speaker was 45 cm. The testing setup can be observed in Figure 5.4.

The first part of the laboratory tests consists in performing a calibration of the GNSs. Thus, the calibration procedure is as follows:

1. **Frequency response:** For the range of frequencies from 50 Hz to 12 kHz, a sine-swept signal is applied to the array of GNSs to compute the frequency response [148].

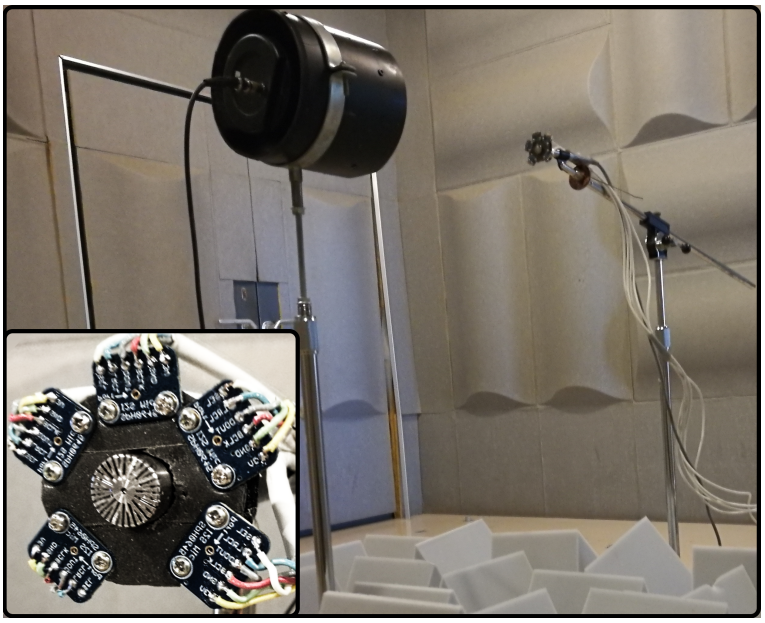

FIG. 5.4: Microphone arrangement for laboratory tests.

2. **Compensation filter:** A filter is designed and implemented based on the inverse of the frequency response of the microphone. The filter is normalized to zero gain on the 1 kHz frequency.

3. **Global calibration:** Once the frequency response of the microphone is flattened, a global calibration value is computed to reference the GNSs to the sound level meter at 94 dB@1 kHz. Thus, a signal of 1 kHz is applied to the array of GNSs for 3 minutes. The mean difference of the L_{Aeq} for the GNSs and the sound level meter is computed and used as the global calibration value.

4. **Validation:** The calibration is validated applying pink and white noise at 70 and 80 dBA (bandwidth of the speaker, from 50 Hz to 12000 kHz) to the GNSs and computing the Leq, L_{Aeq} and Leq_{fc} for the total measurement time.

Once the calibration is done, the accuracy tests as stated in [3] are performed as suggested in [115], to verify whether the GNS has an equivalent accuracy of a Type 2 sound level meter. Furthermore, in order to test the actual precision of the GNSs when measuring real traffic noise, 30 minutes of measurements were taken outside of an open window at an approximated height of 6 m. The setup of the

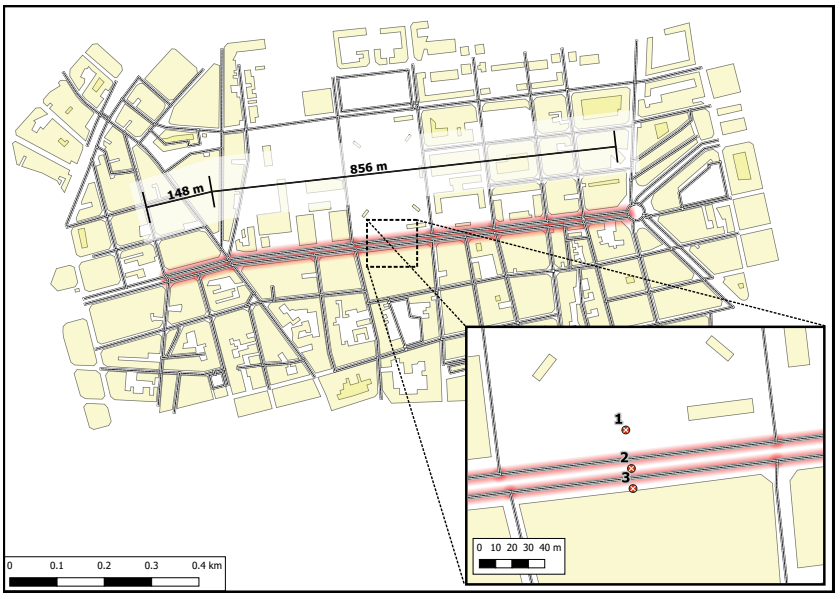

FIG. 5.5: Map of the place under study (Abat Marcet, Terrassa, Spain). The road is highlighted in red and the fixed measurement points are indicated as a circle: 1) Free field, 2) Center and 3) Façade.

microphones was the same as the one used for the laboratory tests, but the array of microphones was protected by a wind shield.

5.2.2 Mobile measurements

5.2.2.1 Study area

The second part of this research consists in the mobile sampling and the comparison to the static one. The selected street is a main avenue with 3 lanes by each side of the road and a two-way bicycle exclusive lane in the center. The width of the street is approximately 33 meters including sidewalks (22 m of traffic lanes) with an approximated traffic flow of 1000 vehicles per hour. Both, fixed and mobile measurements were taken simultaneously in the area under assessment. Three GNSs were put at an approximated height of 1.5 m in an L-shaped segment of the avenue, with buildings on one side and a soccer field on the other. Thus, one GNS was located in the free field conditions, another one at the middle of the avenue and the last one was put at 1 m from the façade. The measurement configuration and more information about the place under study is shown in Figure 5.5.

FIG. 5.6: Bike with the GNS mounted in the lower part of the seat. The microphone is located at the top of a tube at an approximated height of 2 m.

Five passes-by for each side of the road were taken using one GNS mounted in a bicycle (Figure 6.2). Special care was taken about speed, road irregularities and self generated noise by the bike to avoid external noise sources. Thus, the speed of the bike was always below 5 m/s to avoid applying any corrections. The microphone was also provided with a windshield.

5.2.3 Measurements analysis

A comparison of the noise level measured by the mobile GNSs when passes near to the static receiver is proposed. The procedure is based on the one shown in [66], where an analysis of mobile (walking person) and static measurements is done. It is proposed to join mobile samples to compute its equivalent level (aggregation of mobile samples) according to a distance of aggregation which ensures that both, the fixed and the mobile receivers are measuring the same acoustic environment.

To compare the A-weighted ($L_{Aeq,fix}$) and the 1/3OB ($Leq_{fc,fix}$) equivalent noise levels sampled by the static GNS, and the A-weighted ($L_{Aeq,mob}$) and the 1/3OB ($Leq_{fc,mob}$) equivalent noise levels sampled by the mobile one, the data should be

synchronized in time and space to study the data representative of the same sound environment. The following procedure is carried on to perform the analysis for each pass-by:

1. **Time and space synchronization:** The closest point between the mobile measurement and the fixed station is obtained. Then, for 20 s of measurements centered at the closest point, the mobile signal is shifted in time until the maximum correlation coefficient between $L_{Aeq,fix}$ and $L_{Aeq,mob}$ is obtained.

2. **Spatial aggregation:** To ensure the spatial representativeness, the 35 m radius suggested in [66] is then used for the aggregation of mobile noise measurements taking the static receiver position as a reference. The $L_{Aeq,mob}$ and $Leq_{fc,mob}$ of the set of samples within this aggregation radius is computed for the mobile measurements.

3. **Fixed-Mobile noise levels:** The $L_{Aeq,fix}$ and $Leq_{fc,fix}$ are computed for the same time-lapse as the aggregated mobile noise measurements. Thus, the noise level difference as $L_{Aeq,fix} - L_{Aeq,mob}$ and $Leq_{fc,fix} - Leq_{fc,mob}$ are finally computed.

The process is repeated 10 times (10 passes-by) for the three static receivers.

5.3 Results

5.3.1 Laboratory tests

5.3.1.1 Calibration

The frequency response of the microphone with the compensation filter response is shown in Figure 5.7a. The standard deviation of the global calibration value was ±0.27 dBA, which ensures that the same value can be used for the 5 GNSs. The calibration validation is shown as a box-plot in Figure 5.7b. It is performed using white and pink noise signals to validate the 1/3OB equivalent levels as well as the Leq and L_{Aeq}. It can be observed that the variability within GNSs is, for

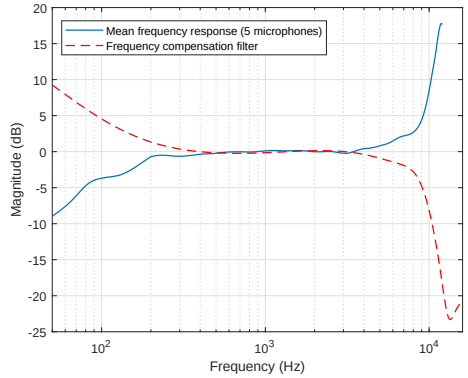

(a)

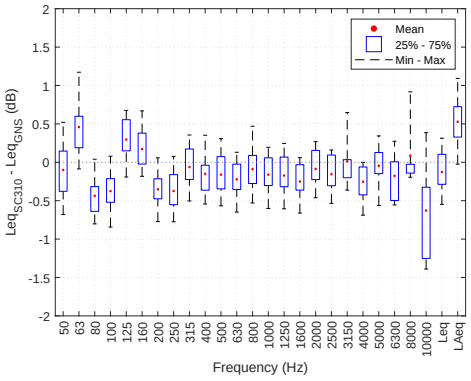

(b)

FIG. 5.7: (a) Mean frequency response of 5 SPH0645LM4H-B microphones. The frequency response of the compensation filter is also shown. (b) Box plot showing the 25%-75% percentiles, the data range and the mean differences of the Leq, L_{Aeq} and Leq_{fc}, between the sound level meter and the 5 GNSs (white and pink noise signals at 70 and 80 dBA, 20 samples in total).

most of the frequencies, under ±1 dB. Furthermore, all the 1/3OB are within ±1 dB from the reference sound level meter.

5.3.1.2 Accuracy tests

A summary of the testing results is presented in Table 5.2. It is observed that the GNS is able to measure noise levels with an equivalent accuracy as a Class 2 sound level meter for frequencies between 63 Hz to 10 kHz, which is suitable for typical environmental noise evaluation.

Frequency weighting

Frequency	Measure (dB)	Limit (dB)	Comply
63 Hz	-24.4	-26.2 ± 2	Passed
80 Hz	-21.8	-22.5 ± 2	Passed
100 Hz	-18.2	-19.1 ± 1.5	Passed
125 Hz	-15.7	-16.1 ± 1.5	Passed
160 Hz	-13.3	-13.4 ± 1.5	Passed
200 Hz	-10.9	-10.9 ± 1.5	Passed
250 Hz	-8.6	-8.6 ± 1.5	Passed
315 Hz	-6.5	-6.6 ± 1.5	Passed
400 Hz	-4.7	-4.8 ± 1.5	Passed
500 Hz	-3.2	-3.2 ± 1.5	Passed
630 Hz	-1.8	-1.9 ± 1.5	Passed
800 Hz	-1.0	-0.8 ± 1.5	Passed
1 kHz	0.0	0 ± 1	Passed
1.25 kHz	0.5	0.6 ± 1.5	Passed
1.6 kHz	0.9	1 ± 2	Passed
2 kHz	1.2	1.2 ± 2	Passed
2.5 kHz	1.3	1.3 ± 2.5	Passed
3.15 kHz	0.9	1.2 ± 2.5	Passed
4 kHz	0.9	1.0 ± 3	Passed
5 kHz	0	0.5 ± 3.5	Passed
6.3 kHz	-1.5	-0.1 ± 4.5	Passed
8 kHz	-3.2	-1.1 ± 5	Passed
10 kHz	-5	-2.5 [+5;-∞]	Passed

Self generated noise

Measure	Min	Max	Std
33.5 dBA	31.5 dBA	35.5 dBA	1.6 dBA

Long-term stability

Measure (Init/End)	Error	Limit	Comply
94.5 dBA	$0.2E^{-3}$ dBA	± 0.3 dBA	Passed

Level linearity

Frequency	Measure (Min,Max) (dBA)	Range	Comply
1 kHz	44.2, >115	70.8	Passed
4 kHz	42.1, >117	74.9	Passed
8 kHz	43.3, >116	72.7	Passed

Tone-burst

Time (ms)	Δ (dB)	Target (±lim (dB))	Comply
1000	0.0	0 (± 1)	Passed
500	0.0	-0.1 (± 1)	Passed
200	-0.1	-1.0 (± 1)	Passed
100	-2.3	-2.6 (± 1)	Passed
50	-4.3	-4.8 (+ 1, -1.5)	Passed
20	-8.6	-8.3 (+ 1, -2.0)	Passed
10	-11.6	-11.1 (+ 1, -2.0)	Passed
5	-14.6	-14.1 (+ 1, -2.5)	Passed
2	-18.6	-18.8 (+ 1, -2.5)	Passed
1	-21.4	-21.0 (+ 1, -3.0)	Passed
0.5	-23.3	-24.0 (+ 1, -4.0)	Passed
0.2	-26.2	-27.0 (+ 1, -5.0)	Passed

TABLE 5.2: Results of the accuracy test compared to the requirements for a Class 2 sound level meter indicated in IEC61672 [3, 4].

5.3.1.3 Traffic noise static measurements

A segment of 100 s of the 1 hour sampled noise (each second samples) is shown in Figure 5.8. It is observed that the $L_{Aeq,1s}$ measurements of the GNSs are quite similar to the sound level meter ones.

Figure 5.9 shows the Leq_{fc} of the GNS and the sound level meter for the half hour of traffic noise sampling. A box plot showing the mean value, 25%-75% percentiles and data range of the estimation error is also shown. It can be seen that the L_{Aeq} and Leq mean estimation errors are below ± 0.5 dB, being the second one almost zero. For the Leq_{fc}, for frequencies below 5 kHz, the estimation error is under ±1 dB from the reference. For the higher frequencies, the obtained difference is due to the low noise levels at these frequency bands, which are below the noise floor of the GNSs and also below the minimum level to ensure linearity (33.5 dB and 44.2 dB, respectively, as shown in Table 5.2).

5.3.2 Mobile measurements

5.3.2.1 GPS position accuracy

The position error was calculated based on the perpendicular distance of the actual measurement location to the closest point of the bicycle exclusive lane (Figure 5.10). The average position error of the whole set of sampled points is 7.8 m with

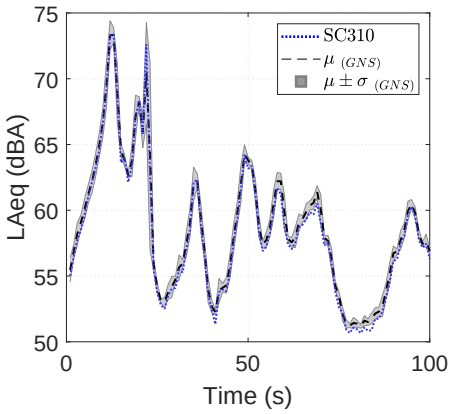

FIG. 5.8: 100 s of urban audio sampled at 1 s, the noise level measured by SC-310 sound level meter compared to the average value of the 5 GNSs and its standard deviation.

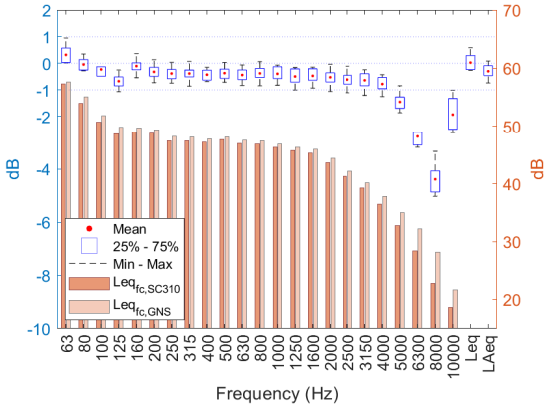

FIG. 5.9: Box-plot of the mean, the data range and the 25%-75% percentiles of the noise level difference between the GNDs and the sound level meter. The average of the Leq_{fc} measured by the 5 GNDs and the one sampled by the SC310 sound level meter is also shown.

a standard deviation of 6.2 m (the position accuracy specified by the GPS module manufacturer is 3 m). The difference in the accuracy position could be due to the placement of the GNS and its antenna, that were put under the seat of the bicycle driver, which would probably affect the signal reception as the sky-view is reduced [149]. The difference obtained between the actual position and the one obtained by the GPS is accurate enough to georeference the receiver to its corresponding street, which is the objective of adding the positioning information. The speed was also computed for the whole measurement time obtaining an average of 3.1 m/s.

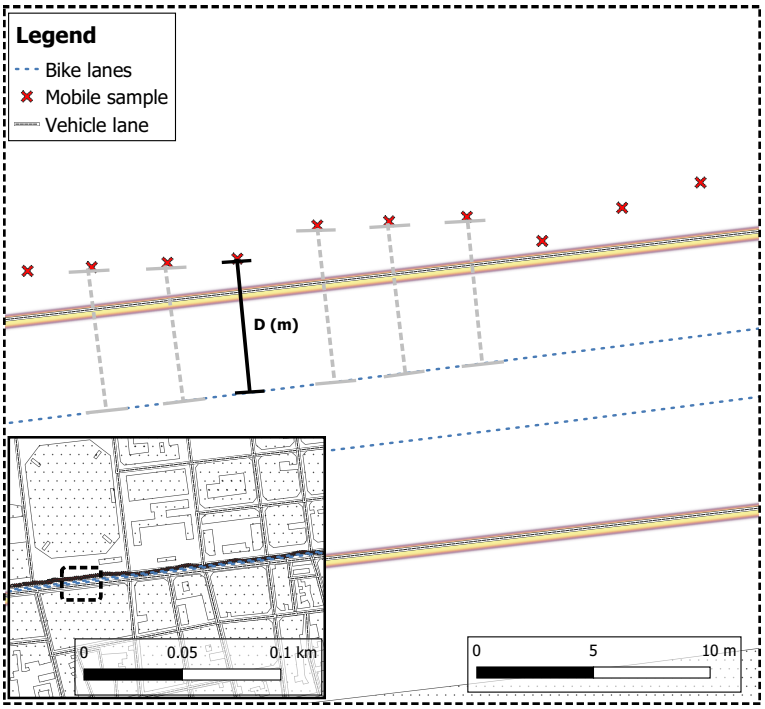

FIG. 5.10: Perpendicular distance of actual measurement to the closest point in the bicycle exclusive lane.

5.3.2.2 Fixed/Mobile comparison

Figure 5.11 shows a box-plot of the Leq_{fc} and L_{Aeq} difference between the static noise sensors minus the noise level of the mobile one for the 10 passes-by. As can be observed, the equivalent levels of the mobile measurement are most of the time higher than the fixed ones, which could be expected since the bicycle is just next to the source. Furthermore, a different pattern is observed in the noise levels measured by th GNS placed near the façade (Figure 5.11c) compared to the free-field and the center ones (Figure 5.11a and 5.11b, respectively), for the frequency bands under 250 Hz, an increase in the noise level around 4 dB is seen, which is probably caused by the façade reflections [150]. The observed variability between the passes-by, i.e. high data range in Figure 5.11, could be caused due to the relative position of the sources and the static and mobile receivers is different for each pass-by.

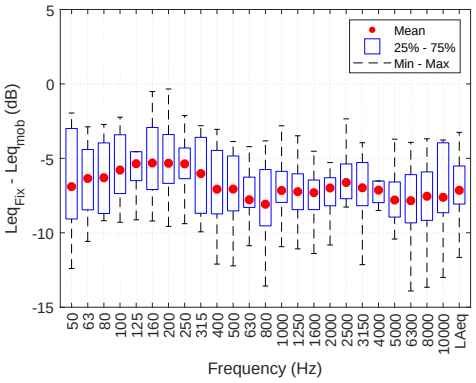

(a)

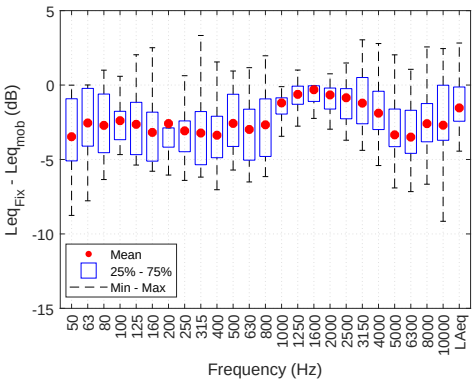

(b)

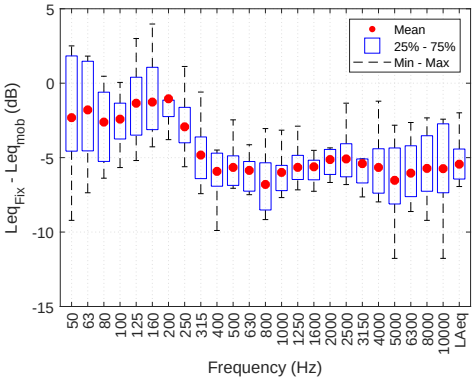

(c)

FIG. 5.11: Noise level difference between free field (a), central (b) and façade (c) fixed stations to the mobile one for Leq_{fc} and L_{Aeq}.

5.4 Analysis and discussion

The present study encourages a change in the static measurement approach by designing a noise sensor to perform mobile measurements. The huge amount of static receivers previously required, could be replaced by a small set of GNSs which would cover larger areas. Depending on the place under assessment, with just a few devices, that could be mounted in different type of vehicles, a noise map could be produced with less resources and without compromising accuracy, since the proposed noise sensor was tested to have an equivalent accuracy as a Class 2 sound level meter [3, 115].

The design of the device incorporates a digital microphone to acquire the acoustic signals, thus, the pre-amplification stage is avoided which reduces the size of the prototype, the possible sources of electrical noise and the final production price. Compared to other low-cost proposed hardware [56, 57, 60, 115, 151], the cost for assembling one unit is greatly reduced (in most of the cases around 40%), which could be decreased even more if the whole set of components are integrated in a single PCB rather than using the manufacturers evaluation boards. Additionally, the incorporation of a GPS module into the system, enables the device to perform the georeferencing of samples automatically.

The capability of the GNS to produce $^1/_3$OB spectrum, which is not common for low-cost sensor, could be useful when analyzing the noise measured while moving compared to static measurements, since the attenuation at each $^1/_3$OB are observed to be different depending on the position of the static receiver. The noise level measured at the center of the avenue is very near to the one measured with the mobile GNS. Thus, a transfer function between a static receiver at the center of the street and one located at the façade, could be developed to estimate the perceived noise level at the façade, which is the parameter required by the normative [11]. A wider set of static and mobile measurements that could also be based on simulations, which expands the variety of street configurations, could confirm that the spectrum difference between the fixed and mobile measurements follows a pattern, which has been suggested to be affected by the distance to the façade and the height of the measurement [66] as well.

The preliminary tests performed in this research confirmed that several factors should be addressed before making a noise map based on mobile measurements,

which could be related to the selected vehicle such as:

- Microphone/GNS position [65]
- Max speed [152]
- Self generated noise [60]

or related to the data processing, such as

- Samples aggregation [108, 122]
- Equivalent façade level [66]
- Crossway uncertainty [109, 129]
- Outlier detection [64]
- Sampling routes [60]
- Required samples (pass-by) [131]

Mounting the GNS in a bike has been shown to be a good option to deal with the noise of the vehicle itself and the max speed limitation. For the case of the GNS position, it was observed that the GPS antenna should be placed trying to avoid the screening of the bike driver to improve the position accuracy as suggested in [149].

Finally, for the case of the nocturnal noise measurements where the background and the actual traffic noise are very low, since the levels measured by the GNS are expected to be above 40 dB as seen in Section 5.3.1.2 (linearity and self generated noise), a technique based on street categorization and a short number of long-term static measurements could be used to estimate the L_{night} from the day-time measurements [36], instead of performing mobile measurements at night that, apart from being more expensive and resources demanding, would require longer measurement time to acquire representative values.

5.5 Conclusions

The development of a noise sensor designed to perform mobile noise measurements was introduced. The inclusion of a digital microphone simplifies the design of the noise sensor and reduces its cost since only 4 core elements are required: Microcontroller, Micro SD card, GPS and Microphone.

It was confirmed that with low-cost hardware it is possible to generate reliable noise measurements (equivalent to a Class 2 sound level meter for L_{Aeq}). Furthermore,

more complex tasks such as the $^1/_3$OB spectrum computation was also shown to be possible with accurate results. Since the hardware and programming of the GNS is the same, a very low variability within the set of GNSs was observed during the calibration and accuracy tests. Moreover, the same parameters were used for the calibration of the 5 GNSs tested, which suggest that the obtained calibration parameters could be used for further devices produced.

It was shown that the bicycle is a good option to perform mobile measurements. Anyway vehicles that are already in transit such as public transportation or delivery services, could also be used to perform the mobile measurements but further consideration should be taken.

Finally, the preliminary tests confirmed practically that in order to produce a noise map based on mobile measurements, several factors should be considered that could be related to the vehicle where the device is mounted or to the data processing to produce the noise map.

Chapter 6

Validation of noise mapping based on mobile measurements

6.1 Introduction

The main tool used to present the noise levels of a region are the noise maps. Since the European Noise Directive [11] was implemented, which states that noise maps and actions plans for noise reduction should be performed every 5 years by the Member States, several efforts have been done to improve the noise mapping processes with the aim to provide a more accurate representation of the acoustic condition of the place under study and to reduce the resources needed to do so.

One approach to obtain the noise levels to compute a noise map is through on-site measurements, which usually requires an expert to record noise levels at several sampling points for long periods. Thus, procedures addressed to reduce the number of measurement points have been proposed [17, 34, 36, 38, 91, 113]. Furthermore, it has also been shown that long-term indicators can be estimated based on short-term samples [17, 49–53]. Nowadays, many low-cost noise sensors have been developed which have been shown to provide accurate results [115, 151, 153], to replace the expensive equipment required to perform the noise measurements. Most of them are designed to be used as nodes in sensor networks [57–59, 114], with the aim to increase the spatiotemporal coverage through the placement of a large amount of devices all over the place under assessment. Moreover, the sampling approaches have been evolving since nowadays the citizens are enabled to perform noise measurements using their own smartphones [61–63] or low-cost hardware specially designed for that purpose. To deal with the random space and time distribution of samples in the citizen oriented sampling and the uncertainties introduced by the sampling methodology itself, an approach of mobile measurements has emerged as an option to increase the temporal and spatial coverage, where the measurements could be performed in transit or by setting-up specific mobile receivers [60, 65, 66]. Although these new sampling techniques and technologies offer lots of benefits, there are some drawbacks that should be addressed. The representativeness of the sampled data should be assured [61, 62, 66], which is not only limited to the data processing, it is also important to know the accuracy of the measurement equipment [154, 155]. Furthermore, to deal with the spatial heterogeneity of samples, some methodologies to improve the precision of noise mapping should be developed [30, 122, 156].

Computational methods can also be used to calculate the noise levels that will be represented in a noise map. The process to compute the noise level at a receiver

is usually separated in two sections: one related to the noise attenuation which is commonly computed using ray tracing models [16] and the other one is the calculation of the sound power emitted by the sources, usually vehicles, which are commonly modeled based on statistics, that estimates the generated noise levels according to traffic properties such as speeds, accelerations, type of paving and more [15]. It is a common practice to use average speeds and traffic flows to model the noise sources which reduces the computational processing but disregards the actual traffic dynamics [108]. Thus, depending on the resources in terms of information and computational power that can be used, performing dynamic simulation based on micro-traffic representations, as it considers the events that occur within a traffic network, is an option to obtain more representative noise levels [109, 110]. Moreover, to emulate the on-site noise measurements which would capture the whole sound environment that is not only limited to traffic noise, efforts to include most of the possible noise sources that exists in a real scenario has been done [30, 111, 112]. Anyway, since nowadays the computation of a noise map is usually based in national methods and for a local scale, a direct comparison of results between different countries is not possible. For this reason, one of the goals of the Noise Directive was to standardize the calculation methods, to carry it out, CNOSSOS [107] has emerged as a possible solution.

The present research aims to validate the noise sampling with mobile receivers by comparing the mobile noise measurements to static ones, whether the static measurements are performed experimentally or simulated. For that, on-field noise measurements are taken with mobile receivers simultaneously to reference static ones. Then, the same scenario is dynamically modeled to perform noise calculations that will be compared to the experimental results. The dynamic modeling methodology is based on micro-traffic simulations since the mobile receivers would also measure the different events that are found within the traffic network, which are represented by this type of noise modeling.

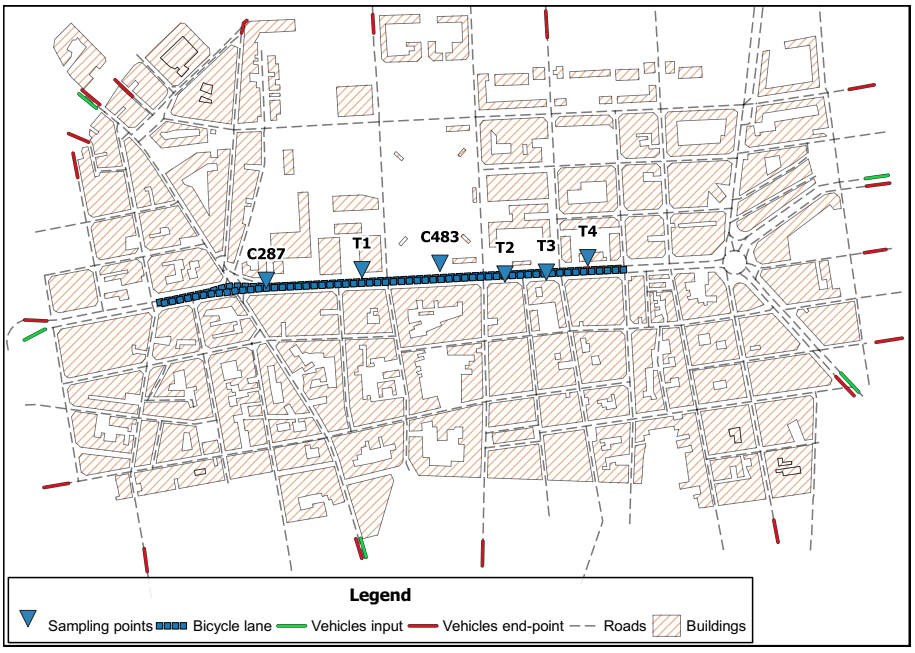

FIG. 6.1: Zone under study located in the north of Terrassa, Catalunya, Spain.

6.2 Methodology

6.2.1 Study area

For the vehicles in the micro-traffic simulation, the zone under study is an area of about 1.86 km^2 located at the north of the city of Terrassa, Catalunya, Spain, which includes around 32 km of traffic network. For the case of the mobile receiver (bicycle), the study is focused within a road segment of around 800 m in the main avenue Abat Marcet, which is a 6 lanes road (3 each side) with a two-ways bicycle exclusive lane in the middle. The map of the study zone, the location of the static sampling points and the inputs and end-points of the vehicles for the micro-traffic simulation can be seen in Figure 6.1.

Therefore, an analysis of the noise levels measured with the mobile and static measurement points is performed, where the noise levels in the static measurement points are taken as a reference to be estimated by the mobile measurements. Once the experimental tests are carried out, the testing conditions are also simulated. The steps followed to carry out the analysis are as follows:

(a) On-site sampling: Noise measurements sampled with mobile and static receivers are taken simultaneously in the place under study. The traffic flow is

also accounted during the measurement time discerning 3 types of vehicles: light, heavy and motorcycles.

(b) Micro-traffic simulation: The experimental sampling scenario is reproduced based on a micro-traffic simulation, which is needed to perform the noise level calculations.

(c) Dynamic noise modeling: Using the output data of the micro-traffic simulation, the noise levels are computed for different static receivers.

(d) Data processing and approaches comparison: Equivalent noise levels are computed for the mobile and the static receivers intended to compare the sampling approaches, where the noise levels of the static receivers are obtained experimentally or through simulations.

6.2.2 On-site sampling

In order to perform the noise measurements with the mobile receiver, which aims to obtain the L_{Aeq} at each second, a low-cost georeferenced noise sensor was mounted on a bicycle, with the microphone placed at an approximated height of 2 m, as shown in Figure 6.2. Furthermore, 4 low-cost noise sensors and 2 CESVA SC310 were put at lampposts (approximately 3 m height) and in tripods (approximately 1.5 m height) respectively, in different segments of Abat Marcet (see sampling points in Figure 6.1). Then, 1 hour of mobile measurements were taken along the avenue, simultaneously to the 6 static measurement points. A vehicle count at sampling points C297 and C483 was also performed in order to further reproduce the sampling conditions.

6.2.3 Micro-traffic simulation

The software used to model the actual traffic conditions is the micro-traffic simulation package SUMO [157], which is an open source software able to perform road traffic simulations by reproducing all the dynamics that would occur in a traffic network.

In order to match the real traffic scenario in Abat Marcet, apart from the vehicle counts that are used as traffic flow calibration points, the traffic lights and the

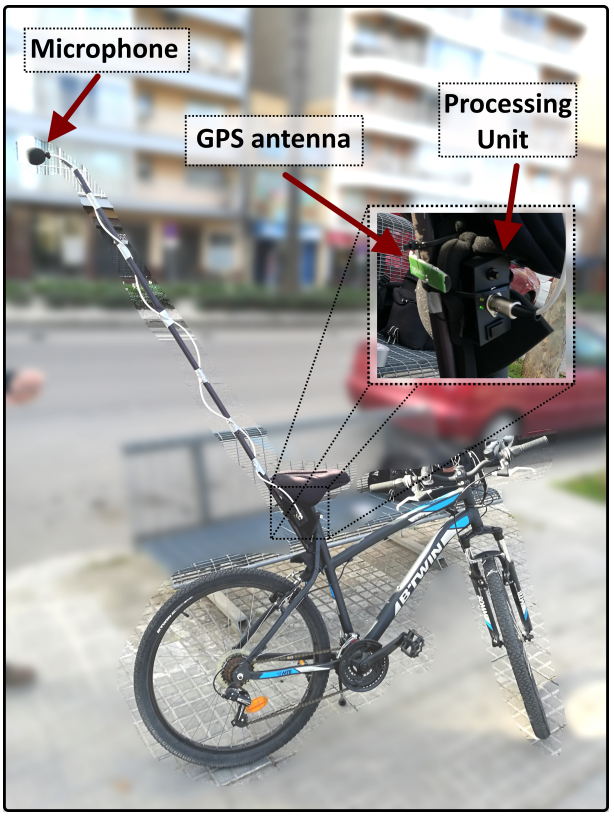

FIG. 6.2: Noise sensor mounted under the seat of the bike with the GPS antenna attached to the tube. The approximate height of the microphone is 2 m.

public transportation (buses) were also configured to match the real scenario for the studied period.

To ensure that there is traffic flow in the surrounding streets, which would also contribute to the noise levels measured by the receivers, the traffic demand was set by flow definitions and turning ratios, i.e., the streets junctions are configured based on the probability that the vehicle turns to one side or another or continues straight.

In order to simplify the routing of vehicles to the road under study, the vehicles enter only at certain specific streets and their end-point is any street that leads out of the study zone (see vehicle inputs and end-points in Figure 6.1). Thus, in order to lead just a small amount of vehicles to the vicinity of Abat Marcet which contributes but not spoils the results, the initial junction configuration is set to route the majority of the traffic, higher than 70% of vehicles depending on the junction, along the studied street as shown in Figure 6.3. The junctions and traffic demand is adjusted until the simulated traffic flow matches the vehicle

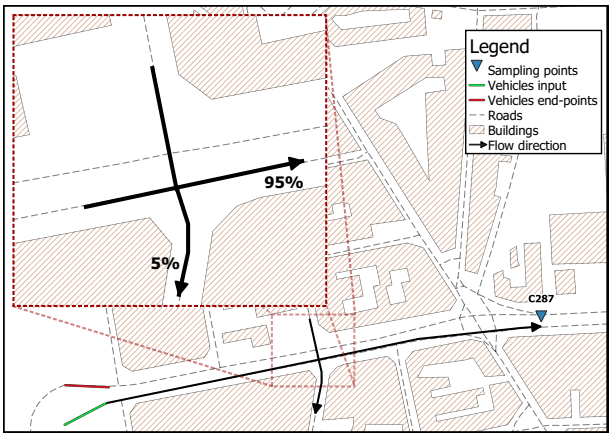

FIG. 6.3: Example of a junction configuration with 95% of cars routed with direction to the calibration point (sampling point C287) and 5% routed to other street.

count for the two points where the traffic count was performed.

Then, to obtain the possible routes that SUMO could use for the simulation, once the input demand and the junctions turn ratios are set, the JTRROUTER module of the SUMO package is used. The output of SUMO in its raw output configuration is the position lat/lon $x(t)$, the speed $v(t)$, the vehicle id (id), type of vehicle (vtype), among others at each time-step of 1 s ($\Delta t = 1$s). The acceleration $a(t)$ is computed based on the change of the speed for each Δt.

6.2.4 Dynamic noise modeling

Once the micro-traffic simulation is calibrated, the acoustic part of the simulation is performed. The output of SUMO is used to compute the noise levels for each Δt at the 6 static receivers located at the same coordinates as the experimental ones. Furthermore, a set of receivers are located all along the bicycle lane to observe the estimation error variability, which could be affected by the traffic events along the road. The procedure followed to compute the noise levels is based on the steps suggested in [30, 109, 110]. A summary of the main steps are:

(a) **Traffic modeling**: It comprises a simulation of individual vehicle trajectories at each Δt. To simplify the computations, the vehicles are matched into a fixed grid (sources). The fixed grid is created by dividing the traffic lanes into equidistant points of 3 m, as shown in Figure 6.4. Then, the vehicles

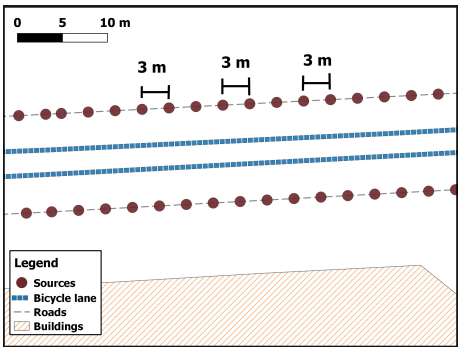

FIG. 6.4: Roads segmented into 3 m spaced points (fixed grid of sources).

are linked to their closest fixed point. The fixed points without any vehicle attached are removed.

(b) **Noise emission**: Consists of the calculation of the spectrum power of each individual vehicle at each Δt. The parameters used as input are the id, $v(t)$, $a(t)$, vtype and $a(t)$ obtained from the micro-traffic simulation. The calculation of the noise emission is based on the CNOSSOS [107] standard and it is performed using the Geographical Information System OrbisGIS which includes the Noise Modeling plug-in (v2.2.0) [124, 125].

(c) **Sound propagation**: Six receivers at the same position as the experimental measurement points were set. Furthermore, similar to the fixed grid of sources (Figure 6.4), a set of measurement points were located each 3 m along the bicycle lane to act as static receivers to assess the variability of the estimation error along the road. Thus, using again OrbisGIS and the noise modeling plug-in, which performs the noise propagations based on the NMPB [126] method, the attenuation between each receiver and its surrounding sources (within a radius of 250 m), where the reflections and diffractions are computed only for walls within 50 m from the sources-receivers propagation line, is calculated with the following parameters:

- Reflection order: 2
- Diffraction order: 1
- Road surface: dense asphalt concrete [107]
- Wall absorption: 0.2
- Temperature: 20 °C

Therefore, the noise level at each receiver can be computed based on the sum of the power emission of the surrounding vehicles (fixed sources) and its attenuation at each Δt.

(d) **Indicators calculation**: The noise indicator used to compare the noise levels measured by the static measurement points and the mobile receivers is the L_{Aeq}, which is calculated for the total measured time (temporal aggregation) for the case of the static receivers, and computed for samples within different radius (spatial aggregation) for the case of the mobile receivers. More details are presented in Section 6.2.5.

6.2.5 Data processing

For each static receiver, $\boldsymbol{i}$, whether it is simulated or experimental, the equivalent noise level of the whole measurement time, 1 hour, is computed according to the formula:

$$L_{Aeq,i} = 10log\left(\frac{1}{T}\sum_{t=1}^{T} 10^{\frac{L_{Aeq,i}(t)}{10}}\right) \tag{6.1}$$

where $T = 3600$ s.

For the mobile measurements, as shown in Figure 6.5, a spatial aggregation of samples that are within a buffer of radius $\boldsymbol{r}$ from 1 m to 100 m of each static sampling point is performed. Then, for the set of samples within the buffer, the equivalent level is computed according to the following equation:

$$L_{Aeq,i,r} = 10log\left(\frac{1}{M}\sum_{n\in N} 10^{\frac{L_{Aeq}(n)}{10}}\right) \tag{6.2}$$

where $\boldsymbol{N}$ is a subset of mobile measurements (time-steps) that are within the buffer and $\boldsymbol{M}$ is the number of elements of this subset. Then, the indicator used to compare the sampling approaches is based on the Root Mean Square Error (RMSE), which is computed between the aggregated mobile samples and the static ones for each $\boldsymbol{r}$ as:

$$RMSE_r = \sqrt{\left(\frac{1}{R}\sum_{i=1}^{R}(L_{Aeq,i}^2 - L_{Aeq,i,r}^2)\right)} \tag{6.3}$$

where R corresponds to the number of receivers to be evaluated, i.e., $R = 6$.

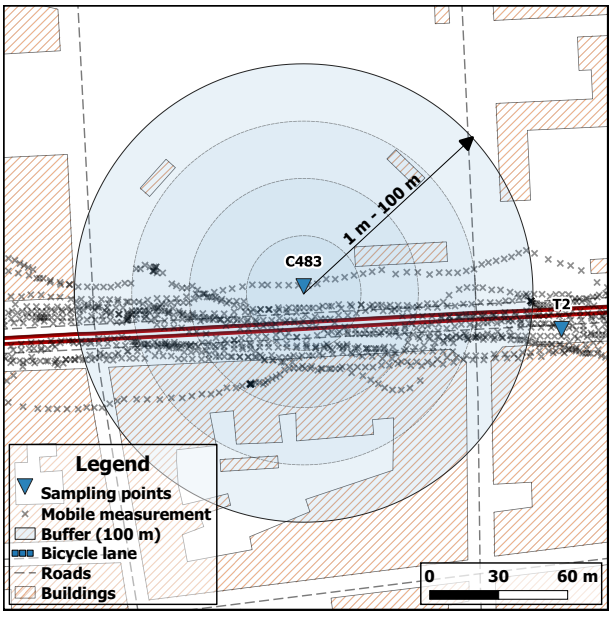

FIG. 6.5: Aggregation of samples that are within a buffer of radius from 1 m to 100 m.

Thus, in order to compare the noise levels measured by the mobile receiver and the static measurement points, the $RMSE_r$ is computed as follows:

(i) Mobile vs Static experimental: The $RMSE_r$ is computed using only experimental data for both, the mobile and the static measurements.

(ii) Mobile vs Static simulated: The $RMSE_r$ is computed between the mobile noise measurements and the simulated static receivers placed at the same positions as the experimental static measurements.

Furthermore, to assess the spatial variability along the road of the noise levels computations from the mobile sampling, a noise map of the estimation error for the 3 m spaced simulated receivers, R_{3m}, is also computed (Item (c) in Section 6.2.4). Thus, for each $i \in R_{3m}$ an aggregation of mobile samples will be performed using Equation 6.2 for the minimum radius where the $RMSE_r$ has reached a stabilization. Then, the noise level difference ε of the static minus the mobile noise levels centered to the $RMSE_{min}$ is computed as follows:

$$\varepsilon = |L_{Aeq,i} - L_{Aeq,i,min}| - RMSE_{min} \tag{6.4}$$

FIG. 6.6: Traffic count at each street for the micro-traffic simulation.

	C483		C287	
Type	**On-site**	**Sim.**	**On-site**	**Sim.**
Cars	465	495	349	351
Heavy	13	5	10	9
Motorcycles	32	34	20	16

TABLE 6.1: Simulated and measured vehicle count in 1 h in Abat Marcet street at points C483 and C287.

6.3 Results and analysis

6.3.1 Micro-taffic simulation

Figure 6.6 shows a map that illustrates the traffic flows for the micro-traffic simulation at the different streets. As expected, the traffic flow is mainly directed to Abat Marcet, as a result the secondary streets have low traffic flow. Table 6.1 shows a comparison of the vehicles counts at the calibration points for the experimental counting and the micro-traffic simulation. It can be seen that the values are very close, which should bring similar noise levels for the simulated and the actual noise measurements.

6.3.2 Dynamic noise modeling

Figure 6.7 compares the $L_{Aeq,1hr}$ measured experimentally and computed through the simulation for each of the 6 static measurement points. The higher noise level differences are found at points C287 and T1. The possible reason is that, since the vehicle counts were only performed for Abat Marcet, the vehicular traffic going along the street perpendicular to Abat Marcet (Rellinards Avenue, near point

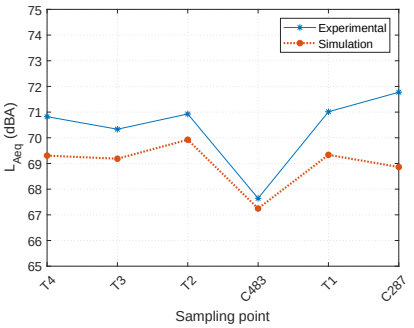

FIG. 6.7: Comparison between the on-site measurements and the simulated results of L_{Aeq} at the fixed receivers.

C287) could be underestimated. Then, since it would have a greater traffic flow, it would increase the noise level in the experimental tests in both measurement points due their proximity. Nonetheless, the noise level difference between the experimental results and the simulation stills under the range observed in the literature [15].

6.3.3 Mobile vs Static sampling

Figure 6.8 shows the $RMSE_r$ of the aggregated mobile samples for the experimental and simulated static measurement points, as proposed in Section 6.2.5. It can be observed that the $RMSE_r$ for the experimental and simulated static sampling points differs in less than ± 0.5 dB for all the aggregation radius. Furthermore, for both calculations of $RMSE_r$, after an aggregation radius of about 10 m, the reduction of the $RMSE_r$ is very low when the radius of aggregation is increased. Additionally, the $RMSE_r$ seems to stabilize after 25 m.

6.3.3.1 Map of the L_{Aeq} estimation error

Based on the results shown in Figure 6.8, the selected radius to compute the aggregated noise levels at the mobile receivers is $r = 25$ m, since after that radius the $RMSE$ is stabilized. The noise level differences between each $i \in R_{3m}$ and the aggregated mobile measurements are shown in Figure 6.9. The estimation difference is normalized to the $RMSE_{25m}$ value to appreciate better the differences. It can be seen that most of the errors fall within ± 2 dB. It can also be seen that the higher estimation errors ($|\varepsilon| > 2$ dB) are mainly found near to intersections.

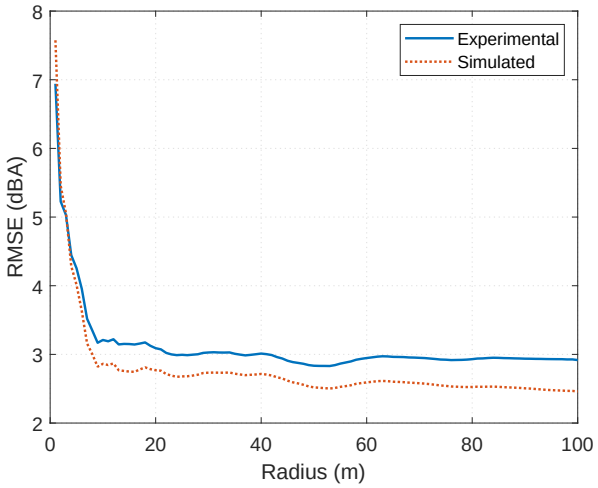

FIG. 6.8: RMSE between the aggregated noise levels of the mobile receiver and the experimental and simulated receivers.

FIG. 6.9: Noise level differences for each $i \in M$ simulated static receiver and the aggregated noise levels of the mobile measurements.

6.4 Discussion

The present research showed that calculating the L_{Aeq} on a real scenario to produce noise maps, from noise levels sampled by mobile receivers, is possible within certain estimation error that stills inside the range of other known error sources for the production of noise maps [15].

It was observed that by aggregating the noise levels of the mobile receiver, the estimation accuracy is improved. In Figure 6.8, it was observed that a stabilization of the aggregation radius was achieved. The possible cause of this stabilization is that the present study is focused only in one main avenue, which has almost constant traffic flow along the study path, thus, the L_{Aeq} for the whole street is very similar, therefore, adding data over a long distances does not add different values. The advantage of the observed stabilization is that it would allow to aggregate more samples, which would be equivalent to sample for longer time which is required for the estimation of long-term equivalent levels based on short-term sampling [17, 49–53].

Furthermore, since the mobile sampling considers the whole set of sources that can be found on a real scenario and also increases the spatial resolution of samples, it could be an option to calibrate noise maps with high spatial resolution, such as those ones where interpolation techniques are used [14, 30, 122]. Moreover, mobile sampling could be used to perform the dynamic update of noise maps that has been proposed in different studies [158–161] of which one of their limitation for scalability has been shown to be the number of measurement stations [14]. Additionally, since it has been seen that a very detailed information is required to properly model complex roads intersections, such as the one near to point C287, the mobile measurements could also be used to calibrate this type of simulations when there is lack of traffic information.

Finally, the use of low-cost hardware specifically designed for mobile measurements, i.e. that performs automatically the measurement georeferencing, is a good option to reduce the resources needed to create a noise map. Furthermore, since low-cost hardware have been shown to provide accurate noise measurements, the reliability of the samples is ensured when performing the sampling in a bicycle, since the speed and the bicycle generated noise is within acceptable values. Anyway if one wanted to use another vehicle, it should be possible but the noise

contribution of the vehicle itself should be removed as well as other factors such as the air flow, outliers detection, max speed, and more [60, 65].

6.5 Conclusion

It was shown that mobile sampling is a good option to increase the spatio-temporal coverage of samples to create a noise map. The proposed study considers both approaches of acquiring noise levels at a static receiver: measurements and simulations. It was observed that the simulation allows to estimate reasonably the noise level perceived by a mobile receiver. Anyway, more detailed information is required when assessing complex cross streets such as the one found near to measurement point 287.

The noise level difference between the mobile and the fixed measurement, which is under an acceptable estimation error, could be a good estimator of the noise level received in the façade as required by the regulations to be presented in a noise map. Thus, a noise map could be computed based only on mobile measurements, or the mobile measurements could be used to calibrate or validate noise maps based on simulations.

Finally, it was observed that mounting a noise sensor in a bicycle, brings reliable measurements and it is a proper vehicle for performing mobile noise measurements.

Chapter 7

Conclusions and further work

7.1 Conclusions

The present research has established the basis of a complete framework to perform mobile sampling, that allows creating noise maps with good accuracy and representative values but with a high reduction in the required resources.

The first step involved the development of a spatio-temporal sampling strategy that allows to estimate the long-term equivalent noise levels. Then, through a spatial stratification for traffic categories and a temporal stratification that separates working-days and weekends, a sampling strategy that estimates the weekend equivalent noise level based on measurements performed only on working-days, was proposed. For the L_{day}, $L_{evening}$ and L_{den} equivalent periods, a reduction up to 38% of the required sampling days compared to random sampling strategy was achieved. For the night period, it was shown that the temporal and spatial stratification are influenced by noise related to recreational activities and land use. Through clustering procedures, it was shown that the weekdays stratification is modified to Friday and Saturday for the weekend days instead of Saturday and Sunday. Moreover, the street classification was observed to be performed based on the level of influence of leisure activities. The new stratification led to a reduction up to 47% in the required sampling days for L_{night}.

Thus, in order to sample the equivalent time to the minimum sampling days as required by the developed spatio-temporal sampling strategy, the mobile sampling approach is proposed, with the advantage that the spatial resolution is increased as well. Based on a micro-traffic simulation coupled to acoustic modeling, the statistical requirements to perform the mobile sampling were shown. It was observed that the mobile sampling is a good option to increase the spatio-temporal resolution of sampling. Furthermore, the results brought the minimum requirements such as the aggregation of mobile measurements, which for the studied conditions was shown to be 34 m, and the number passes-by, which depends on the traffic flow, that should be set in order to reduce the estimation error.

To perform the mobile sampling on a real scenario, using a MEMS digital microphone for the acoustic signal acquisition, a micro-controller to process the data and a GPS for the automatic georeferencing of samples, a low-cost noise measuring device was designed and implemented. It was shown that the proposed prototype is able to measure the A-weighted equivalent noise level (63 Hz to 10 kHz) with

an equivalent accuracy as a Class 2 sound level meter. Furthermore, a reduction in cost of about 40% compared to other low-cost devices was obtained, with the addition that the proposed hardware is able to obtain the signal spectrum for each 1/3 octave band in the mentioned frequency range, that allows to perform a more complete analysis of the mobile measurements.

The designed measuring device was mounted on a bicycle. A first round of preliminary mobile measurement were taken along a main avenue that confirmed the proper working of the noise sensor. It was also observed that mounting the device in a bicycle reduces the external factors that could affect the noise representativeness such as the vehicle self generated noise or the maximum speed limitation. Simultaneously to static measurements, a second round of on-site mobile measurements was conducted at the same avenue. A dynamic simulation of the same scenario was also performed. The comparison of the on-site mobile measurements to the real and simulated static ones validated the requirements for noise mapping previously obtained only through simulations. The results also suggest that the reduction in the estimation error due to the aggregation of samples can arrive to a stabilization value which would allow to add up mobile samples at larger radius (ideally up to the street length), that would be equal to increase the measurement time.

The steps followed in the present research allowed to identify and face some of the challenges to create noise maps based on mobile measurements of environmental noise. The proposed sampling strategy, apart from reducing the required number of sampled days for L_{day}, $L_{evening}$, L_{night} and L_{den}, allows to know an approximation of the uncertainty when estimating the long-term equivalent levels.

Furthermore, the mobile sampling approach, which is not new but has not been deeply studied before, was shown to be feasible and, when using vehicles already in transit, enables a high reduction in the required resources to produce a noise map without disregarding accuracy and representativeness. That, if it is complemented with accurate low-cost hardware, enhance even more the mobile sampling scheme.

The combination of mobile measurements and the proposed spatio-temporal sampling strategy, would allow the creation of noise maps in an easier, faster and cheaper way, which would help to extend the noise level assessment to agglomerations even with lower population than the indicated in the Noise Directive, or to allow the noise level assessment in cities or countries under development with

lower resources dedicated to this environmental field.

7.2 Further work

The present research laid the foundation of performing mobile sampling which opens many possible future works to expand and improve the methodology. Some of them are mentioned in this section.

Vehicle selection

The proposed vehicle to perform the mobile sampling was a bicycle since it has less self produced noise. Also, its driving speed would not require a correction due to the airflow. Anyway, a different vehicle could be selected but tasks such as the removal of the noise contribution of the vehicle itself or the placement of the microphone should be studied.

Sampling routes

Depending on the vehicle where the device is mounted, whether it is public transportation or other vehicle already in transit, an optimization of the routes is required to reduce the estimation error and to represent the whole set of acoustic environments within a city.

Mobile samples aggregation

The possibility that the aggregation radius of mobile samples can be extended for samples taken within the same street is interesting. If the aggregation radius stabilizes at a minimum value, it would allow to increase the aggregation radius which equals to extend the measurement time. The on-site measurements taken in this research suggested that it is possible but further tests in different scenarios are required to validate it.

Façade noise level

According to the regulations [11], the equivalent level to be presented in noise maps is the one perceived in façade. Since for the assessment of a city, several factors could affect the way sound is propagated, a transfer function could be investigated to find out a mathematical relation between a receiver placed at the center of the street and the noise level perceived in the façade.

Sensor networks and real-time noise mapping

The developed noise sensor can be complemented with a wireless module for data transmission that would allow to create a sensor network of mobile nodes. Thus, the possibility to dynamically update noise maps based on mobile samples arises. Moreover, a deeper research is required in order to properly combine static and mobile measurements to estimate nocturnal noise levels.

Bibliography

[1] Metropolitan Area of Barcelona (AMB), Geoportal of Cartography., last visited september 2018. URL: https://geoportalcartografia.amb.cat/AppGeoportalCartografia2/index.html.

[2] Knowles, Datasheet: SPH0645LM4H-B Crawford, https://www.knowles.com/docs/default-source/model-downloads/sph0645lm4h-b-datasheet-rev-c.pdf, Accessed: 2019-03-22.

[3] I. E. Commission, et al., Electroacoustics-sound level meters-part 1: Specifications (iec 61672-1), Geneva, Switzerland (2013).

[4] I. E. Commission, et al., Electroacoustics-sound level meters-part 3: Part 3: Periodic tests (iec 61672-3), Geneva, Switzerland (2013).

[5] M. Basner, W. Babisch, A. Davis, M. Brink, C. Clark, S. Janssen, S. Stansfeld, Auditory and non-auditory effects of noise on health, The Lancet 383 (2014) 1325–1332.

[6] S. A. Stansfeld, M. P. Matheson, Noise pollution: Non-auditory effects on health, British Medical Bulletin 68 (2003) 243–257.

[7] L. Sobotova, J. Jurkovicova, Z. Stefanikova, L. Sevcikova, L. Aghova, Community response to environmental noise and the impact on cardiovascular risk score, Science of the Total Environment 408 (2010) 1264–1270.

[8] R. Makarewicz, M. Galuszka, Empirical revision of noise mapping, Applied Acoustics 72 (2011) 578–581.

[9] M. Raimbault, D. Dubois, Urban soundscapes: Experiences and knowledge, Cities 22 (2005) 339–350.

[10] K. T. Tsai, M. D. Lin, Y. H. Chen, Noise mapping in urban environments: A Taiwan study, Appl. Acoust. 70 (2009) 964–972.

[11] European Comission, Directive 2002/49/EC relating to the assessment and management of environmental noise, 2002.

[12] F. A. de Noronha Castro Pinto, M. D. Moreno Mardones, Noise mapping of densely populated neighborhoods - Example of Copacabana, Rio de Janeiro - Brazil, Environmental Monitoring and Assessment 155 (2009) 309–318.

[13] WG-AEN, Good Practice Guide for Strategic Noise Mapping and the Production of Associated Data on Noise Exposure, 2003.

[14] W. Wei, T. Van Renterghem, B. De Coensel, D. Botteldooren, Dynamic noise mapping: A map-based interpolation between noise measurements with high temporal resolution, Appl. Acoust. 101 (2016) 127–140.

[15] J. Prezelj, J. Murovec, Traffic noise modelling and measurement: Interlaboratory comparison, Appl. Acoust. 127 (2017) 160–168.

[16] N. Garg, S. Maji, A critical review of principal traffic noise models: Strategies and implications, Environ. Impact Assess. Rev. 46 (2014) 68–81.

[17] J. Romeu, M. Genescà, T. Pàmies, S. Jiménez, Street categorization for the estimation of day levels using short-term measurements, Applied Acoustics 72 (2011) 569–577.

[18] D. Montes González, J. M. Barrigón Morillas, G. Rey Gozalo, The influence of microphone location on the results of urban noise measurements, Appl. Acoust. 90 (2015) 64–73.

[19] A. V. Vasilyev, New Methods and Approaches to Acoustic Monitoring and Noise Mapping of Urban Territories and Experience of it Approbation in Conditions of Samara Region of Russia, Procedia Eng. 176 (2017) 669–674.

[20] M. Hamed, W. Effat, A gis-based approach for the screening assessment of noise and vibration impacts from transit projects, Journal of Environmental Management 84 (2007) 305–313.

[21] S. Kephalopoulos, M. Paviotti, F. Anfosso-Lédée, D. Van Maercke, S. Shilton, N. Jones, Advances in the development of common noise assessment methods in Europe: The CNOSSOS-EU framework for strategic environmental noise mapping, Sci. Total Environ. 482-483 (2014) 400–410.

[22] S. Givargis, H. Karimi, A basic neural traffic noise prediction model for Tehran's roads, Journal of Environmental Management 91 (2010) 2529–2534.

[23] D. W. Morley, K. D. Hoogh, D. Fecht, F. Fabbri, M. Bell, P. S. Goodman, P. Elliott, S. Hodgson, A. L. Hansell, J. Gulliver, International scale implementation of the CNOSSOS-EU road traf fi c noise prediction model for epidemiological studies, Environ. Pollut. 206 (2015) 332–341.

[24] J. Romeu Garbí, S. Jiménez Diaz, M. Genesca Francitorra, Á. Sánchez Venegas, Recreation noise in acoustic mapping, in: 39th International Congress on Noise Control Engineering, 2010, pp. 1–10.

[25] E. M. Salomons, S. A. Janssen, H. L. Verhagen, Local impact assessment of urban traffic noise, Noise Control Engineering Journal 62 (2014) 449–466.

[26] A. Can, T. Van Renterghem, M. Rademaker, S. Dauwe, P. Thomas, B. De Baets, D. Botteldooren, Sampling approaches to predict urban street noise levels using fixed and temporary microphones., Journal of Environmental Monitoring 13 (2011) 2710–9.

[27] J. M. Barrigón Morillas, C. Prieto Gajardo, Uncertainty evaluation of continuous noise sampling, Applied Acoustics 75 (2014) 27–36.

[28] International Organization for Standardization, ISO 1996-2:2007. Acoustics – Description, measurement and assessment of environmental noise – Part 2: Determination of environmental noise levels, 2007.

[29] V. Gómez Escobar, J. M. Barrigón Morillas, G. Rey Gozalo, R. Vílchez-Gómez, J. Carmona Del Río, J. A. Méndez Sierra, Analysis of the Grid Sampling Method for Noise Mapping, Archives of Acoustics 37 (2012) 499–514.

[30] P. Aumond, L. Jacquesson, A. Can, Probabilistic modeling framework for multisource sound mapping, Appl. Acoust. 139 (2018) 34–43.

[31] H. D. Kluijver, J. Stoter, H. de Kluijver, J. Stoter, Noise mapping and GIS: Optimising quality and efficiency of noise effect studies, Comput. Environ. Urban Syst. 27 (2003) 85–102.

[32] C. Asensio, M. Ruiz, I. Pavón, M. Ausejo, M. Recuero, Uncertainty in noise maps isolines: The effect of the sampling grid, Acta Acustica united with Acustica 97 (2011) 237–242.

[33] J. M. Barrigón Morillas, C. Ortiz-Caraballo, C. Prieto Gajardo, The temporal structure of pollution levels in developed cities, Science of the Total Environment 517 (2015) 31–37.

[34] C. Prieto Gajardo, J. M. Barrigón Morillas, G. Rey Gozalo, R. Vílchez-Gómez, Can weekly noise levels of urban road traffic, as predominant noise source, estimate annual ones?, The Journal of the Acoustical Society of America 140 (2016) 3702–3709.

[35] G. Rey Gozalo, J. M. Barrigón Morillas, C. Prieto Gajardo, Urban noise functional stratification for estimating average annual sound level., The Journal of the Acoustical Society of America 137 (2015) 3198–208.

[36] J. Romeu, S. Jiménez, M. Genescà, T. Pàmies, R. Capdevila, Spatial sampling for night levels estimation in urban environments., The Journal of the Acoustical Society of America 120 (2006) 791–800.

[37] A. L. Brown, K. C. Lam, Urban noise surveys, Appl. Acoust. 20 (1987) 23–39.

[38] J. M. B. Morillas, V. G. Escobar, J. A. M. Sierra, R. Vílchez-Gómez, J. M. Vaquero, J. T. Carmona, A categorization method applied to the study of urban road traffic noise, The Journal of the Acoustical Society of America 117 (2005) 2844–2852.

[39] E. Murphy, E. A. King, Strategic environmental noise mapping: Methodological issues concerning the implementation of the EU Environmental Noise Directive and their policy implications, Environment International 36 (2010) 290–298.

[40] G. Zambon, R. Benocci, G. Brambilla, Cluster categorization of urban roads to optimize their noise monitoring, Environmental Monitoring and Assessment 188 (2015) 26.

[41] H. Doygun, D. Kuşat Gurun, Analysing and mapping spatial and temporal dynamics of urban traffic noise pollution: A case study in Kahramanmaraş, Turkey, Environ. Monit. and Assess. 142 (2008) 65–72.

[42] A. Can, G. Guillaume, B. Gauvreau, Noise indicators to diagnose urban sound environments at multiple spatial scales, Acta Acust. united with Acust. 101 (2015) 964–974.

[43] V. S. Wang, E. W. Lo, C. H. Liang, K. P. Chao, B. Y. Bao, T. Y. Chang, Temporal and spatial variations in road traffic noise for different frequency components in metropolitan Taichung, Taiwan, Environ. Pollut. 219 (2016) 174–181.

[44] X. Han, X. Huang, H. Liang, S. Ma, J. Gong, Analysis of the relationships between environmental noise and urban, Environ. Pollut. 233 (2018) 755–763.

[45] J. Barrigón, V. Gómez, J. Méndez, R. Vílchez, J. Vaquero, Effects of Leisure Activity Related Noise in Residential Zones, Build. Acoust. 12 (2005) 265–276.

[46] M. J. Ballesteros, M. D. Fernández, J. A. Ballesteros, Acoustic evaluation of leisure events in two mediterranean cities, Appl. Acoust. 89 (2015) 288–296.

[47] M. J. Ballesteros, A. J. Torija, M. D. Fernandez, J. A. Ballesteros, Differences between road traffic and leisure noise in urban areas. Developing a model for automatic identification, Acta Acust. United Ac. 102 (2016) 35–44.

[48] E. Ottoz, L. Rizzi, F. Nastasi, Recreational noise: Impact and costs for annoyed residents in Milan and Turin, Appl. Acoust. 133 (2018) 173–181.

[49] C. H. Ng, S. K. Tang, On monitoring community noise using arbitrarily chosen measurement periods, Applied Acoustics 69 (2008) 649–661.

[50] H. Safeer, J. Wesler, E. Rickley, Errors due to sampling in community noise level distributions, Journal of Sound and Vibration 24 (1972) 365–376.

[51] C. Prieto Gajardo, J. M. Barrigón Morillas, Stabilisation patterns of hourly urban sound levels, Environmental monitoring and assessment 187 (2015) 4072.

[52] E. Gaja, A. Gimenez, S. Sancho, A. Reig, Sampling techniques for the estimation of the annual equivalent noise level under urban traffic conditions, Applied Acoustics 64 (2003) 43–53.

[53] L. Brocolini, C. Lavandier, M. Quoy, C. Ribeiro, Measurements of acoustic environments for urban soundscapes: choice of homogeneous periods, optimization of durations, and selection of indicators., The Journal of the Acoustical Society of America 134 (2013) 813–821.

[54] A. J. Torija, D. P. Ruiz, Á. Ramos-Ridao, Required stabilization time, short-term variability and impulsiveness of the sound pressure level to characterize the temporal composition of urban soundscapes, Applied Acoustics 72 (2011) 89–99.

[55] M. Hueso, A. Giménez, S. Sancho, E. Gaja, Measurement techniques of noise level in various urban scenarios. Day selection and representative period, Applied Acoustics 116 (2017) 216–228.

[56] I. Hakala, I. Kivel, I. Kivelä, J. Ihalainen, J. Luomala, C. Gao, Design of low-cost noise measurement sensor network: Sensor function design, Proceedings - 1st International Conference on Sensor Device Technologies and Applications, SENSORDEVICES 2010 (2010) 172–179.

[57] J. Segura-Garcia, S. Felici-Castell, J. J. Perez-Solano, M. Cobos, J. M. Navarro, Low-cost alternatives for urban noise nuisance monitoring using wireless sensor networks, IEEE Sens. J. 15 (2015) 836–844.

[58] P. Rawat, K. Deep, H. Chaouchi, J. Marie, K. D. Singh, H. Chaouchi, J. M. Bonnin, Wireless sensor networks: A survey on recent developments and potential synergies, J. Supercomput. 68 (2014) 1–48.

[59] P. W. Wessels, T. G. H. Basten, Design aspects of acoustic sensor networks for environmental noise monitoring, Appl. Acoust. 110 (2016) 227–234.

[60] R. M. Alsina-Pagès, U. Hernandez-Jayo, F. Alías, I. Angulo, Design of a mobile low-cost sensor network using urban buses for real-time ubiquitous noise monitoring, Sensors (Switzerland) 17 (2017) 1–21.

[61] E. D'Hondt, M. Stevens, A. Jacobs, Participatory noise mapping works! An evaluation of participatory sensing as an alternative to standard techniques for environmental monitoring, Pervasive Mob. Comput. 9 (2013) 681–694.

[62] S. S. Kanhere, Participatory Sensing: CrowdSourcing Data from Mobile Phones in Urban Spaces, 12th IEEE International Conference on Mobile Data Management (MDM) (2011) 3–6.

[63] C. A. Kardous, P. B. Shaw, Evaluation of smartphone sound measurement applications., The Journal of the Acoustical Society of America 135 (2014) EL186–92.

[64] A. Can, G. Guillaume, J. Picaut, Cross-calibration of participatory sensor networks for environmental noise mapping, Appl. Acoust. 110 (2016) 99–109.

[65] G. Bennett, E. King, J. Curn, Environmental noise mapping using measurements in transit, ... Conf. Noise ... (2010) 1795–1810.

[66] G. Guillaume, P. Aumond, P. Chobeau, A. Can, Statistical study of the relationships between mobile and fi xed stations measurements in urban environment, Build. Environ. 149 (2019) 404–414.

[67] J. C. Blanco, I. Flindell, Property prices in urban areas affected by road traffic noise, Applied Acoustics 72 (2011) 133–141.

[68] W. H. Organization, et al., Health as the pulse of the new urban agenda: United nations conference on housing and sustainable urban development, quito, october 2016, 2016.

[69] E. A. King, H. J. Rice, The development of a practical framework for strategic noise mapping, Applied Acoustics 70 (2009) 1116–1127.

[70] D. W. Morley, J. Gulliver, Methods to improve traffic flow and noise exposure estimation on minor roads, Environmental Pollution 216 (2016) 746–754.

[71] E. A. King, E. Murphy, H. J. Rice, Implementation of the EU environmental noise directive: Lessons from the first phase of strategic noise mapping and action planning in Ireland, Journal of Environmental Management 92 (2011) 756–764.

[72] P. Cohen, O. Potchter, I. Schnell, The impact of an urban park on air pollution and noise levels in the Mediterranean city of Tel-Aviv, Israel., Environmental pollution (Barking, Essex : 1987) 195 (2014) 73–83.

[73] L. Maffei, M. Masullo, Electric vehicles and urban noise control policies, Archives of Acoustics 39 (2014) 333–341.

[74] Y. Avsar, B. D. Gumus, The application of noise maps for traffic noise reduction, Noise Control Engineering Journal 59 (2011) 715–723.

[75] F. Zuo, Y. Li, S. Johnson, J. Johnson, S. Varughese, R. Copes, F. Liu, H. J. Wu, R. Hou, H. Chen, Temporal and spatial variability of traffic-related noise in the City of Toronto, Canada, Science of the Total Environment 472 (2014) 1100–1107.

[76] S. Jiménez, M. Genescà, J. Romeu, A. Sánchez, Estimation of night traffic noise levels, Acta Acustica united with Acustica 94 (2008) 563–567.

[77] C. P. Gajardo, J. M. B. Morillas, V. G. Escobar, R. Vílchez-Gómez, G. R. Gozalo, Effects of singular noisy events on long-term environmental noise measurements, Polish Journal of Environmental Studies 23 (2014) 2007–2017.

[78] P. Mioduszewski, J. A. Ejsmont, J. Grabowski, D. Karpiński, Noise map validation by continuous noise monitoring, Applied Acoustics 72 (2011) 582–589.

[79] R. Khaiwal, T. Singh, J. P. Tripathy, S. Mor, S. Munjal, B. Patro, N. Panda, Assessment of noise pollution in and around a sensitive zone in North India and its non-auditory impacts, Science of the Total Environment 566-567 (2016) 981–987.

[80] V. Bruno, F. Fradet, P. Sylvain, The Development of a Permanent Network for Measuring Environmental Noise at the Urban-Area Level, acoucité (2009).

[81] D. Geraghty, P. Mcdonald, I. Humphreys, Analysis of Urban Noise in Dublin Using Long-Term Data From a Publically Accessible Permanent Monitoring Network, Transp. Res. Board, 94th Annu. Meet. 15-3943 (2015).

[82] D. I. Mihajlov, M. R. Prascevic, Permanent and Semi-permanent Road Traffic Noise Monitoring in the City of Nis (Serbia), Low Frequency Noise, Vibration and Active Control 34 (2015) 251–268.

[83] K. Vogiatzis, Environmental noise and air pollution monitoring in the athens ring road ('attiki odos') an important parameter for a sustainable urban development, International Journal of Sustainable Development and Planning 10 (2015) 528–543.

[84] A. Czyzewski, J. Kotus, M. Szczodrak, Online urban acoustic noise monitoring system, Noise Control Engineering Journal 60 (2012) 69–84. Cited By 4.

[85] Dublin City Council, Dublin City Council Annual Report and Accounts 2010, 2011.

[86] WHO Regional Office for Europe, Burden of disease from environmental noise. Quantification of healthy life years lost in Europe, 2011.

[87] T. Münzel, F. P. Schmidt, S. Steven, J. Herzog, A. Daiber, M. Sørensen, Environmental Noise and the Cardiovascular System, J. Am. Coll. Cardiol. 71 (2018) 688–697.

[88] M. Basner, S. McGuire, WHO environmental noise guidelines for the european region: A systematic review on environmental noise and effects on sleep, Int. J. Env. Res. Pub. He. 15 (2018).

[89] F. Rudzik, L. Thiesse, R. Pieren, J. M. Wunderli, M. Brink, M. Foraster, H. Héritier, I. C. Eze, C. Garbazza, D. Vienneau, et al., Sleep spindle characteristics and arousability from night-time transportation noise exposure in healthy young and older individuals, Sleep (2018).

[90] M. Foraster, N. Künzli, I. Aguilera, M. Rivera, D. Agis, J. Vila, L. Bouso, A. Deltell, J. Marrugat, R. Ramos, J. Sunyer, R. Elosua, X. Basagaña, High blood pressure and long-term exposure to indoor noise and air pollution from road traffic, Environ. Health Persp. 122 (2014) 1193–1200.

[91] G. Quintero, A. Balastegui, J. Romeu, Annual traffic noise levels estimation based on temporal stratification, J. Environ. Manage. 206 (2018) 1–9.

[92] Ajuntament Barcelona, Tourism activity of Barcelona destination (text in Catalan), last visited May 2018. URL: https://ajuntament.barcelona.cat/turisme/sites/default/files/2016_activitat_turistica_de_la_destinacio_barcelona_1.pdf.

[93] I. ISO, 16032. acoustics-measurement of sound pressure level from service equipment in buildings-engineering method, International Organization for Standardization (2004).

[94] P. J. Rousseeuw, Silhouettes: A graphical aid to the interpretation and validation of cluster analysis, J. Comput. Appl. Math. 20 (1987) 53–65.

[95] A. K. Jain, Data clustering: 50 years beyond K-means, Pattern Recog. Lett. 31 (2010) 651–666.

[96] G. Quintero, J. Romeu, A. Balastegui, Seasonal, monthly and daily stratification for annual noise level estimation, INTER-NOISE 2017 - 46th Int. Congr. Expo. Noise Control Eng. Taming Noise Mov. Quiet (2017) 1–7.

[97] G. Zambon, R. Benocci, G. Brambilla, Cluster categorization of urban roads to optimize their noise monitoring, Environ. Monit. Assess. 188 (2016) 1–11.

[98] G. Rey Gozalo, J. M. Barrigón Morillas, V. Gómez Escobar, Analyzing nocturnal noise stratification, Science of the Total Environment 479-480 (2014) 39–47.

[99] B. Jakovljevic, K. Paunovic, G. Belojevic, Road-traffic noise and factors influencing noise annoyance in an urban population, Environ. Int. 35 (2009) 552–556.

[100] C. Nugent, N. Blanes, J. Fons, M. S. de la Maza, M. J. Ramos, F. Domingues, A. van Beek, D. Houthuijs, Noise in Europe 2014, 10, European Environment Agency, 2014. doi:10.2800/763331.

[101] P. Frei, E. Mohler, M. Röösli, Effect of nocturnal road traffic noise exposure and annoyance on objective and subjective sleep quality, Int. J. Hyg. Environ. Health 217 (2014) 188–195.

[102] K. Drew, R. Macfarlane, T. Oiamo, M. Stefanova, Desislava, Campbell, How loud is too loud? Health Impacts of Environmental Noise in Toronto, 2017. URL: http://www.toronto.ca/legdocs/mmis/2017/hl/bgrd/backgroundfile-104525.pdf, accessed: October 2018.

[103] C. Drudge, J. Johnson, E. MacIntyre, Y. Li, R. Copes, S. Ing, S. Johnson, S. Varughese, H. Chen, Exploring nighttime road traffic noise: A comprehensive predictive surface for Toronto, Canada, J. Occup. Environ. Hyg. 15 (2018) 389–398.

[104] WHO, Night noise guidelines for Europe, World Health Organization Regional Office for Europe, 2009.

[105] C. Steele, Critical review of some traffic noise prediction models, Appl. Acoust. 62 (2001) 271–287.

[106] G. Licitra, E. Ascari, Gden: An indicator for European noise maps comparison and to support action plans, Sci. Total Environ. 482-483 (2014) 411–419.

[107] Kephalopoulos, Stylianos and Paviotti, Marco and Anfosso-Lédée, Fabienne, Common Noise Assessment Methods in Europe (CNOSSOS-EU), 2012. doi:10.2788/31776.

[108] B. De Coensel, D. Botteldooren, F. Vanhove, S. Logghe, Microsimulation based corrections on the road traffic noise emission near intersections, Acta Acust. united with Acust. 93 (2007) 241–252.

[109] E. Chevallier, L. Leclercq, J. Lelong, R. Chatagnon, Dynamic noise modeling at roundabouts, Appl. Acoust. 70 (2009) 761–770.

[110] A. Can, L. Leclercq, J. Lelong, D. Botteldooren, Traffic noise spectrum analysis: Dynamic modeling vs. experimental observations, Appl. Acoust. 71 (2010) 764–770.

[111] F. Aletta, J. Kang, Soundscape approach integrating noise mapping techniques: A case study in Brighton, UK, Noise Mapp. 2 (2015) 1–12.

[112] Y. R. Chew, B. S. Wu, A soundscape approach to analyze traffic noise in the city of taipei , taiwan, Comput. Environ. Urban Syst. 59 (2016) 78–85.

[113] G. Quintero, J. Romeu, A. Balastegui, Temporal and spatial stratification for the estimation of nocturnal long-term noise levels, Environ. Pollut. 245 (2019) 666–674.

[114] X. Sevillano, J. C. Socoró, F. Alías, P. Bellucci, L. Peruzzi, S. Radaelli, P. Coppi, L. Nencini, A. Cerniglia, A. Bisceglie, R. Benocci, G. Zambon, DYNAMAP – Development of low cost sensors networks for real time noise mapping, Noise Mapp. 3 (2016) 172–189.

[115] C. Mydlarz, J. Salamon, J. Pablo, The implementation of low-cost urban acoustic monitoring devices, Appl. Acoust. 117 (2017) 207–218.

[116] Smartcitizen, https://smartcitizen.me/, 2011. Accessed: 2019-02-15.

[117] NoiseTube, http://www.noisetube.net/, 2008. Accessed: 2019-02-15.

[118] CITI-SENSE, http://www.citi-sense.eu/, 2012. Accessed: 2017-03-14.

[119] E. Kanjo, NoiseSPY: A real-time mobile phone platform for urban noise monitoring and mapping, Mob. Networks Appl. 15 (2010) 562–574.

[120] R. K. Rana, C. T. Chou, S. S. Kanhere, N. Bulusu, W. Hu, Ear-Phone : An End-to-End Participatory Urban Noise Mapping System, Proc. Int. Conf. Inf. Process. Sens. Networks IPSN (2010) 105–116.

[121] P. Aumond, A. Can, V. Mallet, B. De Coensel, C. Ribeiro, D. Botteldooren, C. Lavandier, Kriging-based spatial interpolation from measurements for sound level mapping in urban areas, J. Acoust. Soc. Am. 143 (2018) 2847–2857.

[122] A. Can, L. Dekoninck, D. Botteldooren, Measurement network for urban noise assessment: Comparison of mobile measurements and spatial interpolation approaches, Appl. Acoust. 83 (2014) 32–39.

[123] SYMUVIA, http://www.licit-lyon.eu/themes/realisations/plateformes/symuvia/, 2005. Accessed: 2019-01-12.

[124] J. Picaut, N. Fortin, G. Dutilleux, A simplified approach for making soundmaps within a GIS software, in: Inter-Noise 2011, France, 2011, p. 6p.

[125] N. Fortin, E. Bocher, J. Picaut, G. Petit, G. Dutilleux, An opensource tool to build urban noise maps in a GIS, in: Open Source Geospatial Research and Education Symposium (OGRS), YVERDON-LES-BAINS, Switzerland, 2012, pp. 9p, cartes.

[126] G. Dutilleux, J. Defrance, F. Junker, D. Ecotière, B. Gauvreau, D. van Maercke, E. Le Duc, M. Bérengier, F. Besnard, Road noise prediction 2 - Noise propagation computation method including meteorological effects (NMPB 2008), 2009.

[127] A. Can, L. Leclercq, J. Lelong, J. Defrance, Accounting for traffic dynamics improves noise assessment: Experimental evidence, Appl. Acoust. 70 (2009) 821–829.

[128] American National Standards Institute, ANSI S1.11: Specification for Octave, Half-Octave, and Third Octave Band Filter Sets, 2009.

[129] L. Estévez-Mauriz, J. Forssén, Dynamic traffic noise assessment tool: A comparative study between a roundabout and a signalised intersection, Appl. Acoust. 130 (2018) 71–86.

[130] L. Cristina, L. D. Souza, M. B. Giunta, Urban indices as environmental noise indicators, Comput. Environ. Urban Syst. 35 (2014) 421–430.

[131] L. Dekoninck, D. Botteldooren, L. Int Panis, Guidelines for participatory noise sensing based on analysis of high quality mobile noise measurements, Proc. 41st Int. Congr. Expo. Noise Control Eng. (Inter-Noise 2012) (2012).

[132] A. Can, P. Aumond, Estimation of road traffic noise emissions: The influence of speed and acceleration, Transp. Res. Part D Transp. Environ. 58 (2018) 155–171.

[133] C. Liguori, A. Ruggiero, D. Russo, P. Sommella, Innovative bootstrap approach for the estimation of minimum measurement time interval in road traffic noise evaluation, Meas. J. Int. Meas. Confed. 98 (2017) 237–242.

[134] L. Filipponi, S. Santini, A. Vitaletti, Data collection in wireless sensor networks for noise pollution monitoring, Distributed Computing in Sensor Systems (2008) 492–497.

[135] S. Ferdoush, X. Li, Wireless sensor network system design using Raspberry Pi and Arduino for environmental monitoring applications, Procedia Comput. Sci. 34 (2014) 103–110.

[136] A. J. Lewis, M. Campbell, P. Stavroulakis, Performance evaluation of a cheap, open source, digital environmental monitor based on the Raspberry Pi, Meas. J. Int. Meas. Confed. 87 (2016) 228–235.

[137] M. Ambrož, Raspberry Pi as a low-cost data acquisition system for human powered vehicles, Meas. J. Int. Meas. Confed. 100 (2017) 7–18.

[138] Wirawan, S. Rachman, I. Pratomo, N. Mita, Design of low cost wireless sensor networks-based environmental monitoring system for developing country, Commun. 2008. APCC 2008. 14th Asia-Pacific Conf. (2008) 1–5.

[139] I. Akyildiz, W. Su, Y. Sankarasubramaniam, E. Cayirci, Wireless sensor networks: a survey, Computer Networks 38 (2002) 393–422.

[140] P. Daponte, L. De Vito, F. Picariello, S. Rapuano, I. Tudosa, Prototype design and experimental evaluation of wireless measurement nodes for road safety, Meas. J. Int. Meas. Confed. 57 (2014) 1–14.

[141] V. Villagrán, A. Montecinos, C. Franco, R. C. Muñoz, Environmental monitoring network along a mountain valley using embedded controllers, Meas. J. Int. Meas. Confed. 106 (2017) 221–235.

[142] D. S. Cho, J. H. Kim, D. Manvell, Noise mapping using measured noise and GPS data, Appl. Acoust. 68 (2007) 1054–1061.

[143] N. A. Rahim, M. P. Paulraj, A. H. Adom, S. Sundararaj, Moving Vehicle Noise Classification using Backpropagation Algorithm, 2010 6th Int. Colloq. Signal Process. its Appl. (2010) 1–6.

[144] A. J. Torija, D. P. Ruiz, A. F. Ramos-Ridao, Application of a methodology for categorizing and differentiating urban soundscapes using acoustical descriptors and semantic-differential attributes, J. Acoust. Soc. Am. 134 (2013) 791–802.

[145] T. Christen, A 15-bit 140-μ W scalable-bandwidth inverter-based $\Delta\Sigma$ modulator for a MEMS microphone with digital output, IEEE Journal of Solid-State Circuits 48 (2013) 1605–1614.

[146] P. R. Scheeper, B. Nordstrand, B. L. J. O. Gullov, T. Clausen, L. Midjord, T. Storgaard-Larsen, A New Measurement Microphone Based on MEMS Technology, J. Microelectromechanical Syst. 12 (2003) 880–891.

[147] International Electrotechnical Commission, Electroacoustics – Octave-band and fractional-octave-band filters, 1995.

[148] Q. Meng , D. Sen, S. Wang and L. Hayes, IMPULSE RESPONSE MEASUREMENT WITH SINE SWEEPS AND AMPLITUDE MODULATION SCHEMES, Electr. Eng. (2008) 4–8.

[149] U-blox, Gps antennas. rf design considerations for u-blox gps receivers, https://www.u-blox.com/sites/default/files/products/documents/GPS-Antenna_AppNote_(28GPS-X-08014).pdf, Accessed: 2019-04-03.

[150] D. H. T. Bergmans, N. V. Bøgholm, Measuring environmental aircraft noise: combining new technologies with old ideas., Proc. Internoise 2008 (2008).

[151] J. Noriega-Linares, J. Navarro Ruiz, On the Application of the Raspberry Pi as an Advanced Acoustic Sensor Network for Noise Monitoring, Electronics 5 (2016) 74.

[152] L. Dekoninck, D. Botteldooren, L. Int Panis, Using city-wide mobile noise assessments to estimate bicycle trip annual exposure to Black Carbon, Environ. Int. 83 (2015) 192–201.

[153] M. Marinov, D. Nikolov, B. Ganev, G. Nikolov, Environmental noise monitoring and mapping, in: Proc. Int. Spring Semin. Electron. Technol., 2017, pp. 1–7. doi:10.1109/ISSE.2017.8000992.

[154] C. A. Kardous, P. B. Shaw, Evaluation of smartphone sound measurement applications (apps) using external microphones—A follow-up study, J. Acoust. Soc. Am. 140 (2016) EL327–EL333.

[155] W. Zamora, C. T. Calafate, J. C. Cano, P. Manzoni, Accurate ambient noise assessment using smartphones, Sensors (Switzerland) 17 (2017) 1–18.

[156] M. Hu, W. Che, Q. Zhang, Q. Luo, H. Lin, A multi-stage method for connecting participatory sensing and noise simulations, Sensors (Switzerland) 15 (2015) 2265–2282.

[157] P. A. Lopez, M. Behrisch, L. Bieker-Walz, J. Erdmann, Y.-P. Flötteröd, R. Hilbrich, L. Lücken, J. Rummel, P. Wagner, E. Wießner, Microscopic traffic simulation using sumo, in: The 21st IEEE International Conference

on Intelligent Transportation Systems, IEEE, 2018. URL: https://elib.dlr.de/124092/.

[158] M. Xia-lin, C. Ming, Rendering of Dynamic Road Traffic Noise Map based on Paramics, Procedia - Soc. Behav. Sci. 96 (2013) 1460–1468.

[159] B. De Coensel, K. Sun, W. Wei, T. Van Renterghem, M. Sineau, C. Ribeiro, A. Can, C. Lavandier, D. Botteldooren, Dynamic Noise Mapping based on Fixed and Mobile Sound Measurements, Euro Noise (2015) 2339–2344.

[160] R. Benocci, P. Bellucci, A. Bisceglie, G. Zambon, H. E. Roman, The LIFE DYNAMAP project: Towards a procedure for dynamic noise mapping in urban areas, Appl. Acoust. 124 (2016) 52–60.

[161] P. Bellucci, L. Peruzzi, G. Zambon, LIFE DYNAMAP : making dynamic noise maps a reality (2018) 1181–1188.